

LIBRARIES
MICHIGAN STATE UNIVERSITY
EAST LANSING, MICH 48824-1048

This is to certify that the
dissertation entitled

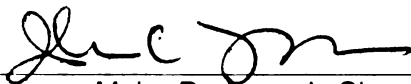
A CANINE MODEL OF IMERSLUND-GRÄSBECK SYNDROME:
GENETIC MAPPING, MUTATION IDENTIFICATION AND
FUNCTIONAL ANALYSIS

presented by

Qianchuan He

has been accepted towards fulfillment
of the requirements for the

Ph.D degree in the Department of Microbiology
and Molecular Genetics



Major Professor's Signature

3/31/05

Date

PLACE IN RETURN BOX to remove this checkout from your record.
TO AVOID FINES return on or before date due.
MAY BE RECALLED with earlier due date if requested.

DATE DUE	DATE DUE	DATE DUE

**A CANINE MODEL OF IMERSLUND-GRÄSBECK SYNDROME: GENETIC
MAPPING, MUTATION IDENTIFICATION AND FUNCTIONAL ANALYSIS**

By

Qianchuan He

A DISSERTATION

**Submitted to
Michigan State University
in partial fulfillment of the requirements
for the degree of**

DOCTOR OF PHILOSOPHY

Department of Microbiology and Molecular Genetics

2005

ABSTRACT

A CANINE MODEL OF IMERSLUND-GRÄSBECK SYNDROME: GENETIC MAPPING, MUTATION IDENTIFICATION AND FUNCTIONAL ANALYSIS

By

QIANCHUAN HE

Imerslund-Gräsbeck syndrome (I-GS, OMIM #261100) is an autosomal recessive disease characterized by congenital selective intestinal malabsorption of cobalamin (vitamin B12) and proteinuria. Some human patients are known to carry mutations in the cubilin gene (*CUBN*), which encodes a multiligand receptor expressed on both enterocytes and kidney proximal tubule cells. A Giant Schnauzer (GS) kindred studied in our lab is a well-established animal model for human I-GS, and has contributed significantly to the research on I-GS and cubilin. Previous experiments demonstrated abnormality of cubilin in the affected dogs, but linkage analysis excluded the *CUBN* as the disease-causing gene.

We performed a whole genome scan linkage analysis and linked the canine *I-GS* to a marker on dog chromosome 8, which is orthologous to human chromosome 14q. Type I markers were developed in the GS kindred to refine the mapping. Haplotype analysis narrowed the candidates region to be between markers *EML1* and *SIVA*, a 5Mb interval predicted from the human genome. *KNS2*, a marker located in the interval, was in complete linkage disequilibrium with *I-GS*, with a multipoint LOD score of 15.4.

One gene in the interval, *AMN* (*amnionless*), was a compelling candidate because it was demonstrated as the second I-GS gene in a recent human study. We cloned the cDNA of canine *AMN* based on human, rat and mouse *AMN* sequences. RT-PCR and genomic PCR disclosed an in-frame deletion of 33 bp in exon 10 of *AMN*, which was

predicted to abolish the hypothetical transmembrane domain of AMN. The deletion segregated with the disease in the GS kindred and was absent in 112 unrelated normal dogs.

We also studied an Australian Shepherd (AS) kindred with similar clinical features to the GS kindred. Linkage analysis of this small pedigree to marker *KNS2* gave a LOD score of 1.7, marginally suggesting linkage of the disease to *AMN*. Mutation screening in *AMN* identified a G>A transition in the start codon, which was predicted to abrogate translation initiation. The mutation segregated with the disease and was not seen in 112 chromosomes of unrelated normal dogs.

A recent study showed that cubilin and AMN form a tight complex, cubam, which is crucial for endocytosis of certain ligands, such as intrinsic factor-Cobalamin (IF-Cbl). Our RT-PCR in multiple canine tissues demonstrated that both genes have high expression levels in ileum and kidney, although they have different expression profiles in some other tissues. In an IF-Cbl pull-down assay, three AMN isoforms were present in the kidney homogenates of a normal dog but absent in the affected dogs of both kindreds. In a heterologous cell transfection system, wildtype canine AMN, but not the 33bp-deletion mutant, assists the membrane expression of cubilin. We therefore demonstrated *in vivo* that the fundamental cause of I-GS is the failure to express functional cubam, and canine I-GS is an orthologue of the human disease. The two pedigrees harboring different *AMN* mutations provide us a unique opportunity to study the functions of AMN and cubilin directly in tissues of both affected and normal dogs, which is nearly impossible in the human study of I-GS patients.

DEDICATION

This dissertation is dedicated to:

Ying Du, my wife, whose love and support give me the most important strength during my graduate studies;

Dr. John Fyfe, a great mentor and scientist, who led me into the field of medical genetics, and shares with me the pleasure, difficulty and hope of the research.

ACKNOWLEDGEMENTS

I am grateful to my committee members, Dr. Karen Friderici, Dr. Ronald Patterson and Dr. John Wang, for their excellent guidance, insight and encouragement. I thank Dr. Friderici for providing me many opportunities to learn human genetics; I thank Dr. Patterson and Dr. Wang for allowing me to participate in their joint seminars, where I constantly learn new knowledge in biochemistry and RNA biology.

I am thankful to all the members in my committee members' labs, for their help and enthusiasms. I cherish the friendship with this group of wonderful people.

I appreciate Dr. Patrick Venta and Dr. Donna Housley for invaluable suggestions to my experiments. I would like to thank Dr. Vilma Yuzbasiyan-Gurkan for the gift of many dog DNA samples.

This thesis would not be possible without the help from Dr. Alejandro Schaffer at NIH, Dr. Paula Henthorn at University of Pennsylvania and Dr. Mette Madsen at University of Aarhus in Denmark. It is always a great pleasure to collaborate with these experts from different fields.

Finally, I would like to thank Adam Kilkenney, Brittany Gregory and Meghan Drummond in our lab for their excellent technical assistance.

TABLE OF CONTENTS

List of tables.....	viii
List of figures.....	ix
List of abbreviations.....	xi
Chapter 1: Literature review.....	1
Vitamin B12 and its physiological importance.....	1
Vitamin B12 absorption review.....	2
Vitamin B12 storage and distribution.....	5
Defects in cobalamin transport.....	5
Defects in cellular AdoCbl and MeCbl synthesis.....	7
Imerslund-Gräsbeck Syndrome.....	8
Cubilin/IFCR/gp280.....	12
AMN.....	18
Canine I-GS.....	25
Summary.....	28
Purpose and outline.....	29
Chapter 2: Genetic mapping of canine Imerslund-Gräsbeck Syndrome in a giant schnauzer family.....	30
Introduction.....	31
Materials and methods.....	34
Results.....	39
Discussion.....	48

Chapter 3: cDNA cloning of canine <i>AMN</i> and mutation screening in the Giant Schnauzer family.....	51
Introduction.....	52
Materials and methods.....	56
Results.....	61
Discussion.....	68
Chapter 4: Linkage analysis and mutation screening of an Australian Shepherd family with Imerslund-Gräsbeck Syndrome.....	72
Introduction.....	73
Materials and methods.....	76
Results.....	79
Discussion.....	88
Chapter 5: Functional studies of canine <i>AMN</i> mutations.....	90
Introduction.....	91
Materials and methods.....	93
Results.....	98
Discussion.....	108
Appendices.....	113
Future direction.....	119
References.....	122

LIST OF TABLES

Table 1. Two-Point LOD score analysis.....	42
Table 2. Genes listed in the <i>EML1-SIVA</i> interval of human genome browser.....	54
Table 3. Primer list for genomic amplification of canine <i>AMN</i>	78
Table 4. Genotyping data of the Giant Schnauzer family.....	115
Table 5. Genotyping data of the Australian Shepherd kindred.....	118

LIST OF FIGURES

Figure 1.1 Vitamin B12 absorption in the gastrointestinal tract.....	2
Figure 1.2 Intracellular transport and processing of vitamin B12.....	8
Figure 1.3 A model of AMN and cubilin assembly in the biosynthetic pathway and recycling in the endocytic apparatus of polarized epithelial cells.....	22
Figure 2.1 Pedigree of dogs of known I-GS status used for linkage analysis.....	40
Figure 2.2 Multipoint LOD score curve showing linkage to I-GS.....	45
Figure 2.3 Haplotype analysis of the GS kindred.	46
Figure 2.4 An iterative strategy to develop new markers for linkage disequilibrium mapping.....	47
Figure 3.1 cDNA sequence of canine <i>AMN</i>	64
Figure 3.2 Alignment of human, dog, and mouse AMN protein.....	65
Figure 3.3 DNA sequencing revealed a 33bp in-frame deletion in canine <i>AMN</i> of the affected dogs.	66
Figure 3.4 Mutation analysis of the 33bp deletion in exon 10.	67
Figure 3.5 Structure prediction of AMN by the TMHMM software.....	71
Figure 4.1 <i>KNS2</i> genotyping of the Australian Shepherd kindred.	75
Figure 4.2. Genomic sequence of canine <i>AMN</i> gene.....	82
Figure 4.3 DNA sequencing revealed a G>A mutation in the start codon of canine <i>AMN</i> in the affected dogs.	86
Figure 4.4 Mutation analysis of the G>A transition in start codon.....	87
Figure 5.1 RNA expression profiles of cubilin and AMN.....	102
Figure 5.2 Specificity test of the anti-AMN antibody.	103
Figure 5.3 Cubilin and AMN expression in normal and I-GS affected dog kidneys <i>in vivo</i>	104
Figure 5.4 Cubilin saturation test.	105

Figure 5.5 Immunofluorescence of double transfected CHO cells expressing cubilin and AMN.....	106
Figure 5.6 Cubilin and AMN expression in CHO cells with wildtype or c.1113-1145del <i>AMN</i> cDNA.....	107
Figure 6 The 5bp polymorphism of <i>AMN</i> identified in a komondor and a beagle.....	114

LIST OF ABBREVIATIONS

Ab	antibody
AdoCbl	adenosylcobalamin
AMN	amnionless
AS	Australian shepherd
BBM	brush border membrane
BMP	bone morphogenesis protein
Caco	colon adenocarcinoma
Cbl	Cobalamin
CFA8	canine chromosome 8
CUBN	cubilin
FISH	fluorescence in situ hybridization
GPI	glycosyl-phosphatidyl-inositol
GS	Giant Schnauzer
HDL	high-density lipoprotein
IF	intrinsic factor
IF-Cbl	intrinsic factor-Cobalamin
IFCR	intrinsic factor-cobalamin receptor
I-GS	Imerslund Gräsbeck Syndrome
LDL	low-density lipoprotein
LOD	logarithm of odds
MeCbl	methylcobalamin
MGA	megaloblastic anemia
MMA	methylmalonyl acidemia
MMAA	MethylMalonic Acidemia linked to the cblA complementation group
MMAB	MethylMalonic Acidemia linked to the cblB complementation group
MTRR	methionine synthase reductase
OMIM TM	Online Mendelian Inheritance in Man TM
OK	opossum kidney
RAP	Receptor Associated Protein
RER	Rough endoplasmic reticulum
SAM	S-adenosyl methionine
TRAF3	TNF receptor associated factor 3
UTR	untranslated region
VE	visceral endoderm
YAC	Yeast artificial chromosome

CHAPTER 1

LITERATURE REVIEW

Vitamin B12 and its physiological importance

Vitamin B12 (cobalamin) has been known as an anti-pernicious factor since 1920s, when it was initially called “extrinsic factor”. A unique feature of vitamin B12 is that a cobalt atom is located in the center of a corrin ring (Banerjee and Ragsdale, 2003 review). Different upper ligands may be linked to the cobalt atom, as shown in vitamin B12 and its derivatives, such as methylcobalamin (MeCbl) and adenosylcobalamin (AdoCbl) (Banerjee and Ragsdale, 2003 review).

All of vitamin B12 in nature is of microbial origin (Rosenblatt and Fenton, 2001 review). The biosynthesis of B12 in microbes is quite complicated, involving more than 30 genes (Roth et al., 1993). Bacteria and archaea use vitamin B12 for acetyl-CoA synthesis, methyl transfer and fermentation, etc (Martens et al., 2002 review). Animals (including humans) need cobalamin but do not synthesize it. Therefore, vitamin B12 must be absorbed from the diet. In animals and man, B12 is known to participate in only two enzyme reactions, which are methionine synthesis and methylmalonyl-CoA isomerization (Okuda, 1999 review). In the cytoplasm, B12 (in the form of MeCbl) is a cofactor for methionine synthase, which catalyzes the conversion of homocysteine to methionine. In the mitochondria, B12 (in the form of AdoCbl) is an essential coenzyme for methylmalonyl-CoA mutase, which converts methylmalonyl-CoA to succinyl-CoA. Defects in these biochemical pathways lead variously to methylmalonic acidemia (MMA), homocystinuria, megaloblastic anemia and neurological symptoms (Stabler and Allen, 2004 review). B12 deficiency may also affect the health of humans indirectly.

Since B12 is required in the synthesis of methionine, B12 deficiency also leads to low level of methionine and subsequent S-adenosyl methionine (SAM) deficiency. This can cause genomic instability in cells, because a low level of SAM may diminish DNA methylation. (Fenech, 2001review; Brunaud et al., 2003).

Vitamin B12 absorption review

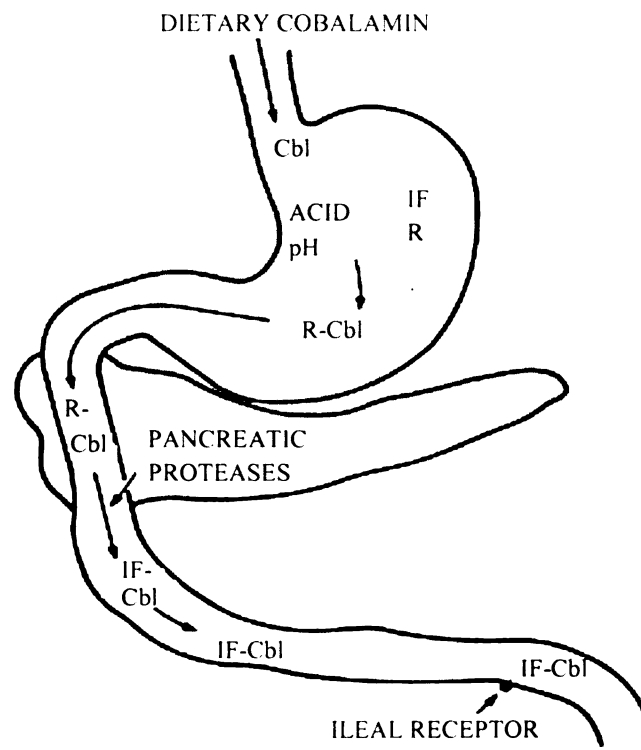


Figure 1.1 Vitamin B12 absorption in the gastrointestinal tract (Seetharam and Alpers, 1982a review). Cbl, cobalamin; IF, intrinsic factor; R, R protein.

Cobalamin (Cbl) absorption is a highly specialized multi-step process in which several proteins are involved (Figure 1.1). Released from food, Cbl is bound to R protein

in the stomach to form a stable complex. R protein, also called TCI or haptocorrin, is a glycoprotein and has high affinity for Cbl at stomach pH (Allen and Majerus, 1972a). R protein is widely distributed in the saliva, bile, blood and other cells (Sennett and Rosenberg, 1981 review). Cbl-TCI complex remains stable in the intestine until pancreatic proteases degrade TCI and release Cbl for binding to intrinsic factor (Allen et al., 1978a). In patients with cobalamin malabsorption due to pancreatic insufficiency, a cobalamin analogue that binds tightly to R protein but not to intrinsic factor can correct the defect, because cobalamin can circumvent the binding to R protein (Allen et al., 1978b). Several individuals were known to have deficient or absent TCI, but they didn't have Cbl malabsorption, and they had no signs of Cbl deficiency except low serum Cbl concentration (Cooper and Rosenblatt, 1987).

Intrinsic factor (IF) was so named because it is produced by the body and was used to prevent pernicious anemia (vitamin B12 was named the extrinsic factor). With R protein degraded by proteolytic enzymes, IF binds to Cbl to form the noncovalent IF-Cbl complex (Tang et al., 1992). IF is a 44 kDa glycoprotein and is highly resistant to proteolytic degradation (Allen and Mehlman, 1973; Allen et al., 1978a). Tissues that produce IF may not be the same in different species. Human IF is synthesized by the gastric parietal cells of the stomach (Levine et al., 1980), whereas canine and feline IF are pancreatic in origin (Vaillant et al., 1990; Fyfe, 1993).

The IF-Cbl complex is endocytosed into enterocytes via intrinsic factor-cobalamin receptor (IFCR), expressed on the apical membrane of the ileal enterocytes (Sennett and Rosenberg, 1981 review). IF-Cbl and IFCR have a disassociation constant of 2.5×10^{-10} M, but Cbl or IF alone has no affinity to IFCR, suggesting that Cbl binding to IF triggers a

conformational change. The binding requires pH between 6 and 9 and is Ca^{2+} dependent (Mathan et al., 1974), explaining why IF doesn't bind to Cbl in the stomach. IFCR was later named cubilin for its unique structural features (discussed later in *Cubilin/IFCR/gp280*). Almost all the absorption of IF-Cbl by cubilin occurs in the ileum, because cubilin is mainly expressed in the ileum (Booth and Mollin, 1959; Xu and Fyfe, 2000). A recent study reported that another protein, amnionless (AMN), is indispensable for the expression and function of cubilin (Fyfe et al., 2004).

The transport of IF-Cbl across the ileal enterocyte to the portal venous plasma takes several hours (Doscherholmen and Hagen, 1959). Three steps are already known, including degradation of IF in lysosomes, binding of Cbl to TCII, and transport of Cbl-TCII into the blood (Kapadia et al., 1983; Ramasamy et al., 1989). Human colon adenocarcinoma (Caco-2) cells were used to study IF-Cbl internalization because they can express both IFCR and TCII and are able to direct Cbl transcytosis (Dix et al., 1990; Ramanujam et al., 1991). Study with Caco-2 cells demonstrated that IF degradation is a prerequisite to release of Cbl into the cytosol (Dan and Cutler, 1994). The accurate location for the formation of TCII-Cbl has not been solved because TCII was synthesized at a low level and didn't accumulate inside the Caco-2 cells (Seetharam, 1999 review).

Although the majority of plasma Cbl is bound to TCI in humans, it is TCII that mainly mediates uptake of Cbl by tissues (Rosenblatt and Fenton, 2001 review). TCII is a 60 kDa non-glycosylated protein (Allen and Majerus, 1972b), distributed in plasma and a host of other extracellular fluids (Cooper and Rosenbaltt, 1987 review). Using ^{125}I -labeled TCII, Youngdahl-Turner et al. (1978) first described a specific TCII-Cbl receptor existing on the cell surface of human fibroblasts, and confirmed that TCII was degraded

within lysosomes. TCII receptors were later observed on human leukemia K562 and HL-60 cells, and the expression level of the receptors is related to the growth conditions of the cells (Amagasaki et al., 1990). The receptor was purified from placenta membranes and characterized to be a 58 kDa glycoprotein with a dissociation constant of 2.6×10^{-10} M (Quadros et al., 1994).

Once TCII-Cbl is endocytosed into the cell, Cbl is released from the lysosomes in a pH-dependent manner (Idriss and Jonas, 1991). Subsequently, Cbl is processed into MeCbl or AdoCbl, and serves as coenzymes for methylmalonyl-CoA mutase or methionine synthase (Marsh, 1999 review).

Vitamin B12 storage and distribution

Experiments with Co^{60} labeled Cbl showed that liver is the reservoir for absorbed Cbl (Schloesser et al., 1958). Some of the Cbl stored in liver is secreted into the intestine through biliary excretion, so called enterohepatic recirculation (Willigan et al., 1958). Other organs showing high concentration of Cbl include pituitary, kidney and pancreas (Cooperman et al., 1960).

Defects in cobalamin transport

Defects in cobalamin transport may lie in problems with one or more of the following steps: gastric intrinsic factor synthesis, pancreatic secretion, intestinal absorption, one of the circulating cobalamin binding proteins (TCII), or cellular absorption.

Defects in intrinsic factor (IF) cause a disease called congenital pernicious anemia (OMIM#261000). Intrinsic factor in these patients either is highly susceptible to degradation in the lumen of the gastrointestinal tract (Yang et al., 1985) or has extremely low affinity to the IFCR (Katz et al., 1974b). The IF gene was cloned and mapped to chromosome 11 (Hewitt et al., 1991). Five patients were found to carry a nonsynonymous variation near the start codon, which changes glutamine to arginine (Gordon et al., 2004). However, since the variant was also carried in two control populations, it is unlikely to be the direct cause of the disease (Gordon et al., 2004). The long awaited mutation in IF gene was identified by Yassin et al. (2004) as a 4 bp deletion in exon 2, resulting in frameshift and predicted loss of the protein. Ten more mutations were identified in the IF gene recently (Tanner et al., PNAS 2005, in press).

Cbl malabsorption due to intestinal defects is called ***Imerslund-Gräsbeck syndrome*** and will be discussed later.

Genetic defects in TCII result in severe megaloblastic anemia in infants. The TCII gene is located on chromosome 22 (Arwert et al., 1986), and the cDNA encodes an extracellular protein of 409 amino acids (Platica et al., 1991). Mutation screening in the TCII gene of an affected child disclosed a compound heterozygote with deletions in both alleles, which led to failed TCII protein expression (Li et al., 1994). However, the most popular TCII variation in Caucasians is a single amino acid substitution, which significantly lowers the concentration of bound B12 and increases the methylmalonic acid concentrations (Miller et al., 2002). Interestingly, it was noticed that human TCII, TCI, and IF gene sequences share high homology at some exon-intron boundary sites,

suggesting that these genes were originated from a common ancestral gene by duplication mechanism (Regec et al., 1995).

However, no patients have been implicated with TC II-receptor deficiency so far. The reason could be that either the deficiency is extremely rare or, most likely, is embryonic lethal, or some compensatory mechanisms exist such that people having TC II-receptor defects do not show any symptoms.

Defects in cellular AdoCbl and MeCbl synthesis

Following entry of Cbl-TCII into the target cells, TCII is digested by enzymes in the lysosomes, with free Cbl released into the cytosol (Figure 1.2). Distinct defects in enzymes required for intracellular transport and processing of B12 have been named as different cbl groups, based on complementation tests (Gravel et al., 1975).

CblG group is due to mutations in the gene encoding methionine synthase (Gulati et al., 1996; Leclerc et al., 1996; Watkins et al., 2002), whereas cblE is caused by mutations in the methionine synthase reductase (MTRR) gene (Wilson et al., 1999; Zavadakova et al., 2002). The AdoCbl metabolism in both groups is intact.

CblA complementation type is linked to mutations in the MMAA (**MethylMalonic Acidemia linked to the cblA complementation group**) gene, which encodes a protein that transports Cbl from cytosol into mitochondria (Dobson et al., 2002a). CblH has similar clinical and biochemical features to cblA, but the molecular basis is unknown.

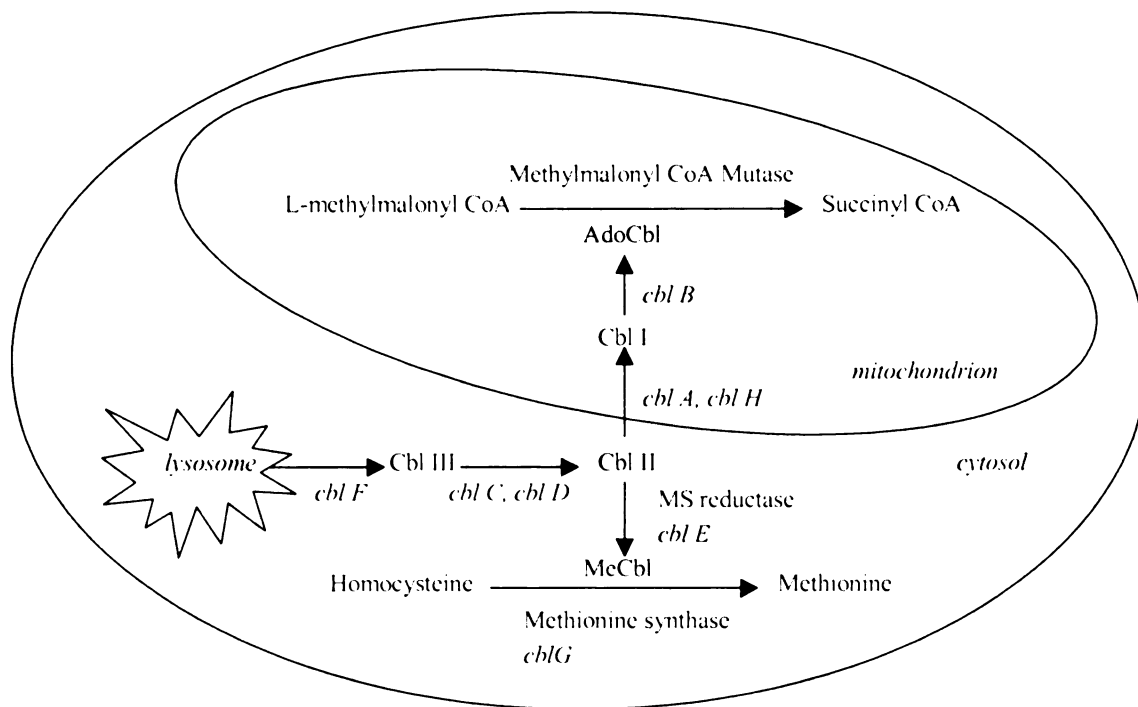


Figure 1.2 Intracellular transport and processing of vitamin B12 (modified from Dobson et al., 2002a)

Mutated MMAB (**M**ethyl**M**alonic **A**cidemia linked to the **cblB** complementation group) gene, encoding the cobalamin adenosyltransferase, is responsible for **cblB** type (Dobson et al., 2002b). The genes responsible for **cblF**, **cblC** and **cblD** remain unknown.

Imerslund-Gräsbeck Syndrome

History and clinical features

Imerslund-Gräsbeck syndrome (I-GS) was first described by Imerslund (1960) in Norway and by Gräsbeck et al. (1960) in Finland. The patients showed familial juvenile vitamin B12 deficiency anemia, methylmalonic acid excretion and proteinuria. By Schilling test, which measures the absorption of orally administered radioactive B12, the

cause of the vitamin B12 deficiency was identified as decreased intestinal absorption from the diet. Other possible causes of the disease were excluded, such as (i) depletion of the vitamin by noxious intestinal bacteria, (ii) general dysfunction of the gastrointestinal tract and (iii) autoimmune mechanisms (Imerslund and Bjornstad, 1963). Since the patients were unresponsive to intrinsic factor, the syndrome is distinct from the congenital pernicious anemia, which is due to the lack of intrinsic factor in the gastric juice. To be diagnosed as I-GS, a patient generally should be no more than five years of age, and not have intrinsic factor insufficiency. However, the most important criteria are that patients are responsive to parenterally administered B12 and Schilling test confirms B12 malabsorption (Mohamed et al., 1966). Most of the patients had mild proteinuria, which was resistant to the parenteral administration of B12. In addition, the clinical features of I-GS may include methylmalonic aciduria (Rubin et al., 1974), homocystinuria (Mohamed et al., 1966), minimal glomerulonephritis (Becker et al., 1977; Rumpelt and Michl, 1979), subacute combined degeneration of the cord (Ismail et al., 1997) and neuropathy (Ludvigsson et al., 1980). Other complications were seen in rare cases, such as dolichocephaly (Ben-Ami et al., 1990), distinct skin lesions (Lin et al., 1994), recurrent urinary tract infection and genitourinary tract abnormalities (Sandoval et al., 2000). Whether these complications are directly related to vitamin B12 deficiency is uncertain.

The defect was deemed congenital, because the time of onset of the symptoms corresponded to the sustaining time of the child's stored vitamin B12 conveyed from the mother in utero (Hippe, 1966). With a single *in vitro* experiment, Mackenzie et al. (1972) stated that the vitamin B12 absorption defect occurred at a stage after the binding

of IF-Cbl to IFCR and before the formation of Cbl-TCII complex, indicating that the IFCR was intact. In contrast to this finding, studies of the absorption of radioactive B12 by ileal biopsy tissues pointed to a defect in the ileal receptor for IF-Cbl binding (Burman et al., 1985). The latter statement was corroborated by experiments showing that I-GS patients have a sharply decreased IFCR activity (Gueant et al. 1995). Thus, I-GS was strongly suggested to be associated with a defect in IFCR.

Epidemiology

More than 200 human cases and familial clusters have been reported world wide (Rosenblatt and Fenton, 1999). Whereas the original patients were identified from Finland and Norway, a number of patients from the Middle East have been reported in the past twenty years (Burman et al., 1985; Ben-Ami et al., 1990; Salameh et al., 1991; Abdelaal and Ahmed, 1991; Altay et al., 1995; Ismail et al., 1997). Other sporadic cases have been reported from Germany (Bienzle et al., 1976), Libya (el Mauhoub et al., 1989), China (Lin et al., 1994), United States (Sandoval et al., 2000), and other countries. It is worth noting that only a few new cases have been diagnosed in Finland and Norway during the past thirty years, which was speculated to be due to the change of population structure (lower inbreeding coefficient) and dietary habits (more meat and therefore more B12) (Aminoff et al., 1995; Kristiansen et al., 2000).

Therapy

Parenteral vitamin B12 treatment resulted in complete clinical and hematological remission except proteinuria (Mohamed et al., 1966). This finding was confirmed by a

long term follow-up study, in which the prognosis of the patients are excellent on intramuscular vitamin B12 therapy, but those who previously had proteinuria symptom keep excreting an average of 750 mg of protein in the urine per day (Broch et al., 1984). A patient with severe neurological abnormalities was reported to have a remarkable recovery from spasticity, truncal ataxia and brain atrophy, by parenteral vitamin B12 therapy (Salameh et al., 1991).

Genetics

Since one of the two patients in the earliest finding was from a consanguineous family, it was speculated that there might be an inherent defect of an acceptor for B12 or transport system in the enterocytes (Gräsbeck et al., 1960). The familial occurrence of the syndrome in other patients also indicated that I-GS was a genetic disease (Imerslund and Bjornstad, 1963). Study of 18 cases in 14 families in Israel demonstrated that both sexes were affected and the parents were unaffected and usually shared common ancestors, highly suggesting that I-GS was an autosomal recessive disease. The gene frequency among Israeli Jews of Tunisian origin was estimated to be 0.025 and the frequency of heterozygotes (carriers) 0.05 (Ben-Bassat et al., 1969). Furuhielm and Nevanlinna (1973) mentioned the gene frequency of I-GS in Finns was between 0.002 and 0.003. They further argued that, while founder effect causes disease allele enrichment in Finland, consanguinity is the main reason causing I-GS in the Jewish families.

Because only anemia responded to parenteral vitamin B12 therapy, it was postulated that the two traits, anemia and proteinuria, are caused by a multi-functional gene or two genes somehow related (Rumpelt and Michl, 1979). Later experiments in canine I-GS

showed IFCR's mistrafficking in both intestine and kidney, suggesting that these defects are associated with a single gene (Fyfe et al., 1991b).

Cubilin/IFCR/gp280

Terminology

People have realized for a long time that IF-Cbl must bind to an ileal receptor before being absorbed by the enterocytes and, therefore, named it the intrinsic factor-cobalamin receptor (IFCR) (Okuda, 1962). cDNA cloning of the rat IFCR disclosed a protein containing 27 CUB domains, thus the receptor was renamed cubilin (Moestrup et al., 1998).

In an independent study, a 280 kDa glycoprotein (gp280) located on the proximal tubule cells and visceral yolk sac membrane was found to be likely involved in endocytosis activities (Sahali et al., 1988). Functional and immunological analysis proved that gp280 is identical to cubilin (Seetharam et al., 1997).

Although one group in France was arguing that IFCR is distinct from cubilin on some limited information (Gueant et al., 2001), it is now generally accepted that cubilin, IFCR, gp280 represent the same protein.

Tissue distribution

Ileum from different species has been used as a source to purify the IFCR (cubilin) in early studies (Marcoullis et al, 1977; Yki-Jarvinen et al., 1979; Kouvonen 1980; Seetharam et al. 1981). Immunocytochemistry localized the IFCR in the crypt, mid-villus, and villus tip areas of the ileal mucosa (Levine et al., 1984). In addition, the IFCR

was found to have high expression in human, canine and rat kidneys and small amounts in rat placenta and liver (Seetharam et al., 1988). Immunomicroscopy revealed that the receptor is located on the apical surface of proximal tubular cells (Seetharam et al., 1988). It is also expressed on rat yolk sac apical membranes (Sahali et al., 1988; Seetharam et al., 1997), and male and female rat reproductive tissues (Van Praet et al., 2003; Argraves and Morales, 2004).

Size and composition

The size and composition of IFCR (cubilin) have perplexed the field for more than 20 years. The porcine IFCR was erroneously claimed to be purified as an 80 kDa protein composed of two subunits (Marcoullis et al, 1977). The IFCR was later purified from canine ileal mucosa by hog IF-Cbl affinity chromatography, showing molecular weight of 180 kDa on SDS-PAGE, disassembling into two subunits at reducing conditions (Seetharam et al. 1981). However, the IFCR purified from dog kidneys showed molecular weight of 230 kDa on SDS-PAGE but 457 kDa by amino acid analysis (Seetharam et al., 1988; Fyfe et al., 1991b). Furthermore, the kidney IFCR remains to be a single band even at strong reducing condition (Seetharam et al., 1988). The apparent inconsistency regarding the molecular weight and compositions of the IFCR was not well explained until the cDNA of the cubilin was cloned in the late 1990s.

IFCR (cubilin) can be affinity purified on a RAP column. Receptor Associated Protein (RAP) is a 39 kDa endoplasmic reticulum protein serving as a molecular chaperone for low density lipoprotein receptor-related protein (Bu et al, 1995). One of its binding partners is megalin, which was indicated to mediate the endocytosis of TCII-Cbl

complexes in kidney proximal tubules (Moestrup et al., 1996). Through a RAP affinity column, the IFCR of rabbit kidney was purified as a 460 kDa protein (Birn H et al., 1997). By immunoscreening of a λ Zap cDNA library constructed from yolk sac cells, the rat cubilin cDNA was first cloned (Moestrup et al., 1998). Rat cubilin has 3623 amino acids if deduced from the cDNA sequence, while the mature protein migrates as a 460 kDa band on SDS-PAGE. If treated with peptidyl N-glycosidase F, the size is reduced to 400 kDa, suggesting that the N-linked oligosaccharides constitute about 60 kDa of mature cubilin (Moestrup et al., 1998). Subsequent cloning of human and canine cubilin cDNA both agree with the size of 400 kDa (Kozyraki et al., 1998; Xu et al., 1999). A likewise explanation for the earlier findings is that the 230 kDa migration band was actually 460 kDa (markers >200 kDa were not used in those studies), and the two subunits detected in intestine were proteolytic cleavage products of cubilin.

Structure and modification

An early study suggested that IFCR (cubilin) has most of its mass in extracellular space and a small portion inserted in the membrane (Seetharam et al., 1982b). cDNA cloning of cubilin helped to dissect the protein's structure. Preceding the mature form of a 3589-aa protein, the human cubilin has a 24-aa signal peptide predicted to be cleaved in the endoplasmic reticulum, and a 10-aa peptide predicted to be cleaved by the trans-Golgi enzyme furin. The most prominent feature of cubilin is that it contains 8 EGF repeats and 27 CUB domains, suggesting cubilin is a multi-ligand receptor. Unexpectedly, as a receptor it has no transmembrane domain or glycosyl-phosphatidyl-inositol (GPI) anchor (Kozyraki et al., 1998). CUB domain 5-8 was demonstrated to be the Cbl-IF binding site

while **CUB** domains 13-14 bind to the receptor associated protein (RAP) (Kristiansen et al., 1999). Two of the EGF repeats contain a Ca^{2+} binding motif (Moestrup et al., 1998), suggested to reflect previous finding that the interaction between IF-Cbl and the receptor is Ca^{2+} dependent (Katz and Cooper, 1974a). Forty-two potential N-glycosylation sites are present in cubilin (Moestrup et al., 1998), but the actual glycosylated sites may vary in different tissues. Studies in dogs suggested that the cubilin in the ileum is more highly glycosylated than that in the kidney, which may help cubilin to resist the proteolytic enzymes in the ileum (Xu and Fyfe, 2000). Study in opossum kidney (OK) cells showed that **IFCR** is also palmitoylated (Ramanujam et al., 1994). Electron microscopy, analytical ultracentrifugation and computer-assisted analysis of bovine cubilin demonstrated that cubilin *in vitro* forms a trimer by a α -helix structure located at the N-terminus (Lindblom et al., 1999). Whether the trimer reflects the *in vivo* structure of cubilin remains unknown.

Functions and Binding partners

IF-Cbl, but not free IF or Cbl, binds to **IFCR** (cubilin). Apical membrane expression of **IFCR** is required for [^{57}Co]Cbl transcytosis across polarized cells, that is, from the apical membrane to the basolateral membrane (Ramanujam et al., 1991). During the transcytosis, IF is degraded in lysosomes and free Cbl is released for further transport by **TCII** (Dan and Cutler, 1994). Defective **IFCR** apparently can cause Cbl malabsorption.

In a different perspective, injection of anti-cubilin to mid-gestation rats resulted in fetal resorption or malformations. Indirect immunofluorescence study suggested that

cubilin **might** be involved in endocytosis activities (Sahali et al., 1988). Further analysis showed **that** in the Ab-treated rat yolk sac both the size and shape of the early endocytosis vesicles **were** abnormal, resulting in disordered intracellular traffic of internalized proteins (Le Panse et al., 1994).

The teratogenic rat phenotype presented above indicates that cubilin may play a role in **development**. As a matter of fact, cubilin activity was observed to rise enormously in the rat **placental** membranes during the third week of pregnancy (Ramanujam et al., 1993). **One** study showed that cubilin can be affinity-purified by galectin-3, a protein **suggested** to play a role in embryo development, from homogenates of murine uteroplacental complex. In addition, cubilin colocalized with galactin-3 on yolk sac membrane in the last week of pregnancy. However, the anti-cubilin doesn't seem to **produce** the teratogenic effects via galactin-3, because the timing of the interaction **between** the two proteins was suggested to be at the late pregnancy (Crider-Pirkle et al., 2002).

Tested in rat visceral yolk sac cells, cubilin also mediates the internalization of immunoglobulin light chains purified from the urine of myeloma patients. However, the **binding** of cubilin with light chain can strongly inhibit the function of the endosome *in vitro*. **Therefore**, excessive light chain present in the urine may lead to proximal tubular cytotoxicity (Batuman et al., 1998).

Megalin (gp330) is a 600 kDa membrane protein belonging to the low density lipoprotein receptor gene family, and mediates endocytosis of several small proteins (Christensen et al., 1992; Saito et al., 1994). Megalin can be purified together with cubilin from a RAP-Sepharose column (Birn et al., 1997), and it was suggested that

cubilin **b**inds to the extracellular domain of megalin (Moestrup et al., 1998). Cubilin binds **a**nd colocalizes with megalin during the endocytosis process, as supported by surface **p**lasmon analysis and electron microscopy, respectively (Moestrup et al., 1998).

Cubilin and megalin act together to reabsorb certain proteins from the kidney proximal tubules. One example is albumin. Cubilin and megalin colocalize predom**i**nantly on the apical membrane of kidney proximal tubule cells, and mediate the reabsorption of albumin from the glomerular ultrafiltrate (Birn et al., 2000; Zhai et al., 2000). Albumin was suggested to bind to cubilin at the same site as IF-Cbl, but with ~500- **750** fold lower affinity (Yammani et al., 2001). Other groups reported that megalin acts **t**ogether with cubilin to mediate the endocytosis of apolipoprotein A-I receptor, a protein belonging to the high-density lipoprotein (HDL) family (Kozyraki et al., 1999; Hammad et al., 1999; Hammad et al., 2000). The list of cubilin's binding partners is grow**i**ng gradually, including transferrin (Kozyraki et al., 2001), vitamin D-binding protein (Nykjaer et al., 2001), hemoglobin (Gburek et al., 2002) and myoglobin (Gburek et al., 2003). Thus cubilin-megalin mediated endocytosis in the proximal tubule appears to be **c**rucial to reabsorb a wide range of proteins.

Another partner of cubilin, AMN, will be discussed later in this chapter.

Cubilin and I-GS

With the rapid progress of molecular genetics and computation tools in the early 90s, **p**osition cloning loomed as a powerful tool to discover the underlying genetic cause of **i**nherited diseases. With six Finnish I-GS families (30 members) and three Norwegian families (11 members), a whole genome scan linkage analysis of human I-GS defined the

minimal **c**andidate interval between markers D10S586 and D10S570, which are 16-cM apart. **T**he highest LOD (**L**ogarithm of the **O**dds) score 5.36 was observed around D10S1**477** (Aminoff et al., 1995). On the other hand, chromosome mapping by FISH (fluores**c**ence in situ hybridization), radiation hybrid, and YAC (Yeast Artificial Chromo**s**ome) screening localized the cubilin gene within a 6 cM region on chromosome 10p 12, close to marker D10S1477 (Kozyraki et al., 1998). Combined with previous **f**indings that the ileal biopsy specimens of I-GS patients have a nearly undetectable IFCR activity (Gueant et al. 1995), these data strongly indicated that cubilin gene (*CUBN*) defects might cause I-GS (Kozyraki et al., 1998). Further linkage disequilibrium mapping and **m**utation screening identified two different mutations in Finnish patients: the first **m**utation (FM1) is a missense mutation in the IF-Cbl binding domain, while the 2nd **m**utation (FM2) is a point mutation in the intron, causing abnormal splicing and **e**ssent**i**ally truncated proteins (Aminoff et al., 1999). Functional analysis demonstrated that **t**he FM1 mutation impaired the binding site of cubilin to IF-Cbl, which subsequently led **t**o vitamin B12 malabsorption (Kristiansen et al., 2000). Four more different **m**utations were later identified in Finnish, Bedouin and Turkish (Tanner et al., 2004). **H**ow**e**ver, no mutations were found in cubilin gene in the Norwegian and Saudi Arabian **f**amilies (Aminoff et al., 1999), suggesting genetic heterogeneity exists.

AMN

Genetics

In 1996, a research group created a new transgenic mouse line by random insertion of **t**he human CD8 α transgene construct (T81) on the C57BL/6J (B6) mouse background.

Mice homozygous for the T81 insertion in chromosome 12 showed prenatal lethal phenotype (Wang et al., 1996). The insertion locus was mapped by interspecific backcross and FISH. Further molecular cloning work recovered the junction site sequence, which helped to pinpoint the insertion site to be close to the *TRAF3* (TNF receptor associated factor 3) gene. Since the mutant does not develop a normal amnion, it was named amnionless (AMN) (Wang et al., 1996). Under the B6 background the mutants stopped embryonic development at E9.5, whereas under the B6x129 background the mutants developed till E10.5 with a shortened trunk, suggesting the genetic background may modify the phenotype. A detailed characterization demonstrated that the $amn^{-/-}$ mutant mouse is unable to generate middle streak derivatives (Tomihara-Newberger et al., 1998). It was found that the T81 transgene fragment (~200 kb) inserted into intron 7 of the *Amn* gene, potentially abrogating expression of the gene product. Targeted mutation of *Amn* and complementation tests confirmed that *Amn* is the gene responsible for the amnionless phenotype in mice (Kalantry et al., 2001). Surprisingly, mutations in *AMN* cause a very different phenotype in humans. In 2003, *AMN* was discovered by positional cloning to harbor mutations in the I-GS patients from Norway and the Middle East. A 1 bp deletion in the 5th codon was found in 3 Norwegian families living in proximity, which apparently resulted in frame shift of the translation. In another Norwegian family, a missense mutation was identified in the 41st codon, which might affect the structure of the protein because it changed a polar amino acid to a nonpolar amino acid at an evolutionarily conserved site. The third mutation, identified in an Israeli family, was a splice site mutation that caused the total loss of exon 4 in the mRNA, which led to early translation termination (Tanner et al., 2003). Since then a total of six

different *AMN* mutations have been found in I-GS families from Norway, Turkey, Israel, United States, and Belgium. According to the distribution pattern of *AMN* and *CUBN* mutations, the relatively high frequency of I-GS in Scandinavian region is due to founder effects, while in the Mediterranean region consanguinity is the reason for rare mutations in both genes to be homozygous (Tanner et al., 2004). Retrospectively, the previous linkage of Norwegian I-GS families to *CUBN* (Aminoff et al., 1995) was probably coincidental and essentially false positive, given that the *AMN* mutations have been identified in the Norwegian families.

Gene, structure and functions

Human *AMN* (Locus ID: 81693 in Pubmed_locuslink) is located between *TRAF3* and *CD42BPB*, on chromosome 14q 32. The gene is 8.5 kb in length, with 12 exons. The mRNA (NM_030943, Pubmed) is about 1.8 kb, including a 22 bp 5'UTR and a 512 bp 3'UTR, encoding a 453 aa protein. The mRNA of human *AMN* is expressed mainly in small intestine, colon, and kidney (Tanner et al., 2003). *AMN* is predicted to have one transmembrane domain, which connects a ~360 aa extracellular domain and a ~70 aa intracellular domain. Amino acids from position 205 to 253 in the extracellular region of *AMN* constitute a cysteine-rich domain, which resembles some bone morphogenic protein (BMP) inhibitors such as chordin (Kalantry et al., 2001; Tanner et al., 2003). The postulated BMP binding motif of *AMN* appears to support that *AMN* may play a role in the mouse development.

Since both *AMN* and cubilin mutations can cause I-GS, it is tempting to think that the two proteins may have some interactions. This hypothesis led to the findings that

cubilin and AMN colocalize in the apical membrane of kidney proximal tubule cells and copurify during affinity purification (Fyfe et al., 2004). Denaturing and nondenaturing gel filtration chromatography suggested that the two proteins bind to each other with a high affinity. Cell-based studies showed that cubilin and AMN must act in concert to mediate the IF-Cbl endocytosis, while neither protein alone is able to internalize the ligand. Immunofluorescence and immunoelectron microscopy demonstrated that cubilin trafficks to the cell surface and endosomes in the presence of AMN, but not without. These data indicate that cubilin and AMN form a complex (*cubam*) in the endoplasmic reticulum or Golgi that is essential for surface expression and endocytic functions (Figure 1.3) (Fyfe et al., 2004).

The findings also help to solve an intriguing puzzle, that is, why cubilin as a receptor doesn't have a transmembrane domain or GPI anchor (Moestrup et al., 1998). It was postulated that cubilin might be anchored on the cell membrane by megalin, or less likely, cubilin might anchor itself on the membrane by its hydrophobic signal peptide (Moestrup et al., 1998). Although a helix structure similar to the membrane-insertion motif was indeed identified in cubilin by computer analysis (Kristiansen et al., 1999), it is now believed that cubilin is anchored by AMN, given the close relationship of the two proteins (Fyfe et al., 2004).

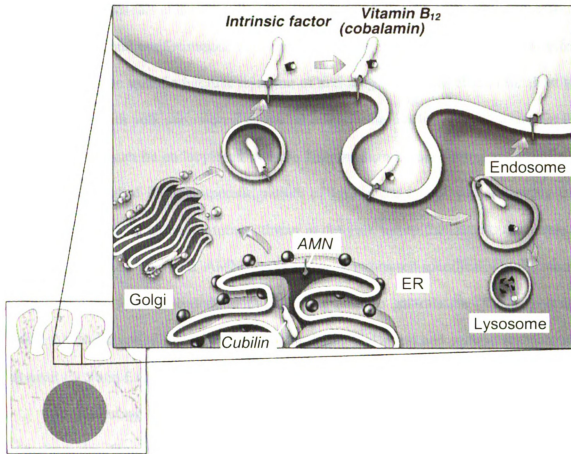


Figure 1.3 A model of AMN and cubilin assembly in the biosynthetic pathway and recycling in the endocytic apparatus of polarized epithelial cells. AMN is required for the folding, trafficking and membrane anchoring of cubilin. It may also mediate the internalization of the ligand and recycling of cubilin (from Fyfe et al., 2004).

Developmental role of cubam?

As mentioned earlier, cubilin is expressed on the epithelial cells of the rat yolk sac. When injected into rats at early pregnancy, anti-cubilin induced a high rate of embryonic resorption and fetal malformations in a dose-dependent manner. This teratogenic effect was deemed to be specific because injection of anti-megalin had no effect (Sahali et al., 1988). Tested with yolk sac visceral epithelial cells, biotin-labeled rat IgG present in the culture medium can be endocytosed into the lysosomes, whereas adding anti-cubilin to the medium resulted in an unspecific pattern of IgG in the cytoplasm, suggesting that cubilin is involved in an endocytotic pathway in the yolk sac epithelial cells (Le Panse et al., 1994). On the other hand, AMN was found to be expressed specifically in the mouse extra-embryonic visceral endoderm (VE) during embryo gastrulation (Kalantry et al., 2001). AMN disruption in mouse leads to developmental arrest and embryo reabsorption between E9.5 and E10.5 (Wang et al., 1996).

An interesting question is whether the two proteins play their roles independently in embryo development or function coordinately as cubam instead. It is unknown yet whether cubilin and AMN exist in the form of cubam in the rat yolk sac or mouse visceral endoderm. However, immunohistochemistry demonstrated that AMN and cubilin colocalized on the apical cell surface of the VE, while in *amn*^{-/-} mouse embryo cubilin failed to reach the cell surface (Strope et al., 2004), suggesting that cubam may exist on the VE apical membrane. If this is also the case in the rat yolk sac, the two similar phenotypes may be fundamentally related, that is, disruption of cubam causes the development defect.

The second intriguing question is whether the developmental defect is due to a general malnutrition problem or due to dysregulation of development signals. Cubilin can mediate the endocytosis of a wide range of plasma proteins, vitamins and lipids (Moestrup and Verroust, 2001), thus dysfunction of cubam may cause malnutrition to the embryo and subsequent development arrest. On the other hand, cubilin has 27 CUB domains (the name of CUB originated from complement subcomponents C1r/C1s, Uegf, and Bone morphogenic protein-1), and AMN has a cysteine-rich module similar to some BMP inhibitors. The structural features of cubilin and AMN suggest that cubam may be involved in the BMP pathway to regulate the embryo development. Since both growth of the embryo and assembly of the middle primitive streak were affected in *amn*^{-/-} mouse, Strope et al. (2004) proposed a unifying model, in which AMN/cubn-mediated endocytosis not only provides necessary nutrients, but also participates in important signaling pathways during embryo development.

Although it appears that cubam is crucial for the embryo development of rat and mouse, humans and dogs having mutations in either *CUBN* or *AMN* do not show any signs of embryo abnormality. The reason may be that cubam is redundant in humans and dogs for embryo development (Tanner et al., 2004). An alternative explanation is that different organizations of embryo-related tissues, as well as different mechanisms for nutrient absorption may have produced such a phenotypic difference in rodents versus human/dogs (Strope et al., 2004).

At this point, none of the three questions have definitive answers. Further investigations are needed to sort out all the possibilities proposed above.

Canine I-GS

Phenotype

Canine I-GS was identified as an autosomal recessive trait in a Giant Schnauzer (GS) family in 1980s. At the age of 2-3 months, the affected dogs became inappetent. Hematological tests demonstrated nonregenerative anemia, hypersegmented neutrophils and erythrocyte anisocytosis. Metabolic screening of the urine discovered extremely high methylmalonic acid (>4,000 mg MMA/g creatinine), suggesting vitamin B12 deficiency. Affected dogs had ~ 10-fold less vitamin B12 concentration in serum than normal dogs. Fecal excretion test of orally administered [^{57}Co]CN-Cbl suggested that affected dogs did not recycle the Cbl through the enterohepatic recirculation. Schilling test showed deficiency in intestinal vitamin B12 absorption, and mild proteinuria was observed. Parenteral, but not oral, vitamin B12 resulted in disappearance of megaloblastic anemia, MMA and other symptoms except for proteinuria. IF and TCII were excluded as the potential causes of the disease. These phenotypes were strikingly similar to the human I-GS. All the data strongly suggested the canine disease is a homologue of human I-GS (Fyfe et al., 1989; Fyfe et al., 1991a).

Comparison of B12 absorption in humans and dogs

Dogs have a mechanism for vitamin B12 absorption similar to humans. It was shown that both IF and IFCR are expressed in dogs (Hooper et al., 1973; Marcoullis et al., 1980). *In vivo* study in dogs with orally administered [^{57}Co]-Cbl demonstrated that Cbl is bound to IF and R protein in the gastric juice and bound to IFCR in the ileum,

indicating that dog also depends on IF-Cbl for B12 absorption (Marcoullis and Rothenberg, 1981).

On the other hand, physiological differences do exist between dogs and humans. In humans, most plasma Cbl is bound to TCI (Gullberg, 1972). In contrast, it is TCII that binds all the plasma Cbl in dogs (Rappazzo and Hall, 1972). Another difference is seen in the biogenesis of intrinsic factor. In human, IF is produced in gastric mucosa, whereas in dogs, the pancreas is the place where the IF is produced (Simpson et al., 1993). However, these physiological differences do not invalidate our statement that the dog family described herein is an animal model of the human I-GS, given that the defect concerned is located at the intestine.

IFCR study

Study of canine I-GS has provided many insights of IFCR (cubilin) and the disease. In immunohistochemical examination of ileal biopsies using a rabbit anti-dog IFCR, cubilin was present on the apical membrane and intracellular spaces of enterocytes in normal dogs, but was retained exclusively in the cytoplasm of enterocytes in affected dogs (Fyfe et al., 1991a). Determined by the $(\text{NH}_4)_2\text{SO}_4$ precipitation method using rat IF- ^{57}Co Cobalamin, the IFCR activity in the affected dog's brush border membrane (BBM) was significantly lower in ileum and renal cortex compared to normal dogs. Although IFCR was present in the homogenates of both ileum and kidney, it was sensitive to Endo H digestion. Endo H insensitivity usually indicates that the protein has completed the Golgi-mediated processing of glycosylation, while Endo H sensitivity suggests that the protein is still in high mannose state. Thus, canine I-GS is caused by

failed BBM expression of IFCR because it did not complete correct folding and glycosylation processing and was detained in an early biosynthetic compartment (Fyfe et al., 1991b; Xu and Fyfe, 2000). These studies provided the first functional evidence that cubilin might be the disease-causing gene, and well explained why both intestine and kidney are affected by the cubilin defect. They also established a solid ground to further explore the fundamental link between human I-GS and canine I-GS. In addition, the canine I-GS has been an invaluable animal model in studying the binding ligands of cubilin, such as apolipoprotein A-I receptor, albumin, transferrin, 25(OH)vitamin D3 and hemoglobin, as mentioned previously in this chapter.

Genetic study

CUBN has been shown to harbor mutations in human I-GS patients in Finland (Aminoff et al., 1999). Therefore, both biochemical and genetic evidences suggested that *CUBN* was a compelling candidate gene in canine I-GS. The canine cubilin cDNA was cloned from a renal tubule cDNA library, encoding a 3,620 aa protein. The protein shares more than 70% identity with human and rat cubilin. Similar to the human and rat cubilin, dog cubilin has a furin cleavage site, 27 CUB domains and 8 EGF domains (Xu et al., 1999). However, linkage study with a 17 bp intronic marker in the cubilin gene elegantly excluded *CUBN* or any gene close to the *CUBN* locus as the disease-causing gene (Xu et al., 1999). Similarly, another plausible candidate gene, megalin, was also ruled out (Xu, unpublished data). These data provided the first convincing evidence that a gene other than *CUBN* is associated with the I-GS, which was confirmed by a human study later in a Saudi Arabian family (Al-Alami et al., 2002). With the biochemical evidences, the canine

I-GS study also pointed out that the yet to be identified gene product functions as an accessory factor to assist the folding and delivery of cubilin to the cell surface.

Summary

Vitamin B12 (cobalamin) is an essential micronutrient for humans and other higher animals, and can be obtained only from the diet. Cobalamin (Cbl) has a highly specialized absorption mechanism, which includes the binding of Cbl with R proteins in the stomach, replacement of the R protein with the intrinsic factor in the intestine, recognition and endocytosis of the IF-Cbl complex by IFCR (cubilin) on the ileal enterocytes. With the IF degraded in the lysosomes, Cbl binds to TCII and is transported into the portal blood. The Cbl complex is recognized by TCII receptors expressed on target cells and endocytosed. Inside the cells, Cbl is processed into MeCbl and AdoCbl, which are cofactors for methionine synthase in cytoplasm and methylmalonyl-CoA mutase in the mitochondria. A defect in any of these steps may cause functional vitamin B12 deficiency, but the selective malabsorption of B12 in intestine due to the IFCR (cubilin) defect is named I-GS. Since cubilin also is expressed on the kidney proximal tubule cells, patients may have proteinuria as well. A canine model of I-GS, created by a natural mutation event, clinically and biochemically resembles the human I-GS. Study of the canine I-GS in the past twenty years has contributed significantly to the understanding of cubilin and the disease. The human I-GS is caused by mutations in either cubilin or AMN. Recent studies demonstrated that cubilin and AMN form a novel complex, called cubam, to endocytose vitamin B12 in the intestine. In our canine model,

although biochemical studies have pointed to the defect in cubilin, the *CUBN* gene was ruled out by genetic study, indicating that another gene may be the disease-causing gene.

Purpose and outline

When this project started in the year of 2000, the cubilin gene was the only known gene that harbored mutations responsible for I-GS. Based on biochemical and genetic studies, we hypothesized that an accessory factor mutated in the affected dogs is required for normal cubilin folding, exit from the ER, and/or transport to the brush border. Therefore, the goal of this thesis work was to map the disease locus, identify the disease-causing gene, and characterize the mutation(s). With the exclusion of cubilin and megalin genes and lack of other candidate genes, we initiated a whole genome scan linkage analysis, with the hope to positionally clone the gene responsible for canine I-GS. Chapter 2 describes the genetic mapping of the Giant Schnauzer family with I-GS to a region orthologous to human chromosome 14q. Chapter 3 includes cDNA cloning of the canine *AMN* and mutation screening in the *AMN* gene. Chapter 4 contains the linkage analysis and mutation identification of a second dog family (Australian Shepherd) with I-GS, which strengthens our finding in chapter 3. Finally, in chapter 5 we did functional analysis to characterize the mutations identified in the Giant Schnauzer and Australian Shepherd families.

CHAPTER 2

GENETIC MAPPING OF CANINE IMERSLUND-GRÄSBECK SYNDROME IN A GIANT SCHNAUZER FAMILY

Most of the studies described in this chapter have been published as (Canine Imerslund-Gräsbeck syndrome maps to a region orthologous to HSA14q) by (He Q, Fyfe JC, Schaffer AA, Kilkenney A, Werner P, Kirkness EF, Henthorn PS) in (Mamm Genome. 2003;14(11):758-64). Henthorn PS and Werner P did the genotyping with microsatellite markers. Kirkness EF provided some of the canine genomic sequences from The Institute for Genomic Research (TIGR). Schaffer AA did the computer-based linkage analysis. Kilkenney A did the genotyping with markers *STN2*, *EML* and *G2A*. I designed the strategy to locate the minimal candidates region, developed makers *EIF5*, *KNS2*, *SIVA* and did the genotyping with these three markers. I also did the haplotype analysis and data interpretation.

Introduction

Imerslund-Gräsbeck syndrome (I-GS) is an autosomal recessive disorder, originally identified in Norway and Finland, that is characterized by selective intestinal cobalamin (vitamin B12) malabsorption and proteinuria (Gräsbeck et al., 1960; Imerslund, 1960). Clinical features of the disease include megaloblastic dyshematopoiesis, neuropathy, methylmalonic acidemia and aciduria, and hyperhomocysteinemia. Severe cobalamin malabsorption can be life-threatening (Babior, 1975). Periodic parenteral, though not oral cobalamin administration restores normal metabolism and hematopoiesis, suggesting that the cellular B12 absorption mechanism is intact. Subsequent to the initial reports, I-GS has been reported in many countries all over the world, but highly concentrated in northern African and Middle Eastern families (Al-Alami et al., 2002; Altay et al., 1995; Ben-Bassat et al., 1969; Burman et al., 1985; Ismail et al., 1997; Mackenzie et al., 1972; Salameh et al., 1991).

People have known for a long time that intrinsic factor-Cobalamin (IF-Cbl) complex must bind to an ileal receptor, later called cubilin, before being absorbed. Cubilin is a multiligand receptor expressed in apical membranes of ileal enterocytes and renal proximal tubular epithelial cells. In the small intestine, cubilin mediates absorption of the intrinsic factor-cobalamin complex (Birn et al., 1997; Seetharam et al., 1997). In proximal tubules, cubilin physiologically mediates reabsorption of several proteins from glomerular filtrate, such as apoA1, albumin, transferrin, and vitamin D-binding protein (Birn et al., 2000; Kozyraki et al., 1999, 2001; Nykjaer et al., 2001). Thus, one gene product has two distinct functions in two different tissues. The cubilin gene (*CUBN*) cDNA was cloned and the gene was mapped to a 6-cM region on Chromosome 10p 12.1

(Kozyraki et al., 1998). This was intriguing because a previous positional cloning project localized the Finnish I-GS to almost the same region on Chr 10p (Aminoff et al., 1995), suggesting that the cubilin gene was the disease-causing gene for I-GS. Two *CUBN* mutations were indeed found in Finnish patients (Aminoff et al., 1999), providing an excellent example that combines biochemical studies with genetic studies to locate the mutated gene. Surprisingly, no *CUBN* mutations were found in the Norwegian or Saudi Arabian patients examined, suggesting that mutations of genes other than *CUBN* also underlie I-GS (Aminoff et al., 1999; Kristiansen et al., 2000). Locus heterogeneity in I-GS was confirmed when the *CUBN* region was excluded by linkage analysis in a Saudi Arabian I-GS family (Al-Alami et al., 2002) and recently with the demonstration of mutations of the amnionless gene (*AMN*) in I-GS patients from Norwegian and Israeli families (Tanner et al., 2003).

Locus heterogeneity in I-GS had previously been supported by findings in a canine model of I-GS. Canine I-GS is an autosomal recessive disorder characterized by juvenile onset of failure to thrive owing to selective intestinal cobalamin malabsorption with mild proteinuria, resembling the human I-GS (Fyfe et al., 1991a). Immunocytochemical and cell fractionation studies of intestinal mucosa and renal cortex demonstrated that, although cubilin has a normal affinity to IF-Cbl in affected dogs, the receptor did not fold properly and was not trafficked to the apical plasma membrane (Fyfe et al., 1991a, 1991b; Xu and Fyfe, 2000). Cubilin, as well as two cubilin-interacting proteins, megalin (LRP2) and receptor-associated protein (RAP), were considered as candidate genes for canine I-GS, but each was excluded by linkage analysis (Xu et al., 1999; unpublished data).

To determine the gene underlying canine I-GS, we undertook a whole-genome scan for genetic linkage in the canine I-GS pedigree. Here, we demonstrate linkage of canine I-GS to markers on canine Chr 8 (CFA8) in a region that is orthologous to human Chr 14q32.2-ter in an interval that contains the *AMN* gene.

Materials and methods

Animals

All dogs were handled according to the principles outlined in the NIH Guide for the Care and Use of Laboratory Animals, with protocols approved by the MSU All University Committee for Animal Use and Care. All dogs were members of a large outbred family in which canine I-GS segregates as a fully penetrant, simple autosomal recessive trait. The I-GS disease phenotype of each dog was determined by monitoring puppies for growth and laboratory abnormalities previously described (Fyfe et al., 1991a) until 12–16 weeks of age and for 3–4 weeks after parenteral cobalamin administration. DNA was available from 128 dogs of known I-GS phenotype. The relationships of these dogs are depicted in the pedigree in Figure 2.1. Blood or tissue samples were stored frozen at –80°C for DNA isolation. The DNA of F100 was initially unavailable but was obtained later for the genotyping with the *KNS2* marker.

Markers and genotyping

DNA was isolated by standard methods (Sambrook et al., 1989). Microsatellite markers for the whole-genome scan, primers, and PCR conditions were those recommended by Richman et al. (2001). Primers and PCR conditions for marker COS8 were from Werner et al. (1999). Fluorescently labeled PCR products were electrophoresed on an ABI Prism 377 Sequencer (Applied Biosystems). Allele sizes and genotypes were determined by using GeneScan® and Genotyper® software (Applied Biosystems).

Based on previous evidence of conserved gene content and order with the distal long arm of human Chr 14 (HSA14q), single nucleotide polymorphisms (SNPs) were sought within genes predicted to reside on distal CFA8. SNPs were developed in the canine orthologues of stonin2 (*STN2*) (Martina et al., 2001), echinoderm microtubule associated protein-like 1 (*EML1*) (Eudy et al., 1997), G protein-couple receptor 2A (*G2A*) (Weng et al., 1998), *EIF5* (Si et al., 1996), and *SIVA* (Prasad et al., 1997). Canine gene sequences were obtained from a database of canine genomic sequence maintained by The Institute for Genomic Research (TIGR). Sequence data were originally obtained from plasmid libraries of small (2 kb) and medium-sized (10 kb) genomic DNA inserts prepared and sequenced at Celera Genomics, as described previously for the human genome (Venter et al., 2001). The finished sequence data consist of 6.2 million reads (average read length, 576 bases), representing approximately 1.2× coverage of the haploid canine genome whose size is estimated at 2.8 Gb (Vinogradov, 1998).

To identify dog sequences for genes of positional interest, we used a three-step procedure. First, human genomic sequences were masked for repetitive elements and searched against the assembled canine genomic sequences by using BLASTN (<http://www.ncbi.nlm.nih.gov/BLAST/>). Second, dog sequences with the highest BLASTN scores were searched back against the current human genome sequence. Third, the matches were evaluated, and dog sequences that were most similar to the human gene originally used for searching were considered to be fragments of a putative orthologue. This procedure can effectively avoid unspecific assignment due to partial homology. Primers for PCR were chosen from exons that flank introns of moderate predicted size.

SNPs were identified by sequencing PCR products amplified from an affected (Hilary i.e. F284) and a carrier (Shorty i.e. F274) dog.

STN2 primers were (JCF236) 5'-AGGTGCAGAGCTGGCTTAGGATGT-3' and (JCF249) 5'-GAGTTGAAGGCATGCTCGTACTTG-3'. The *STN2* SNP altered a *BsII* restriction enzyme recognition site. PCR products were digested with *BsII* (New England Biolab), and DNA fragments were separated on 3% agarose gels.

EML1 primers were (JCF285) 5'-CCTGTAAGCAA GTCGTAAGTGTGG-3' and (JCF286) 5'-GTCTGGCACAA CCTCCTATG-3', and the SNP was detected by *AluI* (New England Biolab) digestion.

G2A primers were (JCF230) 5'-GCCGTCTACCTCTTCTGCCTGTC-3' and (JCF254) 5'-GCTAGGAAGCGGTCACAGGAGAT-3', and the SNP was detected by *TatI* (Fermentas Life Science) digestion.

KNS2 primers were (JCF294) 5'- GAG CCT CTG GAT GAC CTT TTC-3' and (JCF295) 5'- CAC TGC TAT GCT GCT GTT GGA CT-3'.

PCR reactions (50ul): genomic DNA 200ng, 5ul of each primers (2.5pmol/ul), 5ul 10xbuffer, 5ul dNTP (2.5pmol/ul each), 0.5ul Taq polymerase (5U/ul) and 25.5ul H₂O.

PCR cycles: 94°C 3min; 94°C 30', 58°C 30', 72°C 1min for 35cycles; 72°C 10min.

For genotyping, the *KNS2* PCR products were run on the 1% agarose gel, then purified by QIAEX[®] II Gel Extraction Kit (Qiagen, Cat. No. 20021) and sequenced at the University of Michigan DNA Sequencing Core.

EIF5 primers were (JCF298) 5'-GGC GCC ATT TCC TAC GAG-3' and (JCF299) 5'-CTC TGC TTC CTT CAA CCA TTT TAT-3'. The *EIF5* PCR products were gel purified and sequenced.

SIVA primers were (JCF311) 5'-GCT GTG CCA TTG TTG ACC TGC C-3' and (JCF312) 5'-GCT CTG GTC ACT GTC CCG GAG-3'. The SNP was detected by *ScaI* (New England Biolab) digestion or by direct sequencing.

Linkage analysis

Linkage analysis computations were performed with the FASTLINK software package (Cottingham et al., 1993; Lathrop et al., 1984; Schäffer et al., 1994). Loop breakers were chosen by the method of Becker et al. (1998), as implemented in FASTLINK 4.1P. This method is particularly helpful for inbred pedigrees with numerous multiple matings, because it allows a multiply mated loop breaker to break more than one loop. One hundred twenty-eight dogs of the I-GS pedigree were genotyped at one or more CFA8 markers. Omission of dogs from particular marker data sets was because either 1) PCR failed for certain dog/marker pairs, 2) the genotype could be inferred from first-degree relatives, or 3) it became evident that the markers on the proximal portion of CFA8 were not close to the disease gene. LOD scores were calculated with assumptions

of a disease allele frequency of 0.001, full penetrance of the disease trait, and equal marker allele frequencies. The order of microsatellite markers was based on canine linkage maps (Mellersh et al., 2000; Werner et al., 1999), and the order of the three genes, *STN2–EML1–G2A*, was based on their order in the orthologous portion of HSA14. The marker order used here is consistent with the most recently published canine radiation hybrid map (Guyon et al., 2003). Multipoint analysis indicates that the *STN2* gene is most likely between FH2144 and FH2138 on CFA8 but might also be between FH2138 and C08.618. Attempts to use multipoint linkage analysis to place the COS8 marker with respect to *EML1* and *G2A* yielded very flat LOD score curves, indicating that COS8 is close to both *EML* and *G2A*. To confirm that the LOD scores we report are qualitatively robust, we repeated the analyses by using a disease allele frequency of 0.01, penetrance of 0.99, and marker allele frequencies estimated from the data. The latter calculations resulted in nearly identical positive LOD scores.

Results

A whole-genome scan for marker linkage was initiated in the canine I-GS pedigree with DNA from 88 dogs of known I-GS phenotype. The scan was abbreviated when a LOD score >5 was obtained for marker C08.618 examined early in the process. While the high LOD score gave confidence that the I-GS phenotype was linked to CFA8, the peak LOD score was achieved ~10 centiMorgan away from the disease locus. Therefore, we proceeded to genotype other microsatellites from CFA8 and included additional dogs.

We also identified polymorphisms (SNPs) in genes predicted from human-dog comparative mapping to be in the region of interest (Breen et al., 2001). Reciprocal chromosome painting studies demonstrated previously that the entirety of CFA8 is homologous to the entire long arm of HSA14 (Breen et al., 1999; Sargan et al., 2000). Higher resolution conservation of gene order between CFA8 and HSA14q was demonstrated by comparison of loci placed on the most recent canine integrated RH/genetic linkage map (Breen et al., 2001) and Build 30 of the human genome sequence as displayed on the UCSC Genome Bioinformatics website (<http://genome.cse.ucsc.edu/index.html>). One or more SNP markers were genotyped on most of the dogs depicted in Figure 2.1.

Two-point linkage analysis was performed between the I-GS locus and 9 CFA8 markers, including six microsatellites (FH2149, C08.410, FH2144, FH2138, C08.618, COS8) and three SNPs (in genes *STN2*, *EML1*, and *G2A*). This type of analysis considered the relationship between the disease locus and one of the 9 markers at each time. The results are shown in Table 1. Partial analysis of those genotypes indicated that the I-GS locus should be on the distal side of C08.618, where only one other polymorphic

Figure 2.1 Pedigree of dogs of known I-GS status used for linkage analysis. All dogs were derived from two affected purebred Giant Schnauzers (F70 and F100) and three unrelated normal dogs of other breeds (A66, A323, and M874). Dogs F70 and F100 were both inbred (inbreeding coefficients of 0.133 and 0.25 respectively) and related (the sire of F100 is a great grandsire of F70). Squares indicate males, and circles indicate females. Filled symbols indicate I-GS affected dogs, and open symbols indicate clinically normal dogs. Vertical lines descending from the symbol for an animal indicate one or more matings, offspring of which are arranged on horizontal lines connecting the parents. Numbers within symbols indicate the number of dogs of the indicated gender and phenotype that were available for analysis when there was more than one from the depicted mating.

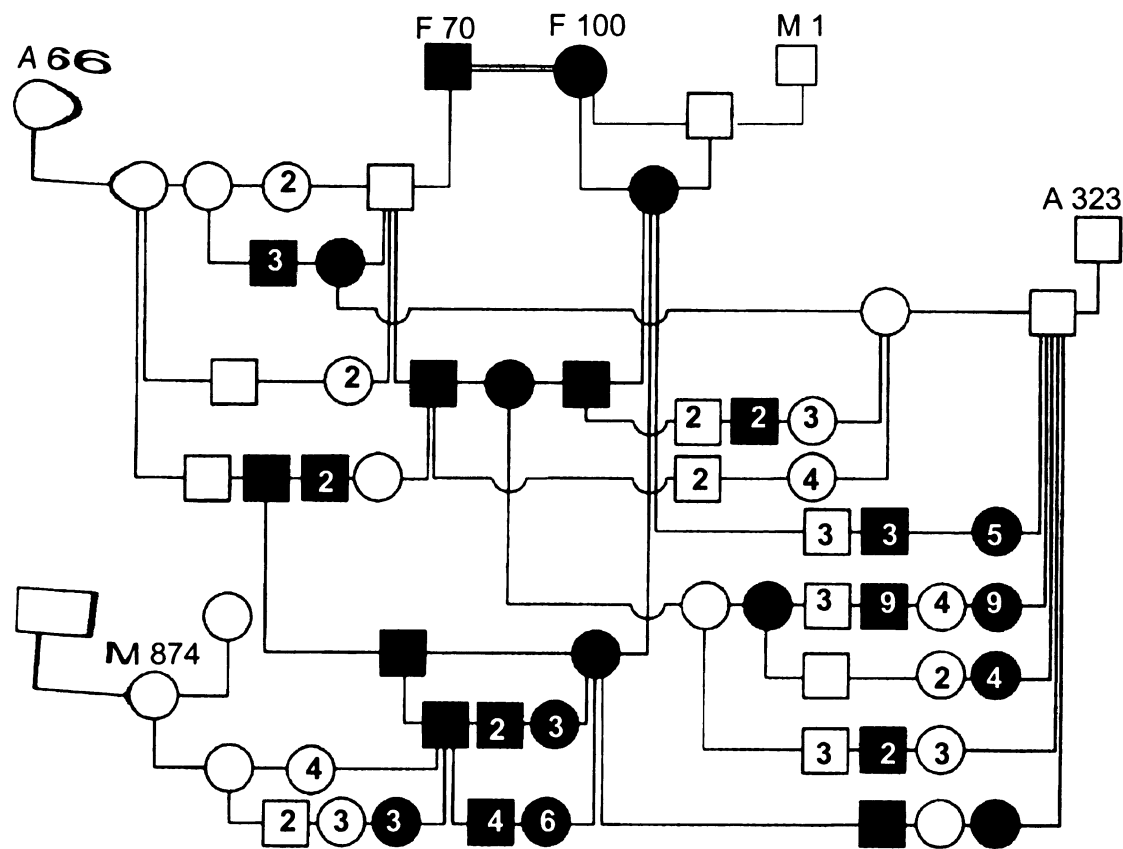


Figure 2.1

Table 1. Two-Point LOD score analysis. Two-point LOD score (Z) values at various recombination fractions (θ) with respect to the canine I-GS locus.

Marker	0.0	0.01	0.03	0.05	0.07	0.10	0.15	Peak LOD	θ of peak
FH2149		-30.49	-19.37	-14.33	-11.20	-8.00	-4.66	0.34	0.416
C08.410		-20.29	-12.02	-8.36	-6.07	-3.79	-1.51	1.05	0.344
FH2144		-17.63	-9.44	-5.86	-3.65	-1.51	0.55	2.26	0.293
STN2		-2.95	1.80	3.73	4.83	5.75	6.32	6.36	0.169
FH2138		0.98	3.86	4.99	5.59	6.03	6.15	6.17	0.135
C08.618		3.65	6.00	6.87	7.29	7.52	7.38	7.54	0.110
EML1		7.60	8.56	8.79	8.79	8.58	7.97	8.81	0.059
COS8	3.31	3.84	4.07	4.11	4.08	3.97	3.68	4.11	0.048
G2A		10.02	10.51	10.52	10.38	10.03	9.24	10.55	0.041

marker, COS8, was initially available (Mellersh et al., 2000). The COS8 marker is near both *EML1* and *G2A*, but attempts to more precisely determine its position were unsuccessful owing to limited informativeness of this marker in the I-GS pedigree and lack of obligate recombinants. We provisionally placed COS8 between *EML1* and *G2A* because this appeared marginally more likely than either extreme placement.

We obtained peak LOD scores for the three most distal microsatellite markers (FH2138, C08.618, and COS8) and the SNPs in *STN2*, *EML1*, and *G2A* that were well above the standard threshold of 3.3 used to declare significant linkage in whole-genome scans (Lander and Kruglyak, 1995), with the score for *G2A* exceeding 10. Peak LOD scores for the six linked markers varied significantly owing to varying informativeness in this pedigree. Therefore, the recombination fraction where the peak LOD score is achieved for each marker, and not the value of that peak, is the most important criterion to consider. By that criterion, *EML1*, COS8, and *G2A* are the markers closest to the gene, since their peak LOD scores occur at recombination fractions of ~ 0.05 or less. The LOD score with COS8 at a recombination fraction of 0 is positive (and not $-\infty$), indicating that there are no obligate recombinants between the disease and COS8 within the pedigree. However, the LOD score with COS8 does not peak at a recombination fraction of 0 because there are two distinct COS8 alleles closely linked to different haplotypes that entered the pedigree separately through dogs F70 and F100.

Using the ILINK program in FASTLINK, we estimated that the recombination fraction between *EML1* and *G2A* was ~ 0.075 . Using that estimate and the LINKMAP program, we generated the multipoint LOD score values plotted in Figure 2.2. The peak LOD score of 11.74 occurs with the I-GS locus placed slightly nearer to *G2A* than

midway between the two markers. The maximum LOD score with the disease gene placed proximal to *EML1* was only 9.8, making it much less likely that the gene is proximal to *EML1*. The maximum LOD score generated with the I-GS locus placed distal to *G2A* was 11.07, obtained when the putative disease gene was placed approximately 4 cM from *G2A*. The 0.6 lower LOD score suggested that this location for the I-GS gene is less likely than the location proximal to *G2A*. The disease gene location between *EML1* and *G2A* was further supported by examination of haplotypes, as illustrated in Figure 2.3. Recombination events and disease status in the dogs shown are most parsimoniously explained by the gene order *EML1*–*I-GS*–*G2A*. In order to further narrow down the disease region, we developed 3 more markers (*KNS2*, *EIF5* and *SIVA*) between *EML1* and *G2A* using an iterative strategy (shown in Figure 2.4). Compared to randomly developing new markers, our strategy is more efficient. We subjected the 3 markers to genotyping (Table 4 in Appendices). Haplotype analysis showed that the minimal candidate region was between *EML1* and *SIVA* (Figure 2.3).

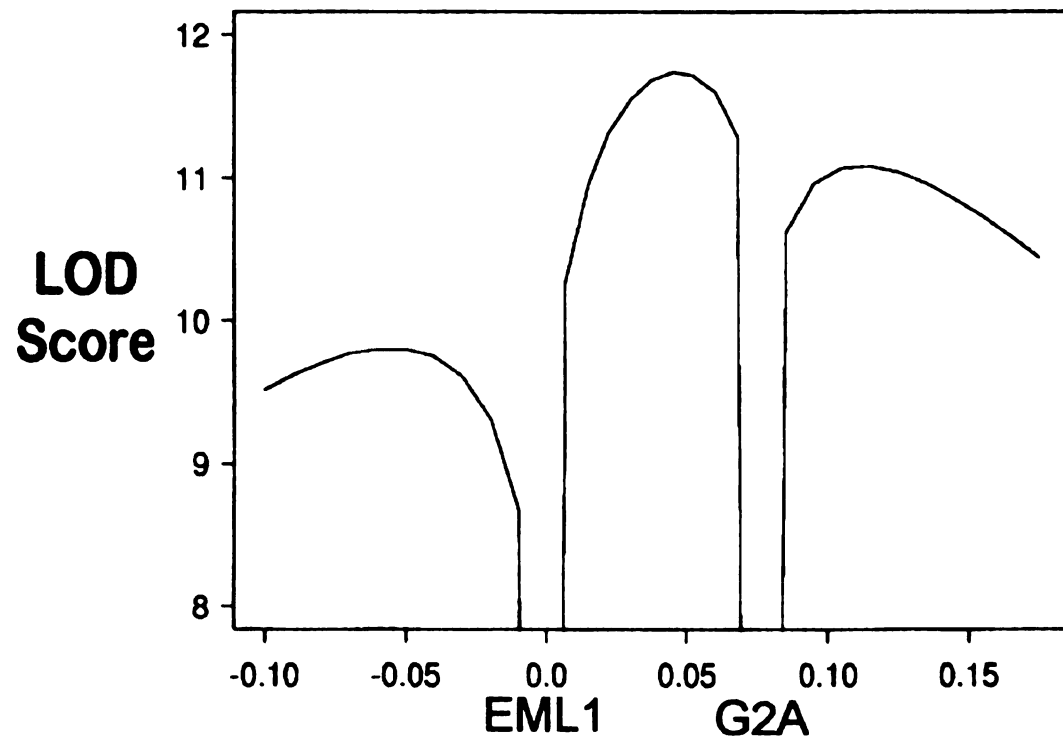


Figure 2.2 Multipoint LOD score curve showing linkage to I-GS. The X-axis shows distance in centiMorgans with respect to the *EML1* marker.

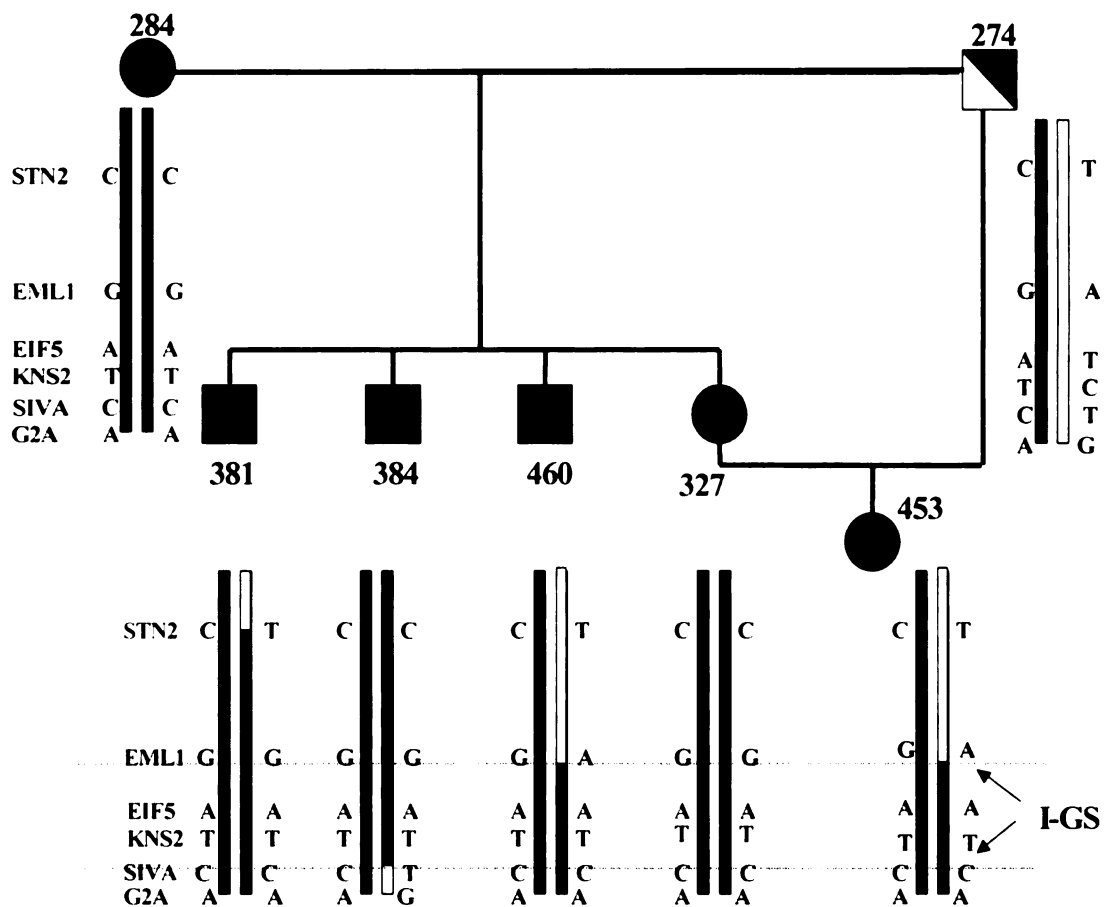


Figure 2.3 Haplotype analysis of the GS kindred. The white bar represents the normal allele, while the black bar represents the disease allele. The minimal candidate region for canine I-GS is between *EML1* and *SIVA*.

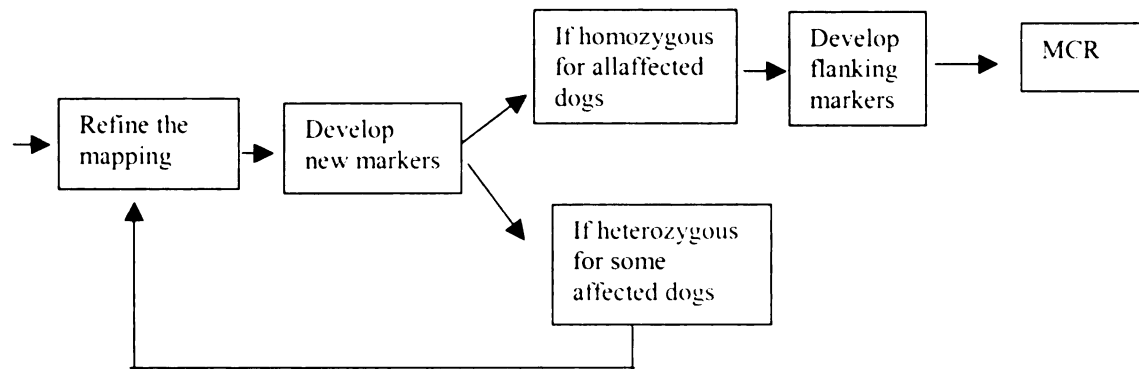


Figure 2.4 An iterative strategy to develop new markers for linkage disequilibrium mapping. MCR represents minimal candidate region.

In order to further minimize the candidate interval already delimited by *EML1* and *G2A*, we first transformed the genetic distances of *EML1* and *G2A* versus *I-GS* into physical distances to locate the *I-GS*. At the *I-GS* position, we would develop a new marker.

I. If the new marker were homozygous in all the affected dogs and heterozygous for all the carriers, we would develop more markers flanking this marker, until we found the nearest heterozygous marker in affected dogs. This minimal homozygous interval would be assigned as the minimal candidate region (MCR).

II. If the new marker were heterozygous for some affected dogs, we would calculate the recombination score or do haplotype analysis to assign the disease gene into one of the smaller intervals divided by the marker. Then, in this smaller interval, we would repeat the process of developing new markers until we defined the minimal candidate region.

Discussion

Results of this investigation indicate that the genetic locus of canine I-GS is on distal CFA8, a canine chromosome that is orthologous to HSA14q. This finding was consistent with our previous report that canine I-GS was not linked to *CUBN* (Xu et al., 1999) and that canine *CUBN* is located on canine Chr 2 (Breen et al., 2001). We obtained compelling LOD scores of >10 for the CFA8 location by using a large canine pedigree specifically bred for investigation of I-GS. Based on the multipoint LOD scores, the disease gene locus is distal to a marker in *EML1*, and examination of haplotypes suggests that it is proximal to a marker in *SIVA*. Within the interval between *EML1* and *SIVA*, the *KNS2* marker was in complete linkage disequilibrium with the disease allele in 20 affected dogs, 11 obligate heterozygous carriers, and 1 unrelated normal dog used for an outcross mating in the I-GS linkage family. The multipoint LOD for canine *I-GS*, *KNS2*, and *G2A*, peaked at 15.4 with θ at 0.0 between *I-GS* and *KNS2*, indicating that the disease-causing gene is very close to *KNS2*. The estimated θ between *KNS2* and *G2A* is 0.05. No recombinants were found for marker *EIF5*. However, it's not possible to accurately deduce the genetic distance between *EIF* and *I-GS* because the number of animals genotyped with *EIF5* is too small.

All genes currently mapped to CFA8, including those reported here, are in the same order as on HSA14q (Breen et al., 2001; Guyon et al., 2003). The *AMN* gene, reported to be mutated in some I-GS patients while this article was in review (Tanner et al., 2003), resides in the 5-Mb interval between *EML1* and *SIVA* in the human genome (Build 30, UCSC Genome Browser <http://genome.ucsc.edu/>).

Prior to this discovery, there had been no previous suggestion that a gene on HSA14q had a role in cobalamin metabolism. Thus, it seems highly probable that the I-GS dogs also have a mutation in the *AMN* gene. One would expect a single homozygous mutation in the affected dogs. Indeed, we hope to use the canine model to clarify the tissues and stages of development at which it is expressed.

The eventual determination of the gene and mutation causing canine I-GS will yield new biological insights, whether the disease gene is *AMN* or not. *AMN* was discovered as the gene disrupted by an insertional mutagenesis event in mouse that caused a recessive prenatal lethal phenotype (Kalantry et al., 2001; Tomihara-Newberger et al., 1998; Wang et al., 1996). Affected mice die at around day 10 of gestation, having failed to develop a portion of the primitive streak during gastrulation. The *AMN* gene encodes a predicted type I transmembrane protein, with an N-terminal signal peptide and a single transmembrane domain that is found on the apical surface of visceral endoderm cells early in development (Kalantry et al., 2001). At this time, essentially nothing is known about the proteins or pathways with which the *AMN* gene product interacts during early embryonic development. The involvement of the *AMN* gene in both early mouse development and in the selective malabsorption of cobalamin in otherwise normal humans was unexpected. A proposed explanation for this phenomenon is that the function of AMN in human and murine embryonic development may differ significantly. Additional work is needed to test this and other hypotheses concerning functions of the *AMN* gene.

Examination of the *AMN* gene in canine I-GS affected dogs combined with the worldwide effort to annotate genes in all species will allow the determination of the gene

involved in canine selective cobalamin malabsorption with proteinuria. Immunocytochemical and cell fractionation studies of canine intestinal mucosa and renal cortex have already demonstrated that, while cubilin is expressed in the appropriate tissues of I-GS affected dogs, the receptor does not fold properly and is not trafficked to the apical membrane (Fyfe et al., 1991a, 1991b; Xu and Fyfe, 2000). The involvement of AMN in this pathology, whether or not it is defective in the affected dogs, can now be examined as the canine I-GS model continues to provide a valuable resource for the development of our understanding of cobalamin metabolism.

CHAPTER 3

cDNA CLONING OF CANINE *AMN* AND MUTATION SCREENING IN THE GIANT SCHNAUZER FAMILY

I designed and performed all the experiments described in this chapter except that Gregory B provided some technical assistance in the genotyping of the unrelated normal dogs.

Introduction

In the previous chapter, we mapped the canine I-GS to an interval between marker *EML1* and *SIVA*, which is syntenic in human, mouse and dog. Referring to the human genome map (<http://genome.uscs.edu/>; build 31), the interval is about 5 Mb in length, containing at least 40 genes (Table 2). *KNS2*, a single nucleotide polymorphism (SNP) marker in the 5 Mb interval, is in complete linkage disequilibrium with the disease allele in our GS kindred. The multipoint LOD score for *KNS2* is 15.4, indicating that the disease-causing gene is very close to this marker. Genes ~ 1 Mb on either side of *KNS2* in the human and mouse genome databases were considered comparative positional-candidate genes and were further triaged by examining EST databases for genes expressed in the known cubilin expressing tissues. *AMN* stood out in this analysis with a vast preponderance of ESTs from kidney and lesser representation in intestine and colon (UniGene Cluster Hs.236720, since retired and replaced by Hs.534494). During the course of this work, three different *AMN* mutations were demonstrated in human I-GS kindreds from Norway and Middle East (Tanner et al., 2003). Combined with the study of human patients, our data highly suggest that *AMN* is also the disease-causing gene for canine I-GS.

AMN gene was originally identified as an essential gene for mouse gastrulation. The gene encodes a transmembrane protein exclusively expressed on the visceral-endoderm of mouse embryo. *AMN* has an extracellular cysteine-rich domain, which resembles several bone morphogenic protein (BMP) inhibitors (Kalantry et al., 2001). Since the *amn*^{-/-} mouse was embryonic lethal, it is not known whether *AMN* defect also causes B12 malabsorption and proteinuria in the mouse. Human (NCBI Nucleotide

accession no. NM_030943), mouse (accession no. BC087954) and rat (accession no. XM_234547) *cAMN* have been cloned, each with 1362 bp, 1377 bp, 1377 bp in length, respectively. The GC content of the three *cAMN* is between 65%~ 71%. Protein alignment of the three gene products suggests that the N-terminal part is evolutionarily more conserved than the C-terminal part. At this point, no sequence information was available for dog *AMN*. In order to screen the canine *AMN* gene for potential mutations, we first cloned the cDNA of canine *AMN* from a cDNA library constructed from dog kidney proximal tubule cells. RT-PCR and genomic PCR in both affected dogs and normal dogs were subsequently performed to locate the mutation in the *AMN* gene.

Table 2. Genes listed in the *EML1-SIVA* interval of human genome browser.

The Human EST hits data were retrieved from the NCBI_Unigene_homo sapiens database (<http://www.ncbi.nlm.nih.gov/entrez/query.fcgi?db=unigene>). Genes that have higher expression in kidney and colon are highlighted.

Locus Name	Position	Human EST hits	Function
<i>SIVA</i>	99.21	kidney 2; colon 3	CD27 binding protein1
<i>FLJ38602</i>	99.18		
<i>FLJ22056</i>	99.16	kidney 3; colon 1	
<i>MGC13251</i>	99.14	kidney 0; colon 0	hypothetic
<i>C14orf2</i>	98.19	kidney 5; colon 0	6.8 kDa mitochondrial proteolipid
<i>PPP1R13B</i>	98.01	kidney 2; colon 2	protein phosphatase regulatory subunit
<i>MGC2550</i>	97.99	kidney 4; colon 0	
<i>XRCC3</i>	97.98	kidney 0; colon 0	Xray repair cross complementing protein 3
<i>KNS2</i>	97.91	kidney 0; colon 1	kinesin 2
<i>MGC2562</i>	97.84	kidney 0; colon 1	
<i>BAG5</i>	97.83	kidney 2; colon 1	Bcl2 associated athanogene 5
<i>FLJ40452</i>	97.81		
<i>CKB</i>	97.8	kidney 4; colon 20	creatine kinase, brain
<i>MARK3</i>	97.66	kidney 3; colon 1	MAP/microtubule affinity regulating kinase3
<i>EIF5</i>	97.61	Kidney 12; colon 1	Eukaryotic translation initiation factor 5
<i>TNFAIP2</i>	97.41	kidney 2 ; colon 0	protein 2 induced by TNFalpha
<i>CDC42BPB</i>	97.21	kidney 4 ; colon 0	CDC42 binding protein kinase beta
<i>AMN</i>	97.2	Kidney 106; colon 7	amniotless protein
<i>TRAF3</i>	97.06	kidney 2; colon 1	TNF receptor-associated factor 3
<i>RCOR</i>	96.87	kidney 1; colon 0	REST-corepressor
<i>MGC21990</i>	96.79		
<i>KIAA0071</i>			
<i>KIAA0329</i>	96.64	kidney 5; colon 3	
<i>CINP</i>	96.63	kidney 1; colon 1	HeLa cyclin dependent kinase 2-interacting protein
<i>FLJ11132</i>	96.61	kidney 6; colon 1	hypothetic
<i>RAGE</i>	96.51	kidney 2; colon 1	renal tumor antigen mapkinase super family
<i>WDR20</i>	96.42		WD repeat protein
<i>HSPCA</i>	96.36	Kidney 49; colon 35	heat shock 90 kDa protein 1, alpha
<i>PPP2R5C</i>	96.09		protein phosphatase 2, regulatory subunitB
<i>DHC1</i>		kidney 15; colon 6	dynein heavy chain cytosolic
<i>DIO3</i>	95.84		thyroxine deiodinase 3
<i>LOC64150</i>	95.83		

Table 2 (cont'd)

<i>DLK1</i>	95.01		delta-like homologue
<i>KIAA1446</i>	94.81		
<i>MGC4645</i>	94.66		
<i>WARS</i>	94.61		Tryptophanyl tRNA synthetase
<i>FLJ38975</i>	94.57		
<i>LOC145604</i>			similar to adaptor-related protein complex 1
<i>Novel</i>			?mitochondrial uncoupling protein
<i>novel</i>			?solute carrier family 25? Ensembl140109
<i>YY1</i>	94.52		YY1 transcription factor
<i>FLJ32960</i>			unknown, alternatively spliced
<i>novel</i>			?degenerative spermatocyte?
<i>RNB6</i>	94.34	kidney 0; colon 0	?actin filament organization neurons?
<i>EML1</i>	94.07	kidney 3; colon 1	echinoderm microtubule associated protein

Materials and methods

Obtaining partial sequence of canine cAMN

Human, mouse, rat *AMN* cDNA sequences were aligned by the MultAlin software (<http://prodes.toulouse.inra.fr/multalin/multalin.html>). Three sets of primers were designed based on the homologous sequences of the three species.

Set 1: JCF321 5'-TSC TGC TGT GGC TGC AGC TCT G-3'

JCF322 5'-CCT TGT CCG CCG GGA ACT GRA C-3'

Set2: JCF323 5'-TCT TCT YCG TGG ACG CCG AGC G-3'

JCF325 5'-GGT CCT CGT CGC GCG WGA ACG T-3'

Set 3: JCF324 5'-ACG TTC WCG CGC GAC GAG GAC C-3'

JCF326 5'-CGG TAC CGC TCC AGG TCA ATT G-3'

Total RNA was extracted from an unaffected dog by Trizol[®] Reagent (Invitrogen). 5 μ g RNA was used to perform the RT reactions (SuperScript[™] First-Strand Synthesis System for RT-PCR, Invitrogen), with Oligo(dT) 12-18mer (Invitrogen). RT-PCR was performed with the three sets of primers shown above, respectively.

PCR conditions:

RT product	2 ul
Primer1	5 ul (2.5 pmol/ul)
Primer2	5 ul (2.5 pmol/ul)
10xPCR buffer without Mg ²⁺	5 ul
25mM MgCl ₂	6 ul
DMSO	2.5 ul
dNTP	5 ul (2.5 pmol/ul each)
AmpliTaq Gold [™] (Roche)	0.5 ul
H ₂ O	19 ul
Total	50 ul

PCR cycles: 95°C 10 min; 95°C 15', 62°C 15', 72°C 1 min for 35cycles; 72°C 5 min.

The PCR product was gel purified and sequenced.

cDNA cloning of canine *AMN*

The primers JCF323 and JCF325 were used for the cDNA cloning of canine *AMN* from a ZAPII™ phage cDNA library (Stratagene) constructed from a pool of dog kidney proximal tubule cell RNA. The PCR with JCF323 and JCF325 was referred to “indicator PCR” in the following steps. The cDNA cloning method was based on a pool-PCR strategy, which was designed to quickly and efficiently clone the target cDNA (Israel, 1993).

Preparing host cells: A single colony of XL1-Blue MRF cultured on a plate (Tetracycline 12.5 ug/ml) was inoculated into 20 ml LB plus 0.2 ml 20% maltose without antibiotics. After culturing at 33°C overnight, the bacteria were harvested by centrifugation at 3,200 rpm for 8 min. The pellet was resuspended in 20 ml 10 mM MgSO₄. 7 ml of the bacteria was transferred to a new tube and centrifuged briefly, with 6.9 ml of the supernatant removed. The pellet was suspended by the residual 0.1 ml MgSO₄.

Infection: The cDNA library was titered as described in the Molecular Cloning: A Laboratory Manual, 2nd ed. (Sambrook et al., 1989; section 2.60-2.61). 5ul of the cDNA library (3×10^7 phages) was diluted into 95 ul SMG buffer (50 mM Tris-Cl, 100 mM NaCl, 10 mM MgSO₄, 0.01% gelatin), and then mixed with the host cells. The mix was incubated at 37°C for 20 min. The mix was diluted into 20 ml LB containing 10 mM MgSO₄, and distributed into 64 wells (100ul/wellx 64wells). Thus only 1×10^7 phages

were actually screened. The wells were sealed by GeNunc Tape (NUNC #BC2689) and incubated at 37°C for 18 hrs with shaking (215 rpm).

Pooling, lysis and PCR: 15 ul of phage culture from each well of the 8x8 matrix was pipetted. 120 ul of phage culture from each row/column was pooled (15 ul x 8=120ul), resulting in 16 pools. 50 ul culture was taken from each pool, and then subjected to 50 ul 100 mM NaOH at 95°C for 10 min, respectively. 20 ul of 1 M Tris-Cl (pH7.4) was used to neutralize each reaction. Finally, 2 ul of the solution in each tube was used as template in the indicator PCR.

Analysis and rescreening: The PCR products were run on 1% agarose gel. A single well that contained the *AMN* clone was identified by the synthesis of a PCR product at the right size. The positive well was titered and diluted. About 1920 phages were used to infect a new 8x8 matrix of host cells, with each well containing 30 phages. The matrix was rescreened by the protocol shown above. A positive well was identified and subjected to the tertiary screening, with each well containing 2 phages before the culture. As a positive well was located, the phages in that well were plated and screened by the indicator PCR one by one. Finally, The target cDNA was PCR amplified with primers T3 and T7 from the positive phage clone or rescued by helper phage into pBluescript plasmid. The PCR product or plasmid was sequenced.

Full length RT-PCR of canine c*AMN*

Primers: JCF334 5'-CGG GCG CGC GGC GGG ATG-3'

JCF332 5'-CTG GCC AGC CCC GCG GTT GC-3'

Total RNA were extracted from an affected dog (F284) and an unrelated normal dog (DCCU6110) by Trizol[®] Reagent. RT reactions were performed with SuperScript[™] First-Strand Synthesis System. The Advantage-GC2 PCR kit (BD BioSciences) was used for the PCR.

PCR conditions:

RT product	2 ul
JCF334	8 ul (2.5 pmol/ul)
JCF332	8 ul (2.5 pmol/ul)
5xPCR buffer	10 ul
GC-Melt	5 ul
50xdNTP	1 ul
GC2-polymerase	1 ul
H ₂ O	15 ul
Total	50 ul

PCR cycles: 94°C 3 min; 94°C 30', 68°C 3 min for 35cycles; 68°C 3 min.

PCR machine: PTC-100[™] (MJ Research).

5'end RT-PCR for canine *AMN*

Primers: JCF379 5'-CGG GCG CGC GGC GGG-3' is located in 5'UTR.

JCF339 5'- CGC TCG GCG TCC ACG GAG AAG A-3' is located in exon 5.

The PCR conditions are the same as those for JCF334+JCF332.

Genomic PCR extraction from blood

DNeasy[®] Tissue Kit (Qiagen) or QIAamp[®] DNA Blood Midi Kit (Qiagen) was used to extract blood DNA.

Genomic PCR for mutation detection

Primers: JCF370 5'-TCC GTT GCA GGC GAA GCC CTC-3' crosses intron 9 and exon 10, while JCF366 5'-CTG CGG GGT GCG TGG AAC CTA G-3' crosses intron 11 and exon 12.

The Thermal AceTM DNA Polymerase Kit (Invitrogen) was used for the PCR.

PCR conditions:

Genomic DNA	100-200 ng
JCF370	5 ul (2.5 pmol/ul)
JCF366	5 ul (2.5 pmol/ul)
10xThermal Ace PCR buffer	5 ul
50x dNTP	1 ul
Thermal Ace polymerase	1 ul
H ₂ O	up to 50 ul
Total	50 ul

PCR cycles: 98°C 3 min; 98°C 30', 65°C 30', 72°C 1 min for 35cycles; 72°C 10 min.

PCR machine: PTC-100TM (MJ Research).

The PCR products were sequenced or run on the 2% agarose gel.

Results

Cloning of canine *AMN* cDNA

To obtain a fragment of canine *AMN* cDNA, we designed 3 sets of primers based on the homology of human, mouse and rat *AMN* cDNA sequences. Only the set of JCF323 plus JCF325 gave a band at expected size in the RT-PCR. DNA sequencing confirmed that the PCR product was homologous to its counterparts in other species. We used this PCR as the indicator PCR to screen the canine cDNA library by a pool-PCR method. At the last round of screening, three colonies were picked from the plate and PCR amplified by T3 and T7 primers, with DMSO added to the reactions. Each of them gave a band at 1.6 kb. Sequencing one of the PCR products demonstrated high homology to *AMN* in other species, indicating it is the cDNA sequence of canine *AMN*.

The full-length canine *AMN* cDNA (deposited to GenBank accession no. AY368152) is 77% GC and comprised of a 15 bp 5' untranslated region (UTR), a 1374 bp open reading frame, and a 152 bp 3' UTR that includes a polyadenylation signal 11 bp 5' of the poly A tract (Figure 3.1). The deduced amino acid sequence of 458 residues is 73 %, 66 %, 65%, 38%, 34%, 33%, and 21% identical to AMN of human (NP112205), mouse (NP291081), rat (XP234547), chicken (XP421397), *Xenopus laevis* (AAH74152), pufferfish (Fugu chrUn:215,972,629-215,974,032; UCSC Genome Browser, Aug 2002 assembly) and fruitfly (NP608515), respectively. Structural features conserved between these species include the predicted signal sequence cleavage site (after Ala 19); 12 cysteine residues in the mature extracellular domain, 9 of which are clustered between residues 205-253; a similarly placed, single predicted transmembrane domain (residues 363-387 of dog AMN); and 2 copies of F/YXNPXF/Y, a well-characterized AP-2 adaptor

protein-binding signal for ligand-independent receptor internalization via clathrin-coated pits (Boll et al., 2002) (Figure 3.2). Potential N-glycosylation sites (dog AMN residues 35 and 39) were found within the first 40 amino acid residues of the protein in all but the chicken and fruitfly sequences.

Mutation screening of canine *AMN*

RT-PCR is a rapid method for mutation screening, although it may not be able to detect certain types of mutations, such as mutations in introns, 5'UTR or 3'UTR etc. *AMN* cDNA of the entire coding region was amplified by RT-PCR from kidney cortex RNA isolated from an I-GS affected dog of the Giant Schnauzer (GS) kindred. Sequencing the product revealed an in-frame, 33 bp deletion in exon 10 (c.1113_1145del), predicting loss of 11 amino acid residues from the transmembrane domain somewhere between residues 370-382 (Figure 3.3). The deletion endpoints could not be determined exactly because they occurred within each of 2 nearly perfect copies of a 24 bp direct repeat sequence that are 79% GC and separated by 9 bp. However, a sequence variation of the repeats allowed us to place the 5' deletion endpoint on or between nucleotides 1106-1113 of the cDNA sequence and the 3' deletion endpoint on or between nucleotides 1139-1145. The same 33 bp deletion in exon 10 was found in PCR products amplified from genomic DNA of affected dogs, and can be detected by simply running the PCR products on the 2% agarose gel (Figure 3.4). The deletion was homozygous in 18 affected dogs, heterozygous in 8 obligate carriers, and was not seen in 224 chromosomes of unrelated normal dogs of various breeds. It must be pointed out that the full-length RT-PCR did not cover the start codon, because primer JCF334 overlapped

the ATG site. We thus did the 5' end RT-PCR, which by sequencing confirmed that no mutation exists in the start codon (data not shown).

Figure 3.1 cDNA sequence of canine *AMN* (deposited to Genbank; Accession number AY368152). The ATG start codon is underlined. The shaded area represents 5' and 3' untranslated region. The polyA signal is underlined near the end of the sequence.

```

1  cgggcgcgcggcggggatgggcgcgctggggcggggccctgctgtggctgca
51  gctgtgcgcgctggcccgggcccgcctacaagctctgggtccccaccacgg
101 acttcgaggccgcgcccaactggagccagaaccggacgccgtgcgcgggc
151 gccgtggtccagtcccccgcgacaaggcggtgtcggtggtggtgcgggc
201 cagccacggcttctcggacatgctcctgccgcgggacggggagttcggtcc
251 tggcctcgggagccggcttcggggccgcggacgccggcagggaccggac
301 tgcggcgcaggcgcccccgcgctcttctcgaccccgaccgcttctcggtg
351 gcacgacccgcgcctgtggcgctccggggacgcggcgcgcgccctcttct
401 ccgtggacgccgagcgcggtgccctgccgccacgacgacgtcggtcttccc
451 cccgacgcctccttccgagtggggctcgggcccggcgcccgcgcccgcgcg
501 cgtcgcgcagcgctccaggttctggggccagacgttcacgcgcgacgaggacc
551 tggctgccttctggcgctcccgcgccggcgccgctgcgcttccacgggccc
601 ggcgctctgcgcgtgggccccggggcctgcgccgacccgtcgggctgcgt
651 ctgcggcgacgcggaggtgcagccctggatctgcgcggccctgctccagc
701 ccctgggcggtcgctgcccgccggcgccctgccccgacgcctccggccc
751 gaggggcagtgctgcgacctctgcggagccatcggtgtcgctgacccacgg
801 cccacctttgacatcgagcggtaaccgggcgcggctgctgcgagccttcc
851 tgccccagtaaccggggctgcaggcgccggtgtccaaggtgcggcgggcgg
901 ccggggccgcacacggaggttcaggtggtgctggcgagaccggggcccca
951 gccgggcggcgcgggggcggtggcccggggccctcctggcgagcgtcgcg
1001 agcacggcgaagccctcggggctcctgtcggcgacagcccgggagtcgggc
1051 gcgcccgtcggggacggctcggcgggcggggcccgtcggtcgggttcgcg
1101 cgcggggctggcgggcgggcgtggcgggccgggctgctgctgctgctgctgg
1151 cgctggcgggcgggcctgctgctgctgcgccgcgctccgaggctcaggtgg
1201 actaagcgcgagcgattgggtcgccacgcccgtcgaggcgcccctgggctt
1251 ctccaacccgggtgttcgacgtggcgggctccgtggggccgggttcacgca
1301 ccccgagcctccccagcgcagcaggcggaagcagcagcaccagccgc
1351 agctaacttcgttaaccgcgtgttcgccgaggccgaggcctgagcaaccgc
1401 ggggctggccagcccctacctgcgccgcgcgcgcccccgcgagatggcc
1451 ccggccttgcgaggtccccgccccctgccacgcacgccttgtccccccag
1501 cccaaggatagggtggctttgcccaataaagcggttctctgc

```

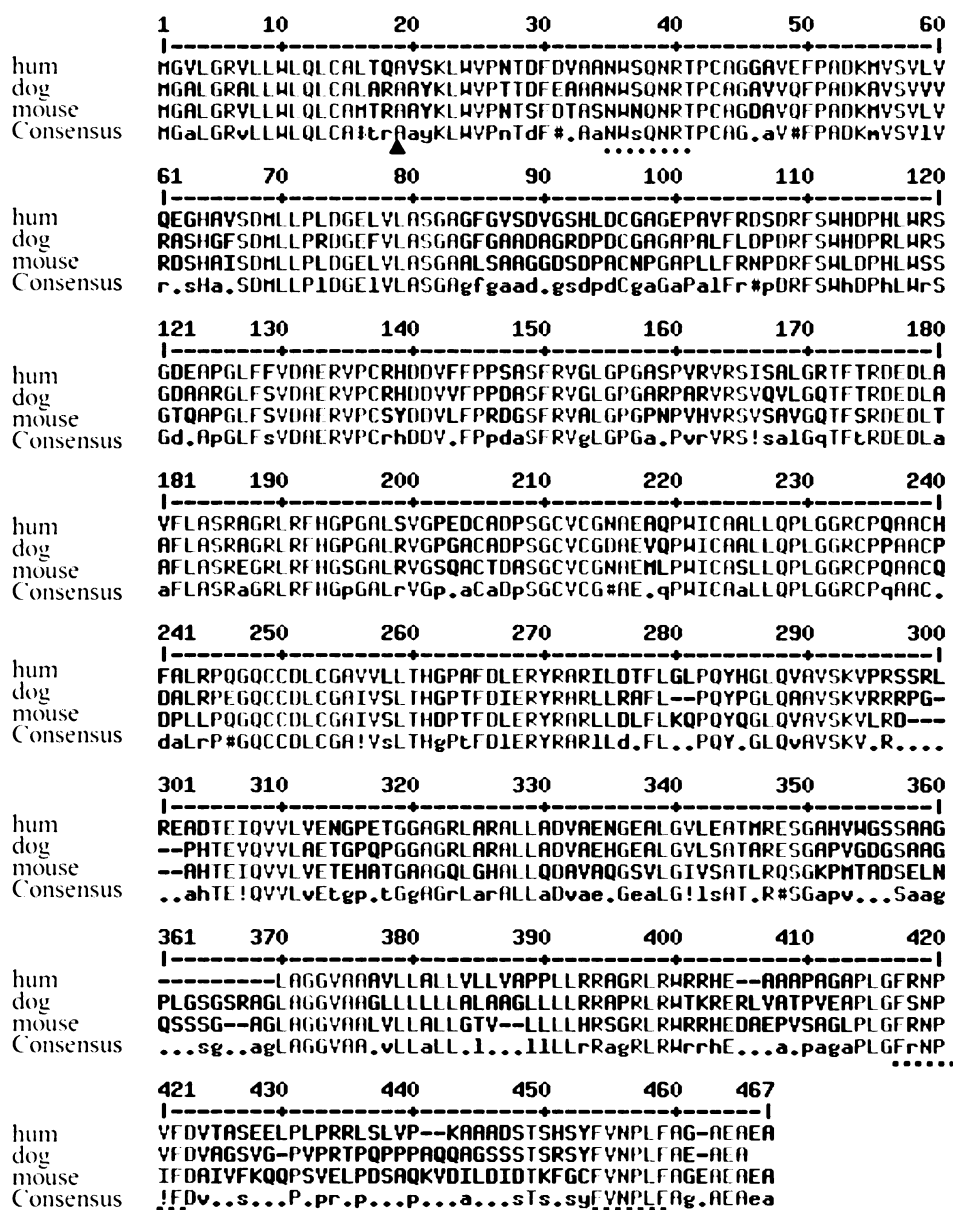


Figure 3.2 Alignment of human, dog, and mouse AMN proteins. The sole transmembrane domain is underlined by a gray bar. Two AP-2 binding signals for ligand-independent receptor internalization are underlined with dashed lines in the cytoplasmic domain (near position 420 and 460). Two nearly tandem N-linked glycosylation motifs (NXS/T) close to the N-terminus are underlined with dots (right before position 40). The predicted signal peptide cleavage site is indicated by an arrowhead.

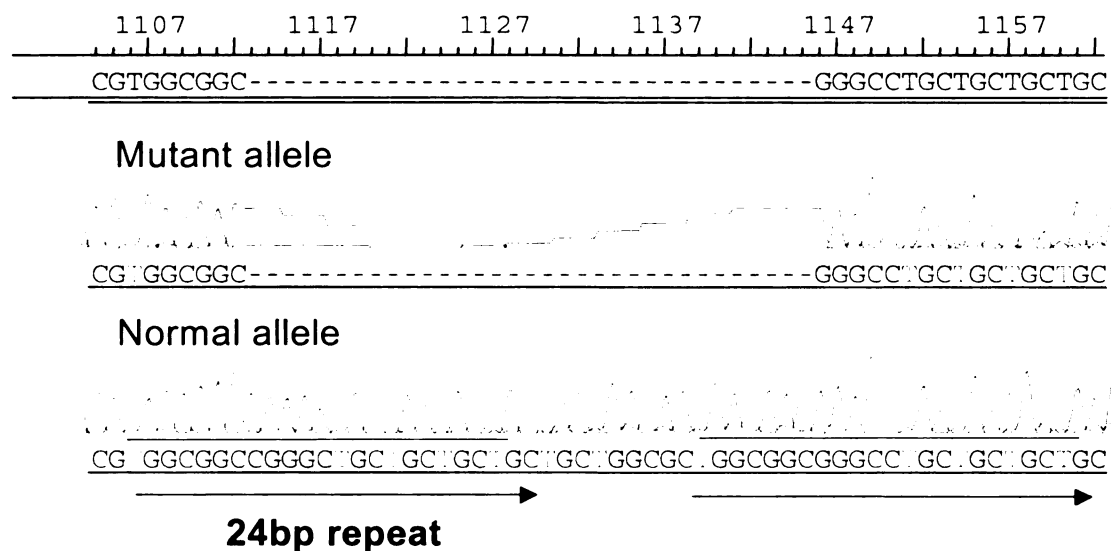


Figure 3.3 DNA sequencing revealed a 33 bp in-frame deletion in canine *AMN* of the affected dogs. The deletion is located in a region containing two 24 bp repeats. The deletion was predicted to delete 11 amino acids in a transmembrane domain.

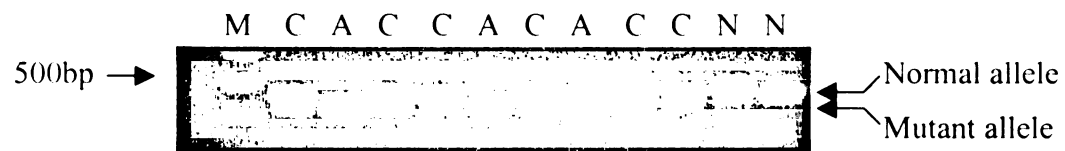


Figure 3.4 Mutation analysis of the 33 bp deletion in exon 10 of *AMN*. Genomic PCR (JCF370 + JCF 366) flanking the 33 bp region were performed in a number of dogs. The PCR products were separated on a 2% agarose gel. The mutant allele migrated faster than the normal allele because of the 33 bp deletion. M, marker. C, carrier. A, affected. N, normal.

Discussion:

Pool-PCR based cDNA cloning method can help to quickly identify the target clone, if used with caution. The potential risk of the method is that the indicator PCR may amplify undesired cDNA, which may lead to wrong directions. We actually experienced undesired cloning of estrogen receptor gene before we cloned the *AMN* cDNA. Thus, a second indicator PCR or sequencing may be necessary to assure that the clone of interest was amplified.

The clone we identified from the cDNA library was thought to be the normal cDNA of canine *AMN*. However, later experiments demonstrated that the cDNA clone was identical to the mutant cDNA, that is, it has the 33 bp deletion. Although it may due to a *in vivo* mutation event during the phage proliferation, a more likely explanation is that the starting mRNA material for the library construction contained some mutant mRNA. This indicates that at least one of the dogs used for kidney pools was a carrier for the mutation.

It has been well known that if significant homology exists, the repetitive sequence region of a chromatid may misalign with its corresponding region in a homologous chromatid during meiosis. As a result, deletion or insertion of repeat units may be generated. Here, the presence of the two 24 bp repeat sequences suggests that the mechanism of the 33 bp deletion was an unequal cross event after misalignment of the repeat sequences during meiosis I.

At least two lines of evidence suggest that the predicted transmembrane domain is a *bona fide* domain. First, protein alignment among multiple species showed that the transmembrane domain is similarly placed near the C-terminus. Second, immunofluorescence studies showed that AMN assisted the anchoring of cubilin on the

cell surface membrane (Fyfe et al., 2004). Since the 33 bp in frame deletion is located in the transmembrane domain, we hypothesized that the deletion might abolish the transmembrane domain. Computerized transmembrane domain prediction (TMHMM Server v. 2.0, Center for Biological Sequence Analysis, Technical University of Denmark), returned a probability of 1.0 for a transmembrane domain between amino acid residues 363 and 387 of the normal sequence, but < 0.05 for the deleted sequence (Figure 3.5). The analysis further indicated that if the mutant product were translated and sufficiently stable, the polypeptide would be entirely extracellular and, therefore, secreted.

A recent study showed that AMN and cubilin forms a novel complex (named *cubam*) on the apical membrane of epithelial cells, where cubilin is responsible for ligand binding while AMN directs membrane localization and endocytosis of cubilin with its ligands (Fyfe et al., 2004). This study provides the first functional evidence to explain why mutations in either *AMN* or *CUBN* cause clinically undistinguishable symptoms in human I-GS patients.

Our experiments showed that *AMN* in the affected dog could be readily amplified at a comparable amount to the normal dog in RT-PCR. Therefore the mutant *AMN* mRNA exists and may be translated. Depending on the stability of the mutant protein, it may be degraded or be secreted. In either way, it is tempting to think that the defect or loss of AMN may disrupt the function of cubam, which is essential for IF-Cbl absorption.

Mutations located in transmembrane domains of membrane proteins have been widely reported, but most of them are short deletions or missense mutations (Gasparini et al., 1991; Kelley et al., 1998; Gomez Lira et al., 2000). Deletion of more than 10 bp in a

transmembrane domain is rarely seen. It would be interesting to find out the structure of the 33 del mutant AMN in the future work.

In conclusion, we have identified the mutation responsible for the I-GS in a Giant Schnauzer family as a 33 bp in frame deletion, which was predicted to abolish the transmembrane domain of AMN and disrupt the functional cubam.

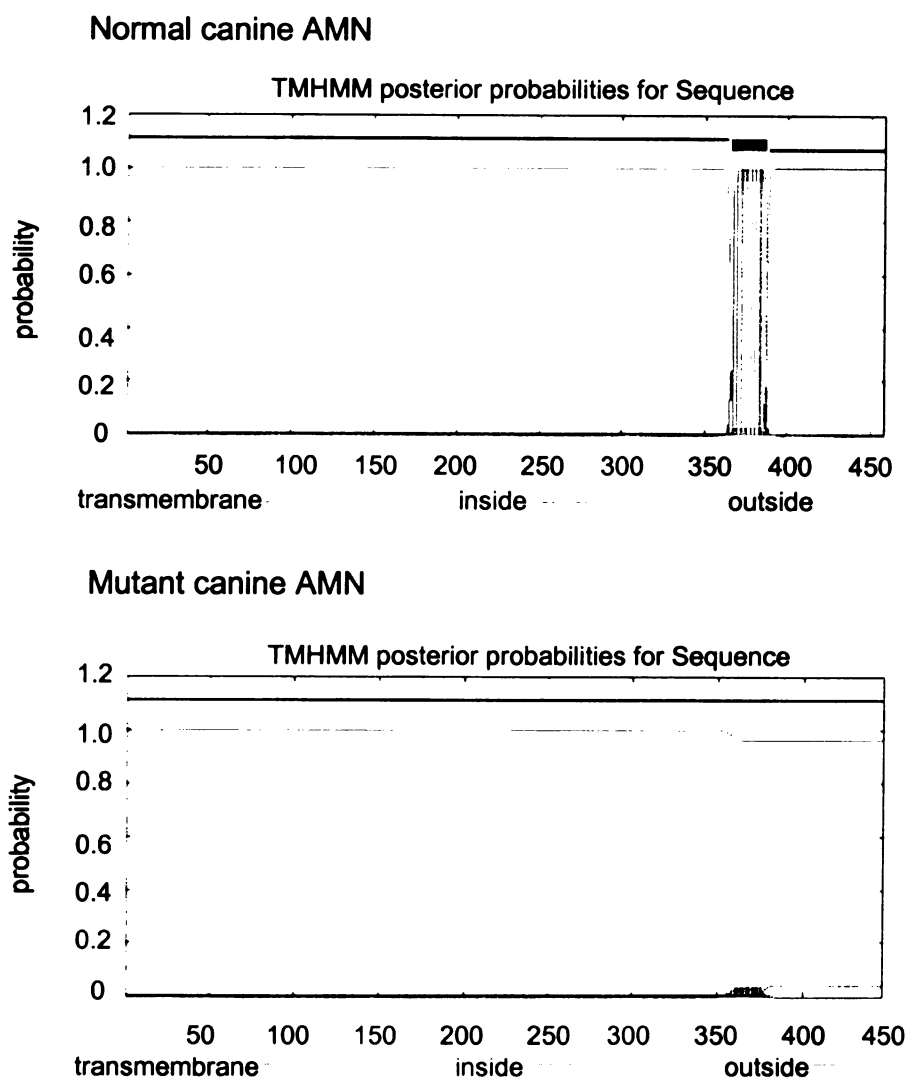


Figure 3.5 Structure prediction of AMN by the TMHMM software. The normal canine AMN (upper panel) was predicted to be a single-transmembrane protein, while the 33del mutant AMN (lower panel) was predicted to lose the transmembrane domain and be secreted out of the cells. Images in this dissertation are presented in color.

CHAPTER 4

**LINKAGE ANALYSIS AND MUTATION SCREENING OF AN AUSTRALIAN
SHEPHERD FAMILY WITH IMERSLUND-GRÄSBECK SYNDROME**

In this chapter, I designed and performed all the experiments, except that Schaffer AA did the computer-based linkage analysis and Kilkenney A did the genotyping with *CUBN*.

Introduction

Imerslund-Gräsbeck syndrome, characterized by cobalamin malabsorption and proteinuria, has been reported in different ethnic groups, such as Norwegian, Finnish, Jewish, Turkish, etc (Gräsbeck et al., 1960; Imerslund 1960; Ben-Ami et al, 1990; Yetgin et al., 1978). The *AMN* c.14delG mutation was commonly seen in Norwegian patients, while *AMN* c.208-2A>G mutation was carried by two Turkish families. Two other distinct mutations of *AMN* have been identified in a USA family and a single Belgium patient, respectively (Tanner et al., 2004). It appears that multiple independent mutation events have occurred in the *AMN* gene during the human history in different subpopulations.

Similarly, an inherited disease may be observed in different breeds of dogs. In the previous chapter, we described a 33 bp deletion in the *AMN* gene identified from a Giant Schnauzer family with I-GS. The deletion leads to loss of 11 aa, which was predicted to abolish the sole transmembrane domain of AMN. This is devastating to the function of AMN, because biochemical and cell-based studies suggested that the transmembrane domain of AMN is essential for anchoring cubilin on the apical membrane, to endocytose certain ligands such as IF-Cbl (Fyfe et al., 2004). In this chapter, we study a second canine I-GS family of purebred Australian Shepherd dogs (AS kindred; Figure 4.1). In this pedigree, three affected littermates exhibited growth failure, methylmalonic aciduria, mild anemia, neutropenia, subnormal serum cobalamin concentrations, and low-molecular-weight proteinuria (Fyfe, unpublished data). Parenteral cobalamin administration produced complete clinical, hematologic, and metabolic remission even

though cobalamin malabsorption and proteinuria remained, suggesting that the AS kindred have the same genetic defect as the GS kindred.

It is therefore intriguing to ask whether the AS kindred carry the same 33 bp deletion as the GS kindred. If not, does another mutation exist in the *AMN* gene? Or does *CUBN* harbor the mutation? The reason to pursue such questions is that different mutations may help to better understand the structure and functions of a protein, as seen in the cases like methylmalonyl-CoA mutase (Janata et al., 1997) and LDL receptor (Jensen et al., 1997) defects. On the other hand, it is also helpful to provide a genetic test for dog breeders to eradicate the disease in the specific dog breed.

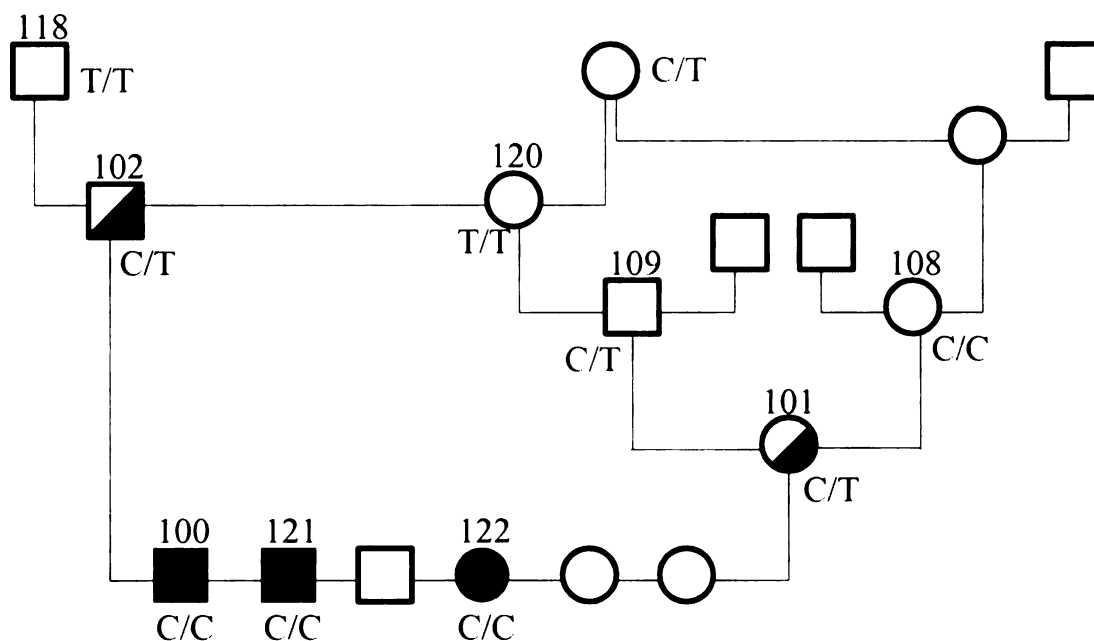


Figure 4.1 *KNS2* genotyping of the Australian Shepherd kindred. Three affected dogs, 100, 121 and 122, are homozygous for the C allele of *KNS2*; two carriers, 101 and 102, are in the heterozygous status of C/T; most of the clinically normal dogs are heterozygous or homozygous for the T allele of *KNS2*. Therefore, the disease appears to segregate with the marker in an autosomal recessive manner. Since *AMN* gene is only ~600 kb from the *KNS2* marker, it suggests that *AMN* may be the disease-causing gene.

Materials and methods

Animals

All dogs were handled according to the principles outlined in the NIH Guide for the Care and Use of Laboratory Animals, with protocols approved by the MSU All University Committee for Animal Use and Care. Blood or buccal brush samples were collected from 28 dogs of the kindred each of which was determined to be affected or clinically normal. The relationships of these dogs are partially depicted in the pedigree in Figure 4.1. Blood or buccal brush were stored frozen at -80°C for DNA isolation.

Markers and genotyping

DNA was isolated by standard methods (Sambrook et al. 1989). To test the linkage of the disease to *CUBN*, an intronic 17 bp variation in *CUBN* previously described (Xu et al., 1999) was chosen as a marker. On the other hand, the *KNS2* marker was chosen to test if the disease is linked to *AMN*, because this marker was only about 600 kb away from the *AMN* gene. Both markers were shown to be informative in this pedigree.

CUBN primers: (JCF119) 5'-GAT CAC AGG CCT ACA GCT CCA TT-3'

(JCF120) 5'-CCA GGC CAA CCA GAG ATC TTC TA-3'

The *CUBN* PCR products were run on the 4% agarose gel, on which two different alleles showed two distinct bands.

KNS2 primers: JCF294 and JCF295 have been described in Chapter 2.

Linkage analysis

Linkage analysis computations were performed with the FASTLINK software package as described in Chapter 2. LOD scores were calculated with assumptions of a disease allele frequency of 0.001, full penetrance of the disease trait, and equal marker allele frequencies.

Mutation screening

DNA samples from affected dogs B122 and B100 and an unrelated normal dog (DCCU6110) were used for mutation screening. The primers and PCR reagents used for genomic PCR amplification are listed in Table 3.

Mutation detection

Primers: JCF563 (5'-GGC TTG GAA GGA AGG CCC CCA-3') is located ~280 bp upstream of the ATG start codon.

JCF387 (5'-CAA GGC GGG GAG CCT CCG AA-3') is located in intron1, ~90 bp downstream of the ATG start codon.

The Thermal AccTM DNA Polymerase Kit (Invitrogen) was used for the PCR.

The PCR products were digested with *Bst*F5 I at 65°C for 2 hours and run on the 2.5% agarose gel. The mutant allele was resistant to the digestion while the normal allele was not.

Table 3. Primer list for genomic amplification of canine *AMN*. Notably, JCF392 (reverse) partially overlaps with JCF422 (forward) located in intron 6. JCF356 (reverse) partially overlaps with JCF370 (forward), which crosses intron 9 and exon 10. JCF334 overlaps with the ATG start codon and amplifies in both normal and affected dogs.

Notations in the PCR reagent column: a, Thermal AceTM Kit (Invitrogen); b, Expand^R High Fidelity PCR System (Roche); c, Advantage^R-GC Genomic polymerase mix (BD Biosciences); d, Taq DNA polymerase (Qiagen).

Set	Primer ID	Primer sequence	location	PCR reagent
set 1	JCF334	5'- CGG GCG CGC GGC GGG ATG-3'	exon1	a
	JCF368	5'- CGT CCG GTT CTG GCT CCA GTT G-3'	exon2	
set 2	JCF388	5'- CTCCGCAGACCTCGTAGGAGTT-3'	intron1	b
	JCF391	5'- AGGCTGGGGAAAGGGTATGGG-3'	intron3	
set 3	JCF416	5'- TGC AGT CCT GCT CCC TCG GCT T-3'	intron3	b
	JCF396	5'- TCTTCCTCGACCCCGACCGCTT -3'	exon5	
set 4	JCF397	5'- CGGCTTCTCTGACCCTCGGACA-3'	intron3	b
	JCF339	5'- CGC TCG GCG TCC ACG GAG AAG A-3'	exon5	
set 5	JCF328	5'- TCG ACC CCG ACC GCT TCT TGT G-3'	exon5	c
	JCF392	5'- AGC GGG GTG AGC GCG GAC AGT-3'	intron6	
set 6	JCF422	5'- ACT GTC CGC GCT CAC CCC GCT T-3'	intron6	c
	JCF423	5'- TCA CCG CAG AGG TCG CAG CAC T-3'	exon7	
set 7	JCF355	5'-GGA GGT GCA GCC CTG GAT CTG-3'	exon7	c
	JCF346	5'-GCC GCC GCC GCA CCT TGG ACA C-3'	exon9	
set 8	JCF335	5'-CCA CGG CCC CAC CTT TGA CAT C-3'	exon8	d
	JCF330	5'- CAC CAC CTG AAC CTC CGT GTG C-3'	exon9	
set 9	JCF362	5'-GCA GGC GGC CGT GTC CAA GGT G-3'	exon9	c
	JCF356	5'-CGA CAG GAC CCC GAG GGC TTC-3'	exon10	
set 10	JCF371	5'- GGA GCA CGG TAA CCG CGG GTG-3'	intron9	a
	JCF366	5'- CTG CGG GGT GCG TGG AAC CTA G-3'	intron11	
set 11	JCF370	5'- TCC GTT GCA GGC GAA GCC CTC-3'	exon10	a
	JCF366	5'- CTG CGG GGT GCG TGG AAC CTA G-3'	intron11	
set 12	JCF351	5'-GTG GAC TAA GCG CGA GCG ATT G-3'	exon11	c
	JCF332	5'- CTG GCC AGC CCC GCG GTT GC-3'	exon12	

Results:

Exclusion of *CUBN*

B100, B121 and B122 were affected littermates descending from B102 and B101. Under the null hypothesis that *CUBN* was the disease-causing gene, B100, B121 and B122 should have identical genotypes for *CUBN*, because both of their parents were carriers and therefore each parent could transmit only one disease allele to the affected offspring. However, the genotyping data of *CUBN* showed that only B100 and B121 shared the same genotype while B122 had a distinct genotype (Table 5 in Appendices). Thus, the null hypothesis should be rejected and we concluded that *CUBN* could not be the disease-causing gene.

Linkage analysis with *KNS2*

11 members of the kindred, including 3 affected siblings were genotyped for a polymorphism in the *KNS2* gene that was also variable in the GS pedigree (Table 5 in Appendices). Assuming that the C allele of *KNS2* is not rare and the disease allele having low probability, two-point linkage analysis was performed and LOD score 1.7 ($\theta=0.0$) was obtained. This suggested, to a slight extent, linkage of the disease to the *KNS2* marker and thereby to the *AMN* gene, because *KNS2* was only ~600 kb from the *AMN* gene.

Mutation screening

As tissues were initially not available, we could not do the RT-PCR in the affected dogs. Although the 7.6X coverage of the dog genome was partially available during our

mutation screening, the *AMN* gene contains several sequencing gaps and the sequencing quality was very poor. We therefore generated most of the genomic sequence of *AMN* in our lab by overlapping PCR and sequencing (Figure 4.2). Sequences of intron 3 and 5' UTR were not obtained because of either technical difficulty or lack of primer sequences. We amplified nearly all the exons and exon-intron boundaries of *AMN* (partial exon 1 was not amplified due to lack of 5'UTR sequence). However, no mutations were identified. Five variations were seen in intron 4, intron 5 and intron 8, but were not located at the 5' or 3' intron-exon boundaries. The variations did not seem to disrupt the site of branching point A either. RT-PCR was performed later with JCF334 and JCF332 as the kidney cortex was obtained from B100. This PCR covered the full-length *AMN* cDNA except the ATG start codon, for JCF334 overlapped the ATG site. With no mutations found, we then did the RT-PCR with JCF379 and JCF339, to include the ATG site in the PCR product. DNA sequencing identified a single nucleotide change (G>A) in the start codon (Figure 4.3).

In order to confirm that the variation was at the DNA level, we amplified the 5' region by genomic PCR. Facing a sequence gap at the 5' region of *AMN*, we first designed primers based on the UCSC Genome Browser on Dog Assembly (July 2004) (<http://www.genome.ucsc.edu/cgi-bin/hgGateway>), and filled in the ~1 kb gap by sequencing the PCR products. With the 5'UTR sequence available, primers JCF563 and JCF387 were designed and subsequently used to PCR the genomic region flanking the ATG site. The G>A variation was confirmed by sequencing, along with some other polymorphisms identified in the 5' region upstream of ATG.

The G>A transition abolished a *Bst**FI* I digestion site, which could be used for convenient genotyping (Figure 4.4). We thus used this method to genotype other dogs in the AS kindred, plus more than 50 unrelated normal dogs. The G>A transition segregated with the disease allele of the AS kindred as expected for an autosomal recessive disorder in 3 affected (A/A), 2 obligate carriers (G/A), and 16 other clinically normal Australian Shepherd dogs (13 G/G and 3 G/A) (Table 5 in Appendices). The mutation was not observed in 112 chromosomes of unrelated normal dogs of various breeds.

Figure 4.2. Genomic DNA sequence of canine *AMN* gene. The italic sequence is upstream of the known *AMN* DNA and may contain the transcription initiation site (the underlined italic sequence represents a polymorphism). The following upper case letters represent exons sequences, while the lower case letters represent intron sequences. The coding regions are shaded. The size of intron 3 has not been determined.

CCCCCCCCCCCCCCCCCCGCTTTCATCATTCTTCCCCACCCAAGCACCAAGCC
 ACCCGGCTCTTGACCGCGGGGTCYCTCGACCCGCCCCCGCCCCGGGCGG
 CCCCCATCACTTCGCGGGGCCCCCAACACCCACTCGTGCTCCGCCACCAGCTCC
 GTGTGCAGCCCCGGGGGGCCTYGCCCCCTCCGCCCCCACCGCCACAGGCCCACT
 GCCGGCGCCCGCAGGGCATCCAGGCGGGGGGGGGTGAGGGGGGCTTGGAAGG
 AAGGCCCCARCCAGGGGGGGCAGAGCAGGTGCAGCCCCGGGCACAGGGCA
 CGGGAGCAGGGAGCCCAGGGGGTCCCTCCCGCCCCAGCTCGCCCCGCCTTGG
 AGCGGGTGGGCGGGCCCCAGGGCTGAGTGTGGGGGCAGGAGCCGCCGCGGCG
 CCCC GG GGCSSGGGAGGTGGTAACGCCCCGCCCCGCCcgccccgccCGCCCCG
 CCGGTCAGGTGGGCCCCGCGGGGCAAGTCCCGGTGGCGGCGACGGGCGCG
 Exon1
 CGGCGGG**ATGGG**CGCGCTGGGCCGGGCCCTGCTGTGGCTGCAGCTGTGCGgta
 agggggccccggggcgcgggcggggggttcggaggtcccccgccttggggccccggacccctcgggcgccggggggggcct
 gcgagccgcgcaccgccccagttcccgctccctgcggggcgcgggcgagcctgactcagttccctccgccttggcgcc
 cggccggcgcggtccccgggcccgggagcttgaaactgcagccccgccccgccccgccccgagccccgcggtcc
 cgcggacacgagtccccagggggcgccctccgcgccccgccccgcgaccccttgtgccgtcggtccctcggttgcgcg
 gccttccccgcccgggcccctctgtccctctgtccagcgccccgcaagccccggggcgaggcgagcgatcttggcggg
 cggcctggagggggcacggggggcgggctccgcagacctcgtaggagtgcgccccgcggcgggggtcccgcggggt
 ctgggccccgggtgcggccgcttccctccggggggggggggcgggcggggagcactcagtcgtgccctccccagCGC
 Exon2
 TGGCCCGGGCCGCCTACAAGCTCTGGGTCCCCACCACGGA**CTTC**GAGGCCGC
 CGCCAACTGGAGCCAGAACCGGACGCCGTGCGCGGGCGCCGTGGTCCAGTTC

CCCGCGGACAAGgtgccccgcgggctcgggagggcgactgggggggctccgggggaggctggggggctcg
 ggggggcccggccaaccgctccttctgcag^{Exon3}GCGGTGTCGGTGGTGGTGCGGGCCAGCCACG
 GCTTCTCGGACATGgtgagggcggggctgcggggggtggcccccggaacccctctgggcctggggcgggct
 cctgggaggtggggaaagggtatgg??????????1~3kb?????????cttgactsgcaggccctgatacc
 tgcccggtccgcgggaacgcggcggcggggcgggaccgtggggcacccgggccaccgtgtgcctgtgctgccgcagC
^{Exon4}TCCTGCCGCGGGACGGGGAGTTCGTCCTGGCCTCGGGAGCCGGCTTCGGGGC
 CGCGGACGCCGGCAGGGACCCGGACTGCGGCGCAGgtgaggggcggggcggggcggggc
 gggagggcggggcccgggscggagggggcggggcctgggcgggcggggcggggcctgagcgggggcggggcctgagc
 gggggcggggggcggggcccggggcggggcggggcggagctcaggagcgcgcggggcggggcag^{Exon5}GCGCCCCCGCG
 CTCTTCCTCGACCCCGACCGCTTCTYGTGGCACGACCCGCGCCTGTGGCGCTC
 CGGGGACGCGGCGCGCGGCCTCTTCTCCGTGGACGCCGAGCGCGTGCCCTGC
 CGCCACGACGACGTCTTCCCGCCCGACGCCTCCTTCCGAGTGGGGCTCG
 GGCCCGGCGCCCGCCCCGCGCGCGTCCGCAGCGTCCAGGTTCTGGGCCAGgtg
 agcggcgctcgggccccctccccgacctgccacgcgcggctgccggcgctcaggggctgtccctcctcgggcggcgc
^{Exon6}cgtcgtgccgccccctccccgcagACGTTACGCGCGACGAGGACCTGGCTGCCTTCCTG
 GCGTCCCGCGCCGGCCGCCTGCGCTTCCACGGGCCGGGCGCTCTGCGCGTGG
 GCCCCGGGGCCTGCGCCGACCCGTCGGGCTGCGTCTGCGGCGACGCGGAGgtg
 agggcgccggcggggggggcgagggggcgagggggcggggggnnnnactgtccgcgctcaccgcgttctccgc
^{Exon7}agtggagGTGCAGCCCTGGATCTGCGCGGCCCTGCTCCAGCCCCTGGGCGGTTCG
 TGCCCGCCGGCCGCCTGCCCCGACGCCCTCCGGCCCGAGGGGCAGTGCTGCG
 ACCTCTGCGgtgagcggccccctccggccccggagagctgccctggctcggccccagcctcagtttccctgacggccct
^{Exon8}gggctcgcggcgccgaccttccgtctgtcgcagGAGCCATCGTGTGCTGACCCACGGCCCC
 ACCTTTGACATCGAGCGGTACCGGGCGCGGCTGCTGCGAGCCTTCCTGgtaacgg

ggccgcgtccccgccccgccctgccccccccgcggggcccgcctcttccgcggcggcggccgggaccccactgcccc
 ccacgcagtcactgaccgcgcacctcccgtcacccgccggccgagggccaggtcccgggacgaccccgctccctcc
 ccag^{Exon9}CCCCAGTACCCGGGGCTGCAGGCGGCCGTGTCCAAGGTGCGGCGGGCGGC
 CGGGGCCGCACACGGAGGTTCAAGGTGGTGCTGGCGGAGACCGGGCCCCAGC
 CGGGCGGCGCGGGGCGGCTGGCCCCGGGCCCTCCTGGCGGACGTGCGGGAGC
 ACGgtaaccgcgggtgccccccccggccggccggccccgcgtgcgggagcctgagcccgccctccgttgagGC
 Exon10
 GAAGCCCTCGGGGTCCTGTGCGCGACAGCCCGGGAGTCGGGCGCGCCCGTCG
 GGGACGGCTCGGCGGCGGGGCCGCTCGGCTCGGGTTCGCGCGCGGGGCTGGC
 GGGCGGCGTGCGGGCCGGGCTGCTGCTGCTGCTGCTGGCGCTGGCGGCGGGC
 CTGCTGCTGCTGCGCCGCGCTCCGAGGCTCAGgtccgcggggcgggggcggggcgggggc
 gggggcggggccgcgtgggggctcacgggcgtcctgttccccag^{Exon11}GTGGACTAAGCGCGAGCGATTGG
 TCGCCACGCCCCGTCGAGGCGCCCCCTGGGCTTCTCCAACCCGGTGTTTCGACGTG
 GCGGCTCCGTGGGGCCGgtgagggggcgcgcgggggacctgccctccccggcctgcggccgccgaccccc
 ttgactccgcgccccgccccag^{Exon12}GTTCCACGCACCCCGCAGCCTCCCCAGCGCAGCAGG
 CGGGAAGCAGCAGCACCAAGCCGCAGCTACTTCGTAAACCCGCTGTTCGCCGA
 GGCCGAGGCCTGAGCAACCGCGGGGCTGGCCAGCCCCCTACCTGCGCCCCGCCG
 CCGCCCCCGCGAGATGGCCCCGGCCTTGCGAGGTCCCCGCCCCCTGCCACGC
 ACGCCTTGTCCCCCCAGCCCAAGGATAGGGTGGCTTTGCCCAATAAAGCGTT
 TCCTGCacccggagtccgttccccagtgccctcctgtgcctgggcttgagcgtggggagccggccagtgtgccctc
 aggtgcccactggtgagcgtgtcctcagaatcctgccctctggccaccagcaagggcagctccaggcactaccgaaaatt
 gcagctgcagagctgcaccagaatgtggggaaggctgccctggagcaggggagcgaggcggcgggtgaggctggctg
 tccagacccccagcagccagtagaacagccagtccttccccagaggaacaggattattctggaatgcagagggaatgacact

gctgcaggatatgcgggctgcggcgggaaccacagcagggcagcctggagaccagggagaggaagaggaggacaagg

g

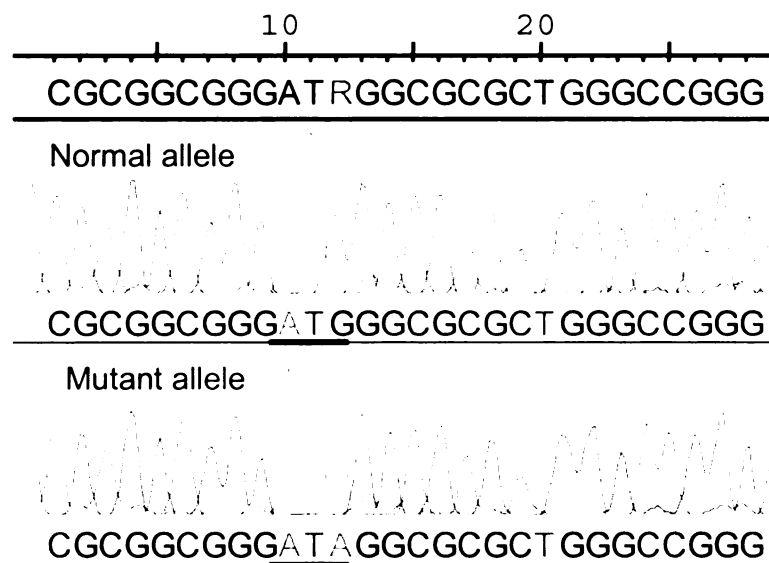


Figure 4.3 DNA sequencing revealed a G>A mutation in the start codon (underlined) of canine *AMN* in the affected dogs. The next in-frame ATG in canine *AMN* is 204 bp downstream, but not within the Kozak consensus context.

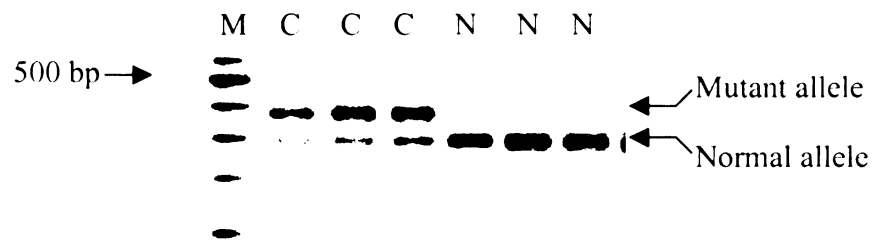


Figure 4.4 Mutation analysis of the G>A transition in start codon. Genomic PCR flanking the start codon were performed in a number of dogs. The PCR products were digested by *BstF5* I for 2 hours and separated on the 2.5% agarose gel. The normal allele was digested into two fragments (284 bp and 95 bp), while the mutant allele was resistant to the enzyme digestion. M, marker; C, carrier; N, normal.

Discussion

CUBN and *AMN* are the two known genes that underlie the I-GS disease. With the *CUBN* gene being ruled out by exclusion linkage analysis, we therefore focused on the *AMN* gene.

Directly testing linkage of the *AMN* gene to the disease was not possible because no informative marker was available in the *AMN* gene. However, since the *KNS2* marker is very close to the *AMN*, we decided to test the linkage indirectly by genotyping *KNS2* in the AS family. The LOD score obtained was 1.7, which means that the likelihood of linkage over nonlinkage is $10^{1.7} = 50$. The score of 1.7 is below the generally accepted score 2.0 for suggestive linkage. Two reasons may explain why the LOD score was not high enough to suggest linkage. First, the number of family members tested is relatively small (11 members), and only 3 affected dogs were in the family. Second, the *KNS2* marker was not in complete linkage disequilibrium with the disease allele in this AS kindred. One unaffected dog B108, who is a carrier of the *AMN* mutation, is homozygous for the disease-associated C allele at the *KNS2* polymorphism. Another unaffected dog B109 who does not carry the *AMN* mutation is heterozygous at the *KNS2* polymorphism site. It appears likely that the C allele of the *KNS2* polymorphism has a high enough frequency that it entered the pedigree on multiple haplotypes, only one of which is associated with I-GS. Nevertheless, *AMN* appeared to be a compelling candidate gene, for which we decided to do an extensive mutation screening.

The *AMN* gene has a 70-80% GC content, which makes the standard PCR condition not useful. High denaturing temperature, GC-Melt reagent, DMSO and some high-temperature-resistant polymerase helped to amplify the sequence, but none of them

worked universally. Although the dog genome sequencing project has been completed recently, there are still 3 gaps in the *AMN* gene, and the sequencing quality of the *AMN* gene is very poor. This is likely due to the high GC-content, because we have also experienced difficulties in sequencing some of the PCR products. Thus, combining genomic PCR with RT-PCR to detect mutations was necessary.

The G>A mutation is predicted to change the initiating methionine into isoleucine. A few rare cases of alternative initiation codons have been described, including ACG (Thr), CUG (Leu) and GUG (Val) (Taira et al., 1990; Tailor et al., 2001), but AUA has never been reported to be able to initiate translation to the best of our knowledge. Eukaryotic translation initiation consensus has been defined as (A/G)CCAUGG. *In vitro* translation experiments showed the G at position +4 and the purine at position -3 are highly conserved (Kozak, 1986; Kozak, 1997). For the canine *AMN* gene, the next in-frame ATG is at position 205-7, but not within the Kozak consensus context. Thus the mutant mRNA is unlikely to be translated. Furthermore, even if translation were initiated in a very rare circumstance, amino-terminal truncation of 68 residues would eliminate the signal peptide sequence required for co-translational rough endoplasmic reticulum insertion and subsequent delivery to the plasma membrane. Therefore, the G>A transition in the start codon is essentially a null mutation.

This finding strengthens our previous conclusion that *AMN* is responsible for the canine I-GS. The two canine pedigrees harboring different *AMN* mutations provide us a unique opportunity to study the functions of AMN and cubilin directly in tissues of both affected and normal dogs, which is nearly impossible in the human study of I-GS patients.

CHAPTER 5

FUNCTIONAL STUDIES OF CANINE *AMN* MUTATIONS

The experiments described in this chapter were carried out as a collaborative investigation involving Mette Madsen and Erik Christensen. Erik Christensen did the immunohistochemistry. For the transfection and immunofluorescence studies of the CHO cells, I designed the experiments and constructed the plasmids, while Mette Madsen carried out cell transfection, Western blots and immunofluorescence of the transfected cells. I did all the other experiments shown in this chapter. The interpretations of the data described here are mine.

Introduction

Mutations in either cubilin or AMN gene cause I-GS in humans. No clinical differences have been reported between patients carrying mutations in *CUBN* vs. *AMN* (Tanner et al., 2004). Cubilin is a 460 kDa, multiligand, apical membrane receptor protein that mediates endocytosis of the intrinsic factor (IF)-cobalamin complex in distal small intestine and of several proteins of the glomerular filtrate in renal proximal tubules (Christensen and Birn, 2002). AMN is an ~ 45 kDa apical membrane protein also expressed in intestinal and proximal tubule epithelia, but whose function is poorly defined (Kalantry et al., 2001; Tanner et al., 2003). Recent studies in human cadaver kidney and transfected Chinese hamster ovary (CHO) cells suggested that cubilin and AMN function as subunits of a receptor complex, now called *cubam*. The complex is Ca^{2+} independent and does not separate under denaturing condition of 2 M urea. Cotransfection of both AMN and a mini-cubilin construct into CHO cells demonstrated that cubilin was expressed on the cell surface and ^{conferred to the cells the ability to} endocytose IF-Cbl. In CHO cells transfected with only the cubilin construct, immunofocal and immunoelectron microscopic examination revealed that cubilin was retained intracellularly, and the internalization of ^{125}I -IF-Cbl was considerably less than in the double transfectants (Fyfe et al., 2004). However, because the disease is completely ameliorated by periodic parenteral cobalamin administration, and the tissues that express the gene products are not readily accessible, there have been no studies that directly assess the effect of *CUBN* or *AMN* mutations on cubam expression in I-GS patients.

Canine I-GS is a well-established animal model of the human disorder (Fyfe et al., 1991a; Fyfe et al., 1991b; Xu and Fyfe, 2000) that has contributed significantly to

understanding of its biological basis as well as molecular aspects of *CUBN* expression and cubilin function (Nykjaer et al., 2001; Kozyraki et al., 2001; Birn et al., 2000; Kozyraki et al., 1999). Cubilin has been implicated in the etiology of canine I-GS for more than ten years. It was demonstrated that cubilin had an abnormal conformation and failed to reach the apical microvillus surface membrane of villus tip enterocytes in the affected dogs (Fyfe et al., 1991a; Xu and Fyfe, 2000). With the mutations in *AMN* already identified in both kindreds, we explored how mutated *AMN* caused the mal-expression and dysfunction of cubilin.

In order to determine the molecular basis of the observed abnormalities of cubilin expression in the canine I-GS model, we studied the expression pattern of both proteins in multiple tissues by RT-PCR, and investigated the mutations' effects on both cubilin and *AMN* expression *in vivo*. Additionally, comparison of these results to expression of mutant canine *AMN* in a heterologous mammalian cell transfection system validates the system for examining functional defects caused by human *CUBN* and *AMN* mutations *ex vivo*.

Materials and methods

mRNA expression pattern in multiple tissues

JCF426 5'AGCCTGCGTGCTGGACATAGAC3'

JCF427 5' CCAGCCCAACCTGATTCACTTA3'

JCF428 5' TCAGGGTGGAGACTTCTCAAATC3'

JCF429 5' GTTGCAGCTTCAGTCTATCTGCT3'

JCF334 and JCF332 have been described in chapter 3.

Total RNAs were extracted from multiple tissues of a normal dog. RT-PCR for *AMN* (JCF334 plus JCF332) was performed with the Expand high fidelity PCR system (Roche). RT-PCR for *CUBN* (JCF426 plus JCF427) and Cyclophilin gene (JCF428 plus JCF429) were performed at standard conditions. Five microliter of PCR products were electrophoresed on 1% agarose gels.

Characterization of the anti-AMN antibody

Anti-canine AMN peptide antiserum was produced by immunization of rabbits with the synthetic peptide TARESGAPVGDGSA (amino acid residues 340-353) of canine AMN. Peptide was synthesized, immunizations performed, and serum harvested in the custom antibody production facilities of ProSci Inc. (Poway, CA) under NIH Animal Welfare Assurance (no. A4182-01). The anti-AMN antibody was affinity purified by the synthetic peptide. The cubam complex was enriched, in bulk, by IF-cobalamin affinity chromatography from pooled fresh frozen kidney of unrelated normal dogs (Fyfe et al., 2004) (provided by Dr. Fyfe). However, this enriched cubam complex still contained many unspecific proteins because of technical limits. The enriched cubam complex was

applied to reducing SDS-PAGE (12%) and transferred to PVDF membrane, then incubated with the preimmune serum, affinity-purified anti-AMN, flowthrough of the peptide-affinity-column-absorbed-serum or secondary antibody only, respectively. The secondary antibody is a goat-anti-rabbit IgG alkaline phosphatase conjugate. The immunoactive proteins were detected by incubating membranes with 5-bromo,4-chloro,3-indolylphosphate (BCIP) / nitroblue tetrazolium (NBT) for 10 minutes.

IF-Cbl Pull down and Western blot

First pull-down: For analysis of AMN expression in biopsy quantities of tissue, 2.7 g kidney cortex was thawed and homogenized in 24 mL of cold 50 mM Tris-Cl (pH 7.4) containing 150 mM NaCl, 1 mM N-ethylmaleimide, 5 mM phenylmethylsulfonyl fluoride. 3-[(3-cholamidopropyl)dimethylammonio]-1-propanesulfonate (CHAPS) was added to 0.6 %, and the homogenate was incubated at 4° C for 2 h with constant agitation. The detergent extracts were centrifuged at 4° C for 40 min at 40,000 g, and the supernatant was collected. The protein concentration was determined by the Lowry method. Rat IF-cobalamin beads were prepared as previously described (Xu and Fyfe, 2000). Supernatant aliquots containing 100 mg of total protein were incubated with 20 ul of rat IF-cobalamin beads with 5 mM Ca²⁺ overnight at 4°C and centrifuged for 15 min at 4,500 g. The beads were washed 3 times with 1 mL of homogenization buffer containing 0.6% CHAPS and 1 mM CaCl₂, then resuspended with 7 ul 4x SDS-PAGE sample buffer and 3 ul 10x DTE. They were boiled for 8 min and subjected to SDS-PAGE (12%), followed by Western blot. The first antibody was affinity-purified rabbit-anti-canine

AMN peptide (residues 340-353 of AMN) (1:40,000), and the secondary antibody was goat-anti-rabbit IgG conjugated with alkaline phosphatase (1:20,000).

Second pull-down: The supernatant after the first pull-down was incubated with rat IF-Cbl beads again. As the protocol described above, the beads were washed and applied to reducing SDS-PAGE (7.5%), followed by Western blot. The first antibody was a rabbit-anti-dog cubilin (1:20,000), and the secondary antibody was a goat-anti-rabbit IgG alkaline phosphatase conjugate (1:20,000).

Immunohistochemistry

Sections of normal and affected dog kidney cortex were fixed briefly in phosphate buffered 4% paraformaldehyde, sliced to 1.5 mm thickness, and immersed for 48 h in phosphate buffered 1% paraformaldehyde. Thin sectioning and peroxidase-labeled immunostaining for light microscopy was as previously described (Birn et al., 2000). Primary antibody was a 1:4000 dilution of previously described rabbit polyclonal anti-canine cubilin serum that did not cross-react with AMN (Xu and Fyfe, 2000; Birn et al., 2000).

Transfection study

I. Plasmid construction

JCF 381 5'-TTT AAA GCT TCG GGC GCG CGG CGG CAT G-3'

JCF382 5'-TTA TAA GCT TGG CCT CGG CCT CGG CGA AC-3'

We did full-length RT-PCR for the normal *AMN* with primers JCF381 and JCF382 to introduce *HindIII* restriction sites, which are underlined above. With the same primers,

we amplified the 33del mutant *AMN* cDNA from a plasmid pGEX-33del-AMN. The PCR products were first cloned into the pCR®-2.1 TOPO® cloning vector (Invitrogen), then subcloned into the vector pcDNA-5xmyc (a gift from Dr. Tanner) at the *HindIII* sites. The plasmids harboring either normal or mutant canine c*AMN* were sequenced to confirm integrity of the inserts before being transfected into the CHO cells.

II. Transfection

The cDNA encoding amino acids 1-1389 of rat cubilin was ligated into the *XbaI* and *HindIII* sites of the expression vector pcDNA3.1/Zeo(-) (Invitrogen) and stable, single-transfected Zeocin-resistant Chinese Hamster Ovary (CHO) cell clones were established as described (Kristiansen et al., 1999). Establishment of stable, double-transfected CHO clones expressing both the cubilin construct and myc-labelled canine AMN was carried out by transfection with the plasmids described in I, and selection with 1 mg/mL Geneticin® (Invitrogen). Expression products of all clones were analyzed by immunoblotting of cell lysates using rabbit polyclonal antibody against rat cubilin and an anti-myc-antibody (Invitrogen) for AMN detection. For endo H digestion, CNBr-activated Sepharose 4B beads (Amersham Biosciences) coupled with porcine IF-cobalamin as previously described (Birn et al., 1997) were incubated with cell lysates of double transfected CHO cells for pull-down of recombinant cubilin. The beads were suspended in 50 mM sodium citrate, pH 5.5, 0.02 % SDS and incubated over night at 37° C with endo H (Roche) prior to SDS-PAGE and immunoblotting.

III. Confocal immunofluorescence microscopy

Immunofluorescent analyses of CHO cells expressing cubilin/AMN(33del), and cubilin/AMN were performed on living non-permeabilized cells. Living cells were

incubated for 90 min at 4°C with a polyclonal antibody against rat cubilin diluted to 10 mg/mL in growth medium. Cells incubated first with the primary antibody at 4°C were fixed for 1 hour at 4°C. Finally, the cells were incubated for 1 hour at room temperature with the secondary antibody: Alexa Fluor 488 goat anti-rabbit IgG (Molecular Probes) diluted 1:200. Stained cells were examined by confocal fluorescence microscopy using a laser scanning confocal unit (LSM510, Carl Zeiss) attached to an Axiovert microscope.

Results

mRNA expression pattern

RT-PCR demonstrated full-length *AMN* transcripts as expected in tissues of known *CUBN* expression, including kidney cortex, jejunum, and ileum (Figure 5.1). Both genes were also expressed in thymus but at very low levels. In addition, *AMN* was expressed in colon, liver, pancreas, and pituitary tissues where *CUBN* cDNA was not detected, and *CUBN* was expressed in placenta where *AMN* was not detected. Shortened RT-PCR amplification products were detected in small amounts in tissues where *AMN* was expressed. Sequencing of one of these that was amplified from ileal RNA demonstrated absence of exons 9 and 10, exactly, and predicted a secreted translation product of 262 residues (~ 30 kDa).

Characterization of the anti-AMN antibody

Although the cubam complex was affinity purified and enriched, numerous other proteins still coexisted with the cubam complex (Fyfe, unpublished data). Therefore, the gel-loaded materials for Western blot not only contained cubilin and AMN, but also contained many unspecific proteins. Three bands between 37 kDa and 50 kDa were seen in the lane blotted against the affinity-purified anti-AMN antibody, but absent in all the other control lanes, such as preimmune serum, flowthrough of the peptide-affinity-column-absorbed-serum, or secondary Ab only (Figure 5.2). Independent study indicated that the highest band represented the full-length AMN, while the two lower bands represented two truncated AMN isoforms (Fyfe, unpublished data). Thus the antibody is specific to the epitope (residues 340-353) of canine AMN.

Pull down assay and Western Blot

We first did anti-AMN Western blot with the kidney cortex homogenate from a normal dog but failed to detect any specific bands, indicating that the AMN protein was expressed at a low level *in vivo* (data not shown). We thus used the IF-Cbl beads to indirectly pull down the AMN via cubilin, because cubilin has been shown to form a tight complex with AMN (Fyfe et al., 2004). Western blot of the pulled-down proteins with the anti-canine AMN peptide serum (Figure 5.3, upper left) demonstrated three immunospecific proteins between 37 kDa and 50 kDa in the normal dog. None of the 3 immunoreactive proteins were observed on Western blots of proteins from kidney cortex of an affected dog of the GS kindred or the AS kindred (Figure 5.3, upper middle and upper right). In order to test if the beads were indeed saturated with cubilin during the first pull-down, we incubated the supernatant of the pull-down assay with IF-Cbl beads for the second time, and subjected the material bound to the beads to Western blotting with anti-cubilin. The cubilin band was present in all the three samples, indicating that the beads in the first pull-down assay were saturated with cubilin in both normal and affected dogs (Figure 5.4).

Renal proximal tubule expression of cubilin in the absence of detectable AMN expression was also examined by immunohistochemistry. As previously demonstrated (Birn et al, 2000; Kozyraki et al, 1999), cubilin immunoreactivity was found predominantly at the apical brush border of the plasma membrane in normal dog proximal tubule epithelial cells (Figure 5.3, lower left). In contrast, cubilin immunoreactivity was found entirely in an intracellular vesicular pattern, with no

detectable labeling of the luminal epithelial cell plasma membrane in proximal tubules, in affected dogs of both kindreds (Figure 5.3, lower panel).

Transfection study and immunofluorescence

To further investigate the effect of the canine *AMN* c.1113_1145del mutation on cubilin expression, we cloned the full-length normal and mutant canine *AMN* open reading frames into a previously described *AMN*-Myc expression plasmid (Tanner et al., 2003) and transfected Chinese hamster ovary (CHO) cells that already expressed a truncated construct of rat cubilin containing the membrane association and IF-cobalamin binding domains (Fyfe et al., 2004). In our efforts to clone the PCR products of the canine *cAMN* into the expression vector, a high mutation rate (>0.002) was observed by directly sequencing the recombinant plasmids. The mutations were deemed to be due to the Taq polymerase, because different plasmid clones showed different mutations while sequencing the total PCR products didn't reveal any mutation. Interestingly, we noticed that about 65% of the mutations in the plasmids were G/C>A/T, indicating that the polymerase tended to incorporate more A/T into the products than it should be. Considering that the *cAMN* is GC-rich (78%), we decided to increase the GC content of the dNTP mix from 50% to ~70% for PCR ((G/C):(A/T)=2.5:1). In addition, the Expand[®] high fidelity PCR system (Roche) was used to decrease the error rate of the DNA polymerase. Consequently, the mutation rate was decreased to about 0.001 and the target plasmid clones were obtained.

Stable double transfectants were selected and incubated with anti-cubilin antibody. The cells were subsequently incubated with fluorescently labeled secondary antibody,

and analyzed by confocal microscopy. Cells transfected with normal canine *AMN* cDNA exhibited surface expression of cubilin, but cells transfected with the mutant *AMN* cDNA did not (Figure 5.5). Presence of the normal and mutant AMN proteins in their respective cell lines was confirmed by Western blot of cell homogenates (Figure 5.6, upper panel). Cubilin in each cell line was examined by Western blot. In cells expressing wildtype canine AMN, cubilin was detected as 2 distinct bands (Figure 5.6, lower panel), the larger of which was endo H resistant and the smaller of which was endo H sensitive (data not shown). In cells expressing the c.1113-1145del mutant AMN, cubilin was detected as a single, endo H sensitive band that comigrated with the smaller species observed in the wildtype AMN cell line.

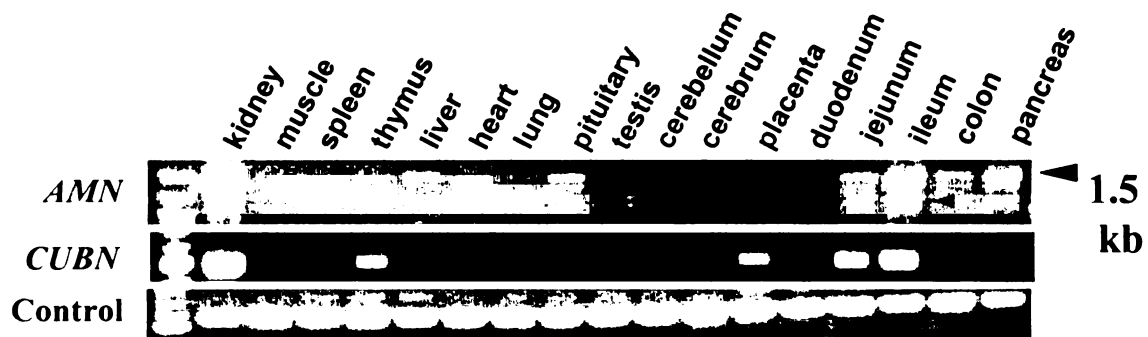


Figure 5.1 RNA expression profiles of cubilin and AMN. Full-length *AMN* and *CUBN* are co-expressed in kidney and ileum, and to a minor extent in jejunum and thymus. Cyclophilin D was used as a control. In the ileum, at least 2 minor bands were seen. Sequencing one of them revealed a product missing exon 9 and 10 exactly, indicating it is an alternative splicing product.

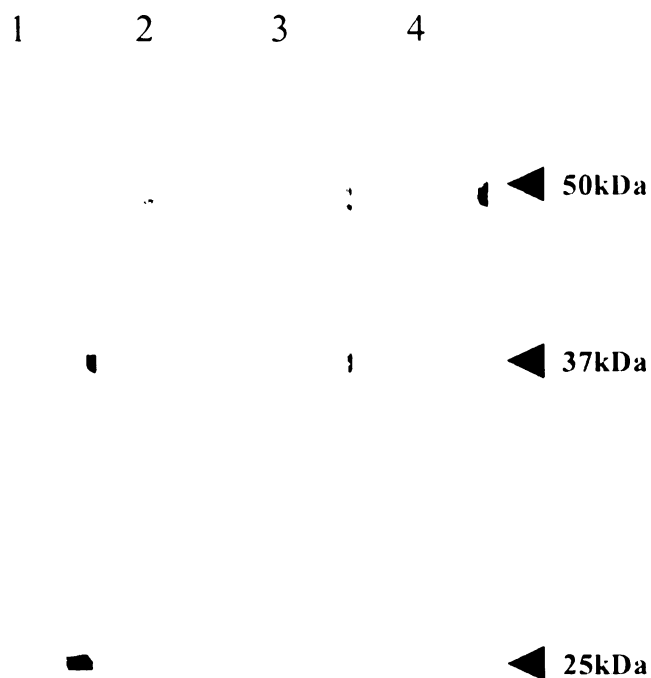


Figure 5.2 Specificity test of the anti-AMN antibody. Affinity-column-concentrated cubam was subjected to reducing SDS-PAGE (12%) and Western blot with different antibodies or serum. It should be pointed out that the concentrated cubam still contained many unspecific proteins because of technical limits. Three bands are present in the anti-AMN lane (lane 2), but absent in the other three control lanes. Lane 1, flowthrough of the affinity-column-absorbed-serum (1:40,000); Lane 2, anti-AMN (1:40,000); Lane 3, secondary antibody only (1:20,000); Lane 4, preimmune serum (1:20,000).

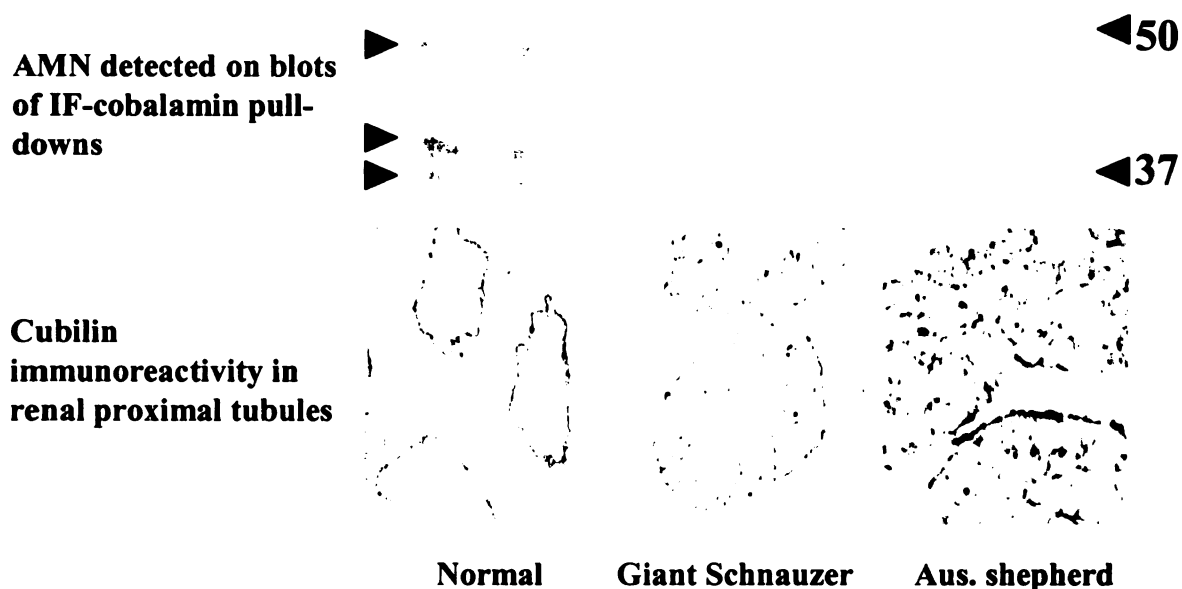


Figure 5.3 Cubilin and AMN expression in normal and I-GS affected dog kidneys *in vivo*. Images in this dissertation are presented in color.

Upper panel: Anti-AMN Western blot of proteins pulled-down by rat IF-Cbl beads from normal (left), GS kindred affected (center), and AS kindred affected (right) dog kidneys. Three AMN isoforms were seen in the normal dog (left), but absent in the affected dogs of both kindreds (middle and right).

Lower panel: Cubilin staining of permeabilized renal cortex in normal (left) and I-GS affected dogs of the GS (center) and AS (right) kindreds expressing 33bp-del *AMN* mutant and G>A *AMN* mutant, respectively. Cubilin showed surface staining in the normal dog, but abnormally intracellular staining in the affected dogs of both kindreds.

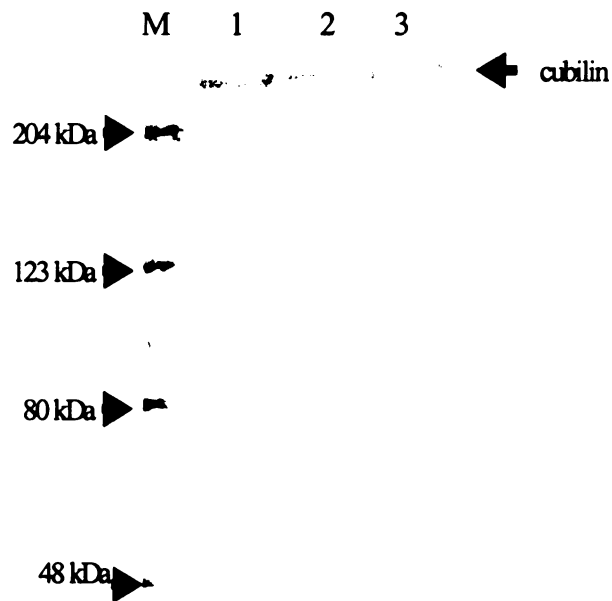


Figure 5.4 Cubilin saturation test. The second pulled-down materials by IF-Cbl beads (described in the Materials and Methods) were subjected to SDS-PAGE (7.5%) and blotted against anti-cubilin. The cubilin band was present in all the three samples, indicating that the beads in the first pull-down were saturated by cubilin. M, marker; Lane 1, a normal dog; Lane 2, an affected dog from GS kindred; Lane 3, an affected dog from AS kindred.

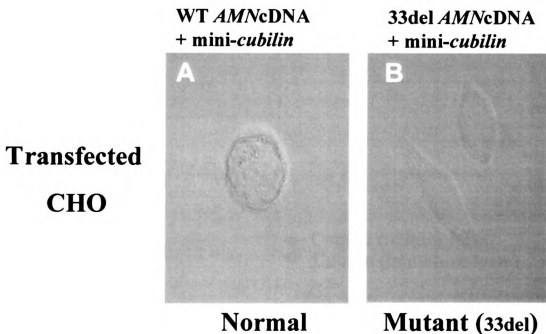


Figure 5.5 Immunofluorescence of double transfected CHO cells expressing cubilin and AMN (the cells were not permeabilized). CHO cell lines expressing a 'mini-cubilin' construct of rat origin were additionally transfected with wildtype (WT) or c.1113-1145del (mut) canine *AMN* cDNA constructs, and stable transfectants expressing cubilin and AMN were selected. Non-permeabilized cells were stained for fluorescence confocal microscopy by incubation at 4°C with anti-cubilin and subsequently with labeled anti-rabbit IgG. Abundant surface cubilin staining was observed in cells expressing wildtype, but not mutant AMN.

Images in this dissertation are presented in color.

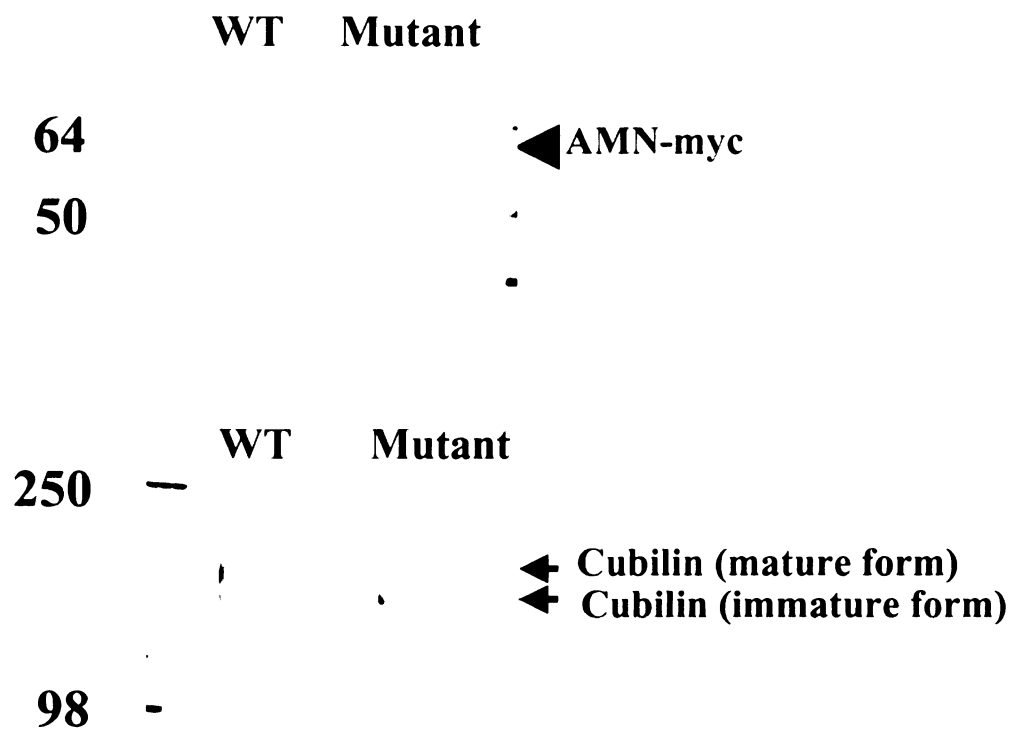


Figure 5.6 Cubilin and AMN expression in CHO cells with wildtype or c.1113-1145del *AMN* cDNA. Note the CHO cells already contain a mini-cubilin construct.

Upper panel: Lysates of double transfectant cell lines were subjected to Western blotting with anti-myc confirming expression of wildtype and mutant AMN.

Lower panel: Lysates of double transfectant cell lines were subjected to IF-Cbl pull-down and Western blotting with anti-cubilin. The upper band is Endo H resistant (data not shown) and observed only in cells expressing wild type AMN. The lower band is Endo H sensitive (data not shown) and seen in both cells. Endo H sensitivity usually means that the protein has not undergone Golgi-mediated oligosaccharides processing. The results suggest that cubilin could not complete the Golgi-mediated glycosylation without the assistance of AMN.

Discussion

I-GS is a unique, recessively inherited disorder characterized by selective intestinal cobalamin malabsorption and proteinuria due to loss of specific receptor functions in intestinal and renal proximal tubule epithelia. Studies in human cadaver kidney suggested that the functional receptor for IF-cobalamin in intestine and for multiple protein ligands in renal proximal tubules is a complex of cubilin and AMN, now called cubam (Fyfe et al., 2004). Although more than 10 different mutations have been identified in the two genes, no studies of *CUBN* or *AMN* expression in human I-GS patient tissues have been reported.

Our data confirmed that both AMN and cubilin have ample mRNA expression in kidney and intestine, where malfunctions of cubam cause detectable defects. However, the tissues that have AMN but not cubilin expression, such as liver, pituitary and pancreas, are all somehow involved in protein secretion. It is tempting to think, although very preliminary at this stage, that AMN may assist some proteins' secretion in those tissues.

In our pull-down assay, 3 isoforms of the AMN proteins were found in the normal kidney, but absent in the two affected dogs' kidney. Independent experiments by LC/MS/MS mass spectrometric mapping and Western blot indicated that the highest Mr band represents the full-length AMN, while the two smaller bands represent C-terminal truncated AMN (Fyfe, unpublished data). Our second pull-down assay assured that the beads of the first pull-down were saturated with cubilin. Previous data (Fyfe et al., 1991b) also indicates that renal cubilin of GS kindred affected dogs has normal affinity ($K_d \approx 1 \times 10^{-10}$ M) for IF-Cbl. Thus, the absence of AMN bands in the affected dogs was

not due to insufficient cubilin in the kidney homogenates, but due to lack of the cubam complex in the kidney homogenates. In conclusion, the pull-down assay demonstrates that no cubam is expressed in the kidney proximal tubule cells of the two affected dogs.

An interesting fact of the canine I-GS disease is that cubilin is affected by mutations in AMN. It was demonstrated that cubilin failed to reach the apical microvillus surface membrane of villus tip enterocytes (Fyfe et al., 1991a). The specific activity of cubilin in the affected dogs' brush border membrane (BBM) was significantly less in ileum and renal cortex than in BBM of the corresponding tissue of normal dogs. In addition, cubilin in kidney of affected dogs was endo H sensitive, indicating that it had not undergone Golgi-mediated N-glycosylation processing, and peptide mapping by trypsin and elastase suggested that the protein was incompletely folded (Fyfe et al., 1991b; Xu and Fyfe, 2000). Those *in vivo* findings were consistent to the results presented here that cubilin expressed in CHO cells with *AMN* c.1113-1145del did not reach the plasma membrane and, as indicated by cubilin endo H sensitivity, was retained in an early biosynthetic compartment. The effects of the canine *AMN* mutation on cubilin expression in this heterologous expression system were identical to those observed when no AMN was expressed (Fyfe et al., 2004). When overexpressed in CHO cells, the AMN deletion mutant protein was detected but was apparently incapable of forming a required quaternary interaction with cubilin. Combined with the immunohistochemistry data, these findings are compatible with an active quality-control function of the RER in proximal tubules and suggest that cubilin and AMN must interact together in the RER for protein stability, to become competent for RER exit, and for efficient apical membrane cubam expression.

We then ask, in the pull-down assay, what is the molecular basis for the absence of the three AMN bands in the two affected dogs? For the AS kindred carrying the start codon mutation, it is very likely that the AMN protein was not translated at all, due to loss of the translation initiation site. However, for the GS kindred carrying the 33 bp deletion, two hypotheses are currently in consideration. The first hypothesis is that the 33del AMN mutant is simply secreted out of the proximal tubule cells. The second hypothesis is that the 33del mutant did not fold properly and was targeted for rapid degradation. Based on the current paradigm of protein biosynthesis, a possible scenario is that the 33del mutant completely enters the lumen of ER (because it loses its anchor domain), then binds to immature cubilin but fails to help cubilin fold correctly, which results in rapid degradation. Previous experiments demonstrated that the IFCR activity in the kidney homogenates of affected dogs was significantly less than that in the normal dogs (Fyfe et al., 1991b). A pulse-chase labeling study in kidney slices indicated that immunoprecipitable renal cubilin of affected dogs had a shortened half-life than that of a normal dog (Fyfe, unpublished data), suggesting that the misfolded cubilin was subject to degradation. However, these facts do not exclude either of the two hypotheses. Further experiments are needed to make more conclusive statements. Unfortunately for this investigation, none of the anti-dog, human or mouse AMN peptide antibodies produced to date function in immunohistochemical detection of AMN in canine tissue.

The three isoforms of AMN could originate from alternative splicing products, or be created by a posttranslational mechanism. Another possibility is that they are simply due to *ex vivo* proteolysis. Interestingly, AMN isoforms were also observed in the IF-Cbl affinity purified materials from human kidney homogenates (Fyfe et al., 2004). Further

study with the CHO transfectants using anti-AMN antibody instead of anti-Myc antibody may provide some clues.

In mice, AMN is expressed exclusively in an extra-embryonic tissue, visceral endoderm, during the early post-implantation stages. *Amn* knockout mice fail to assemble a normal middle primitive streak and have developmental arrest after E7.0 (Tomihara-Newberger et al., 1998). This phenotype is strikingly different from the phenotypes in humans and dogs. Though unknown as yet, cubilin and AMN likely collaborate to perform an essential endocytic function in rodent embryonic tissue that is not required or is performed by redundant mechanisms during human and canine embryogenesis. On the other hand, the three species do share some traits in common. Recently studies with *Amn*^{-/-} ES cell ↔ +/+ blastocyst chimeras demonstrated that cubilin is not properly localized to the cell surface in *Amn*^{-/-} tissues in the embryo and adult mouse (Strope et al., 2004), suggesting that in the enterocytes and proximal tubules cubam is a complex conserved across the mammal species.

Because *AMN*^{-/-} and *CUBN*^{-/-} patients have indistinguishable phenotypes, AMN as an accessory factor may solely serve cubilin for its expression on the cell surface in intestine and kidney. Such a “receptor-accessory factor” concept has been recapitulated in another study, in which melanocortin 2 receptor accessory protein (MRAP), a 19-kDa single-transmembrane domain protein, is responsible for the familial glucocorticoid deficiency (FGD) which can be caused by mutated melanocortin 2 receptor as well (Metherell et al., 2005).

In sum, in both kindreds, effectively null AMN mutations block trafficking of cubilin to the apical plasma membrane and, thereby, all cubam-mediated endocytic

functions, confirming a previous prediction by Xu et al. (1999) that an accessory factor is required for cubilin's surface expression and function. Although some questions have been answered in this study, many questions remain to be explored in the future. For example, what is the fate of the 33del mutant AMN? If stable, what is the structure of the 33del mutant AMN? What happens if AMN alone is expressed in the CHO cells? Can we ascertain the essential role of AMN in dog embryonic development? Are there any other roles of AMN in tissues where no cubilin is expressed? If yes, what are those partners? We hope this canine model of I-GS will continue to help us understand the function of AMN, and hopefully, shed light on the developmental biology.

Appendices

A brief report of mutation screening in a beagle and a komondor dog with I-GS

In addition to GS and AS kindreds, I-GS has also been found in two other breeds of dogs. One of them is a beagle (Shamus) showing typical symptoms of congenital selective cobalamin (Cbl) malabsorption, including failure to thrive, methylmalonic aciduria and anemia. The dog had low serum Cbl concentration. Periodic injections of parenteral vitamin B12 corrected the Cbl deficiency and obliterated all the clinical abnormalities (Fordyce et al., 2000). The other one is a komondor (K101) with similar clinical presentations (Fyfe, unpublished data).

Without fresh tissues to extract mRNA, we isolated blood DNA from the two affected dogs. Genomic PCR were performed as described in chapter 3. Most exons, exon-intron boundaries were amplified and sequenced. Sequences of partial exon 6 and partial exon 10 were not obtained in both dogs either because of failure of the PCR or poor quality of the sequencing results. No mutations were identified. A noteworthy fact is that the 33 bp deletion in GS kindred and the G>A mutation in AS kindred were not observed in either of the two dogs.

A 5 bp deletion was found in both dogs compared to an unrelated normal dog (DCCU6110). The deletion is located at the 3' end of the intron 6, but the accurate deletion sites could not be determined because of the presence of two flanking AG dinucleotide (Figure 6). Two lines of evidence suggest that the deletion is not a mutation. First, the deletion does not change the conserved acceptor sequence (N(C/T)AG | G) for splicing (Mount, 1982). Second, the 5 bp deletion was also present in a normal komondor

dog (K100). We therefore concluded that the 5 bp deletion is a nondeleterious polymorphism.

Allele I.	gtcaccccgttcctccgc <u>ag</u> tgagGTGCAGCCCTGGATCTGCGCGGCCC
Allele II.	gtcaccccgttcctccgc-----agGTGCAGCCCTGGATCTGCGCGGCCC

Figure 6. The 5 bp polymorphism of AMN identified in a komondor and a beagle. The two ag dinucleotide are underlined. The lower case letters represent partial intron 6, while the capital letters represent partial exon 7 of AMN.

At least three possibilities should be considered in future study. First, the mutation(s) may locate in the exon 6 or exon 10 for which we didn't get complete sequences due to technical difficulties. Second, the unsequenced introns, 5'UTR or 3'UTR of AMN may harbor the mutation(s), which may introduce defects by altering the mRNA splicing product. Third, cubilin or another gene may be the disease-causing gene. RT-PCR and linkage analysis will help to clarify these possibilities.

Table 4 Genotyping data of the Giant Schnauzer family. In the “KNS2” column, the shaded genotypes were deduced from genotypes or haplotypes of their first-degree relatives. Notations: 1) In the “I-GS” column: N, Normal; C, Carrier; A, Affected.

2) “?” represents unknown or uncertain genotype.

DOG ID	Sire	Dam	I-GS	Stonin	EML1	EIF5	KNS2	SIVA	G2A
F100			A				TT		
F114			C				CT		
M721			N	CC					
M811			N	CT					
M874	M721	M811	N	CT	GG?		CC		GG
F70			A	CC					AA
F146	F114	F100	A	CC	AG	AA	TT	CT	AG
F150	F70	A66	C	CC	GG		TC	CT	AA
F153	F70	A66	C						
F154	F70	A66	C	CC					AG
F155	F70	A66	C	CC					AA
F227	F150	F146	A	CC	GG		TT	CC	AA
F233	F150	F155	A	CC			TT		
F274	A323	F233	C	CT	AG	AT	TC	CT	AG
F275	A323	F233	C	CC	AG		TC		AG
F283	F150	F146	A	CC	AG		TT	CT	AG
F284	F150	F146	A	CC	GG	AA	TT	CC	AA
F294	F227	F154	A	CC					AA
F303	F227	F275	C		AG				AG
F304	F227	F275	C		AG				AG
F305	F227	F275	C		GG?				AG
F306	F227	F275	C		AG				AG
F307	F227	F275	C		AG				AG
F309	F274	F146	A	CC					
F310	F274	F146	A	CT					
F311	F274	F146	A	CT					
F324	F274	F284	A	CC	GG		TT		AA
F325	F274	F284	C	CT	AG		TC		AG
F326	F274	F284	C	CT	AG		TC		AG
F327	F274	F284	A	CC	GG		TT	CC	AA
F328	F274	F284	A	CC	GG		TT		AA
F329	F274	F284	A	CC	GG		TT		AA
F330	F274	F284	C	CT	AG		TC		AG
F331	F227	F275	C		AG				AG
F342							TT		
F343	F294	F146	A	CC	GG		TT		AA
F348	F283	F275	A						

Table 4 (cont'd)

DOG ID	Sire	Dam	I-GS	Stonin	EML1	EIF5	KNS2	SIVA	G2A
F349	F283	F275	A				TT		
F350	F283	F275	C						
F351	F283	F275	C						
F352?	F283	F275	C						
F353	F283	F275	C						
F354	F283	F275	C						
F355	F283	F275	C						
F358	F274	F284	A	CC	GG		TT		AA
F359	F274	F284	A	CC	GG		TT		AA
F360	F274	F284	A	CC	GG		TT		AA
F361	F274	F284	A	CC	GG		TT		AA
F362	F274	F284	A	CC	GG		TT		AA
F363	F274	F284	C	CT	AG		CT		AG
F366	F274	F146	A	CC					
F367	F274	F146	A	CC					
F368	F274	F146	C	CT					
F369	F274	F146	A	CT					
F370	F274	F146	A	CC					
F372	F274	F146	C	CT					
F373	F274	F146	C						
F374	F274	F146	A	CT					
F375	F274	F146	C	CT					
F380	F274	F284	C						
F381	F274	F284	A	CT	GG		TT		AA
F382	F274	F284	A	CC	GG		TT		AA
F384	F274	F284	A	CC	GG		TT	CT	AG
F388	F274	F327	C	CT	AG?				
F389	F274	F327	C	CC	AG	AT	CT		AG
F390	F274	F327	A	CC	GG		TT		AA
F398	F274	F343	A	CC	GG		TT		AA
F399	F274	F343	C	CT	AG		CT		AG
F400	F274	F343	A	CT	GG		TT		AA
F411	F342	F343					TT		
F414	F342	F343					TT		
F415	F342	F343					TT		
F428	F274	F284	A	CC	GG		TT		AA
F442	F274	F284	C	CT	AG		CT		AG
F445	F342	F343	A	CC	AG		TT	CT	AG
F446	F342	F343					TT		

Table 4 (cont'd)

DOG ID	Sire	Dam	I-GS	Stonin	EML1	EIF5	KNS2	SIVA	G2A
F451	F274	F327	C	CT	AG		CT		AG
F453	F274	F327	A	CT	AG	AA	TT		AA
F454	F274	F327	A	CC	GG		TT		AA
F455	F274	F327	A	CC	GG		TT		AA
F458	F274	F284	A	CC	GG		TT		AA
F459	F274	F284	A	CC	GG		TT		AA
F460	F274	F284	A	CT	AG	AA	TT		AA
F461	F274	F284	A	CC	GG		TT		AA
F462	F274	F284	A	CC	GG		TT		AA
F463	F274	F284	C	CT	AG		CT		AG
F470	F445	F343					TT		
F472	F445	F343					TT		
F477	F274	F284	A	CC					AA
F478	F274	F284	C	CT	AG		CT		AG
F481	F274	F442	A	CC	GG				AA
F482	F274	F442	?	CT	AG				
F483	F274	F442	?	CC	AG				
F484	F274	F442	?	CT	AG				
F485	F274	F442	?	CT	AG				AG
F497	F445	M874	C	CT	AG		TC		GG
F498	F445	M874	C	CC	GG		TC		AG
F499	F445	M874	C	CT	GG		TC		GG
F500	F445	M874	C	CT	AG		TC		GG
F501	F445	M874	C	CC	GG		TC		
F505	F274	F442	A	CC					
F506	F274	F442	?	CC	AG				
F507	F274	F442	?	TT	AG				
F508	F274	F442	?						
F509	F274	F442	?	CT	AG				
F510	F274	F442	?						
F511	F274	F442	?						
F512	F274	F442	?						
F532	F445	F497	C	CT					
F533	F445	F497	C	CT					
F535	F445	F497	A	CC					
F536	F445	F497	A	CC					
F537	F445	F497	A	CC	AA				
F538	F445	F497	C	CT					
F539	F445	F497	C	CT					GG
F540	F445	F497	C	CT					

Table 5 Genotyping data of the Australian Shepherd kindred. The notation “c.normal” represents “clinically normal”.

Lab ID	NAME	Sex	Disease status	<i>AMN</i>	<i>KNS2</i>	<i>CUBN</i>
B100	Buddy Henry	M	affected	AA	CC	II
B101	H. Floxy	F	carrier	AG	CT	IO
B102	H. Boo	M	carrier	AG	CT	II
B103	H. Bits of Clover	F	c. normal	GG		
B104	Twiggy	F	c. normal	AG		
B105	H. Red Chili	M	c. normal	GG		
B106	H. Tux	M	c. normal	GG		
B107	H. Cozy Kitten	F	c. normal	GG		
B108	H. Keeper	F	c. normal	AG	CC	IO
B109	H. Blue Clipper	M	c. normal	GG	CT	IO
B110	Rodeo	M	c. normal	GG		
B111	South Twenty's R.	F	c. normal	GG		
B112	H. Kiss of Rain	F	c. normal	GG	CT	OO
B113	Champ	M	c. normal			
B114	H. Cheerio	F	c. normal			
B115	Snoopy	F	c. normal	AG		
B116	H. Zackery	M	c. normal	GG		
B117	H. Banjo	M	c. normal	GG	CT	II
B118	CR Poke Weed	M	c. normal		TT	IO
B119	Trevor	M	c. normal	GG		
B120	H. Cheshire Cat	F	c. normal		TT	IO
B121	Sidney Daniels	M	affected	AA	CC	II
B122	Maddie Martin	F	affected	AA	CC	IO
B123	Sassy b: 6-30-03	F	c. normal	GG		
B124	Angel	F	c. normal	GG		
B125	Pixie b: 1-20-04	F	c. normal	GG		
B126	Karri b: 1-3-04	F	c. normal	AG		
B127	H. Lacey Lady	F	c. normal	AG		

FUTURE DIRECTION

The beagle and the komondor dog with I-GS will be screened more extensively for potential *AMN* mutations. At the same time, complementation tests (breeding tests) could be done to ascertain that *AMN* is the disease-causing gene. *CUBN* will be considered for mutation screening too. Should *AMN* and *CUBN* be ruled out, the komondor dog family will be expanded for a positional cloning project.

The AMN peptide antibodies currently in our hands only worked under reducing conditions in Western blot, and do not work in the immunohistochemistry. Therefore, we need to develop new antibodies.

More experiments could be done to characterize the 33del mutant AMN. Directly assessing the existence of the mutant AMN in the affected dogs' urine may be difficult, because the amount of the AMN is probably too low. Instead, the cell culture medium of the CHO double transfectants should be examined to see if the mutant AMN is secreted out of the cell. Crystallization could be pursued to study the structure of the normal and mutant AMN.

Current data suggest that cubilin binds to the N-terminal of AMN, but the exact binding site is unknown. Different *AMN* cDNA mutants will be constructed *in vitro* and tested in the CHO cell system to accurately locate the binding site of AMN to cubilin. These mutants may also help to identify the minimal length of AMN's N-terminus that is required for cubilin's folding and surface expression, and the minimal length of AMN's C-terminus for endocytosis.

Should new anti-AMN antibody be available, the CHO cells transfected with wild type cubilin and wild type AMN-5myc will be subject to Western blot with anti-AMN

antibody. If three isoforms are seen as those in the kidney homogenates, further characterizations, such as cubilin-binding ability, glycosylation, cellular localization, will be pursued for the AMN isoforms.

It is not known whether that AMN's surface expression requires cubilin. Single AMN-transfectant of CHO will be subjected to both Western blot and immunofluorescence surface staining, to determine the molecular weight and location of AMN in the absence of cubilin.

Most of the studies of cubam so far were performed with kidney tissues. It may be necessary to directly address the role of cubam in the intestine tissues, where the vitamin B12 malabsorption actually occurs. Affinity chromatography purification, IF-Cbl pull down, Western blot, mass spectrometry mapping may be used to characterize the intestinal cubam complex.

In the tissues where AMN is expressed but cubilin is not, a yeast two hybrid system could be used to look for potential partners for AMN. Briefly, the cDNA of *AMN* would be cloned into the vector pGBKT7 (Clontech) as the bait, and mRNA from the target tissue, say, pancreas, would be reverse-transcribed into double-stranded cDNA. Subsequently the pGBKT7-bait, cDNA pool and another vector pGADT7-Rec (Clontech) are cotransformed into the yeast for screening. Once new partners have been identified, at least three approaches should be considered. First, it should be confirmed that the new protein interacts with cubilin/AMN *in vitro*. Second, the interaction of the new protein and cubilin/AMN should be examined in appropriate cell-based studies. Third, knock out mouse of the new protein could be produced. If the phenotype is embryo lethal, chimera mouse may be made to determine the function of the gene.

To assess the potential role of AMN or cubilin in the embryo development, extra-embryonic tissues (including visceral endoderm and yolk sac) of dogs would be screened for AMN and cubilin expression at RNA level and protein level. In the tissues that have both AMN and cubilin expressions, IF-Cbl pull down assay would be used to detect if cubam exists. If cubam does present in the tissue of interest, it would be intriguing to find out the partners of AMN, since the cysteine-rich domain of AMN has been suggested to be interacting with some BMP inhibitors. These experiments may give us more insights of the signaling pathways involved in embryo development.

REFERENCES

- Abdelaal MA, Ahmed AF. Imerslund-Gräsbeck syndrome in a Saudi family. *Acta Paediatr Scand*. 1991; 80(11):1109-12.
- Al-Alami JR, Tayeh MK, Al-Sheyyab MY, El-Shanti HI. Linkage analysis of a large inbred family with congenital megaloblastic anemia. *Saudi Med J*. 2002; 23(10):1251-6.
- Allen RH, Majerus PW. Isolation of vitamin B12-binding proteins using affinity chromatography. II. Purification and properties of a human granulocyte vitamin B12-binding protein. *J Biol Chem*. 1972a; 247(23):7702-8.
- Allen RH, Majerus PW. Isolation of vitamin B12-binding proteins using affinity chromatography. 3. Purification and properties of human plasma transcobalamin II. *J Biol Chem*. 1972b; 247(23):7709-17.
- Allen RH, Mehlman CS. Isolation of gastric vitamin B 12 -binding proteins using affinity chromatography. I. Purification and properties of human intrinsic factor. *J Biol Chem*. 1973; 248(10):3660-9.
- Allen RH, Seetharam B, Podell E, Alpers DH. Effect of proteolytic enzymes on the binding of cobalamin to R protein and intrinsic factor. *J Clin Invest*. 1978a; 61(1):47-54.
- Allen RH, Seetharam B, Allen NC, Podell ER, Alpers DH. Correction of cobalamin malabsorption in pancreatic insufficiency with a cobalamin analogue that binds with high affinity to R protein but not to intrinsic factor. *J Clin Invest*. 1978b; 61(6):1628-34.
- Altay C, Cetin M, Gumruk F, Irken G, Yetgin S, Laleli Y. Familial selective vitamin B12 malabsorption (Imerslund-Gräsbeck syndrome) in a pool of Turkish patients. *Pediatr Hematol Oncol*. 1995; 12(1):19-28.
- Amagasaki T, Green R, Jacobsen DW. Expression of transcobalamin II receptors by human leukemia K562 and HL-60 cells. *Blood*. 1990; 76(7):1380-6.
- Aminoff M, Tahvanainen E, Gräsbeck R, Weissenbach J, Broch H, de la Chapelle A. Selective intestinal malabsorption of vitamin B12 displays recessive mendelian inheritance: assignment of a locus to chromosome 10 by linkage. *Am J Hum Genet*. 1995; 57(4):824-31.
- Aminoff M, Carter JE, Chadwick RB, Johnson C, Gräsbeck R, Abdelaal MA, Broch H, Jenner LB, Verroust PJ, Moestrup SK, de la Chapelle A, Krahe R. Mutations in *CUBN*, encoding the intrinsic factor-vitamin B12 receptor, cubilin, cause hereditary megaloblastic anaemia 1. *Nat Genet*. 1999; 21(3):309-13.
- Argaves WS, Morales CR. Immunolocalization of cubilin, megalin, apolipoprotein J, and apolipoprotein A-I in the uterus and oviduct. *Mol Reprod Dev*. 2004; 69(4):419-27.

Arwert F, Porck HJ, Frater-Schroder M, Brahe C, Geurts van Kessel A, Westerveld A, Meera Khan P, Zang K, Frants RR, Kortbeek HT, et al. Assignment of human transcobalamin II (TC2) to chromosome 22 using somatic cell hybrids and monosomic meningioma cells. *Hum Genet.* 1986; 74(4):378-81.

Babior BM. Cobalamin Biochemistry and Pathophysiology. 1975; Pg3-Pg14. By John Wiley&Sons, Inc.

Banerjee R and Ragsdale SW. The many faces of vitamin B12: catalysis by cobalamin-dependent enzymes. *Annual Review of Biochemistry.* 2003; 72: 209-247.

Batuman V, Verroust PJ, Navar GL, Kaysen JH, Goda FO, Campbell WC, Simon E, Pontillon F, Lyles M, Bruno J, Hammond TG. Myeloma light chains are ligands for cubilin (gp280). *Am J Physiol.* 1998; 275(2):F246-54.

Becker A, Geiger D, Schaffer AA. Automatic selection of loop breakers for genetic linkage analysis. *Hum Hered.* 1998; 48(1):49-60.

Becker M, Rotthauwe HW, Weber HP, Fischbach H. Selective vitamin B12 malabsorption (Imerslund-Gräsbeck syndrome). Studies on gastroenterological and nephrological problems. *Eur J Pediatr.* 1977; 124(2):139-53.

Ben-Ami M, Katzuni E, Koren A. Imerslund syndrome with dolichocephaly. *Pediatr Hematol Oncol.* 1990; 7(2):177-81.

Ben-Bassat I, Feinstein A, Ramot B. Selective vitamin B 12 malabsorption with proteinuria in Israel: clinical and genetic aspects. *Isr J Med Sci.* 1969; 5(1):62-8.

Bienzle U, Olischlager A, Leupold D, Kohne E, Harnisch R, Kleihauer E. Megaloblastic anaemia in childhood due to vitamin B12 deficiency, report of 3 cases of congenital selective vitamin B12 malabsorption. *Klin Padiatr.* 1976; 188(2):97-103.

Birn H, Verroust PJ, Nexø E, Hager H, Jacobsen C, Christensen EI, Moestrup SK. Characterization of an epithelial approximately 460-kDa protein that facilitates endocytosis of intrinsic factor-vitamin B12 and binds receptor-associated protein. *J Biol Chem.* 1997; 272(42):26497-504.

Birn H, Fyfe JC, Jacobsen C, Mounier F, Verroust PJ, Orskov H, Willnow TE, Moestrup SK, Christensen EI. Cubilin is an albumin binding protein important for renal tubular albumin reabsorption. *J Clin Invest.* 2000; 105(10):1353-61.

Boll W, Rapoport I, Brunner C, Modis Y, Prehn S and Kirchhausen T. The μ 2 subunit of the clathrin adaptor AP-2 binds to FDNPVY and YppO sorting signals at distinct sites. *Traffic.* 2002; 3(8): 590-600.

Booth CC, Mollin DL. The site of absorption of vitamin B12 in man. *Lancet*. 1959; 1(7062):18-21.

Breen M, Thomas R, Binns MM, Carter NP, Langford CF. Reciprocal chromosome painting reveals detailed regions of conserved synteny between the karyotypes of the domestic dog (*Canis familiaris*) and human. *Genomics*. 1999; 61(2):145-55.

Breen M, Jouquand S, Renier C, Mellersh CS, Hitte C, Holmes NG, Cheron A, Suter N, Vignaux F, Bristow AE, Priat C, McCann E, Andre C, Boundy S, Gitsham P, Thomas R, Bridge WL, Spriggs HF, Ryder EJ, Curson A, Sampson J, Ostrander EA, Binns MM, Galibert F. Chromosome-specific single-locus FISH probes allow anchorage of an 1800-marker integrated radiation-hybrid/linkage map of the domestic dog genome to all chromosomes. *Genome Res*. 2001; 11(10):1784-95.

Broch H, Imerslund O, Monn E, Hovig T, Seip M. Imerslund-Gräsbeck anemia. A long-term follow-up study. *Acta Paediatr Scand*. 1984; 73(2):248-53.

Brunaud L, Alberto JM, Ayav A, Gerard P, Namour F, Antunes L, Braun M, Bronowicki JP, Bresler L, Gueant JL. Effects of vitamin B12 and folate deficiencies on DNA methylation and carcinogenesis in rat liver. *Clin Chem Lab Med*. 2003; 41(8):1012-9. Review.

Bu G, Geuze HJ, Strous GJ, Schwartz AL. 39 kDa receptor-associated protein is an ER resident protein and molecular chaperone for LDL receptor-related protein. *EMBO J*. 1995; 14(10):2269-80.

Burman JF, Jenkins WJ, Walker-Smith JA, Phillips AD, Sourial NA, Williams CB, Mollin DL. Absent ileal uptake of IF-bound vitamin B12 in vivo in the Imerslund-Gräsbeck syndrome (familial vitamin B12 malabsorption with proteinuria). *Gut*. 1985; 26(3):311-4.

Christensen EI, Gliemann J, Moestrup SK. Renal tubule gp330 is a calcium binding receptor for endocytic uptake of protein. *J Histochem Cytochem*. 1992; 40(10):1481-90.

Christensen EI and Birn H. Megalin and cubilin: multifunctional endocytic receptors. *Nat. Rev. Mol. Cell. Biol*. 2002; 3(4): 256-266.

Cooper BA and Rosenblatt DS. Inherited defects of vitamin B12 metabolism. *Ann. Rev. Nutr*. 1987. 7: 291-320.

Cooperman JM, Luhby AL, Teller DN, Marley JF. Distribution of radioactive and nonradioactive vitamin B12 in the dog. *J Biol Chem*. 1960; 235:191-4.

Cottingham RW Jr, Idury RM, Schaffer AA. Faster sequential genetic linkage computations. *Am J Hum Genet*. 1993; 53(1):252-63.

Crider-Pirkle S, Billingsley P, Faust C, Hardy DM, Lee V, Weitlauf H. Cubilin, a binding partner for galectin-3 in the murine utero-placental complex. *J Biol Chem.* 2002; 277(18):15904-12.

Dan N, Cutler DF. Transcytosis and processing of intrinsic factor-cobalamin in Caco-2 cells. *J Biol Chem.* 1994; 269(29):18849-55.

Dix CJ, Hassan IF, Obray HY, Shah R, Wilson G. The transport of vitamin B12 through polarized monolayers of Caco-2 cells. *Gastroenterology.* 1990; 98(5):1272-9.

Dobson CM, Wai T, Leclerc D, Wilson A, Wu X, Dore C, Hudson T, Rosenblatt DS, Gravel RA. Identification of the gene responsible for the cblA complementation group of vitamin B(12)-responsive methylmalonic acidemia based on analysis of prokaryotic gene arrangements. *Proc. Nat. Acad. Sci.USA* 2002a; 99(24): 15554-15559.

Dobson CM, Wai T, Leclerc D, Kadir H, Narang M, Lerner-Ellis JP, Hudson TJ, Rosenblatt DS, Gravel RA. Identification of the gene responsible for the cblB complementation group of vitamin B12-dependent methylmalonic aciduria. *Hum Mol Genet.* 2002b; 11(26):3361-9.

Doscherholmen A, Hagen PS. Delay of absorption of radiolabeled cyanocobalamin in the intestinal wall in the presence of intrinsic factor. *J Lab Clin Med.* 1959; 54:434-9.

el Mauhoub M, Sudarshan G, Aggarwal V, Banerjee G. Imerslund-Gräsbeck syndrome in a Libyan boy. *Ann Trop Paediatr.* 1989; 9(3):180-1.

Eudy JD, Ma-Edmonds M, Yao SF, Talmadge CB, Kelley PM, Weston MD, Kimberling WJ, Sumegi J. Isolation of a novel human homologue of the gene coding for echinoderm microtubule-associated protein (EMAP) from the Usher syndrome type 1a locus at 14q32. *Genomics.* 1997; 43(1):104-6.

Fenech M. The role of folic acid and Vitamin B12 in genomic stability of human cells. *Mutat Res.* 2001; 475(1-2):57-67. Review.

Fordyce HH, Callan MB, Giger U. Persistent cobalamin deficiency causing failure to thrive in a juvenile beagle. *J Small Anim Pract.* 2000; 41(9):407-10.

Furuhjelm U, Nevanlinna HR. Inheritance of selective malabsorption of vitamin B12. *Scand J Haematol.* 1973; 11(1):27-34.

Fyfe JC, Jezyk PF, Giger U, Patterson DF. Inherited selective malabsorption of vitamin B12 in giant schnauzers. *Journal of the American animal hospital association.* 1989; 25:533-539.

- Fyfe JC, Giger U, Hall CA, Jezyk PF, Klumpp SA, Levine JS, Patterson DF. Inherited selective intestinal cobalamin malabsorption and cobalamin deficiency in dogs. *Pediatr Res.* 1991a; 29(1):24-31.
- Fyfe JC, Ramanujam KS, Ramaswamy K, Patterson DF, Seetharam B. Defective brush-border expression of intrinsic factor-cobalamin receptor in canine inherited intestinal cobalamin malabsorption. *J Biol Chem.* 1991b; 266(7):4489-94.
- Fyfe JC. Feline intrinsic factor (IF) is pancreatic in origin and mediates ileal cobalamin (cbl) absorption. *J Vet Intern Med.* 1993; 7:133.
- Fyfe JC, Madsen M, Hojrup P, Christensen EI, Tanner SM, de la Chapelle A, He Q, Moestrup SK. The functional cobalamin (vitamin B12)-intrinsic factor receptor is a novel complex of cubilin and amnionless. *Blood.* 2004; 103(5):1573-9.
- Gasparini P, Nunes V, Savoia A, Dognini M, Morral N, Gaona A, Bonizzato A, Chillon M, Sangiuolo F, Novelli G, et al. The search for south European cystic fibrosis mutations: identification of two new mutations, four variants, and intronic sequences. *Genomics.* 1991; 10(1):193-200.
- Gburek J, Verroust PJ, Willnow TE, Fyfe JC, Nowacki W, Jacobsen C, Moestrup SK, Christensen EI. Megalin and cubilin are endocytic receptors involved in renal clearance of hemoglobin. *J Am Soc Nephrol.* 2002; 13(2):423-30.
- Gburek J, Birn H, Verroust PJ, Goj B, Jacobsen C, Moestrup SK, Willnow TE, Christensen EI. Renal uptake of myoglobin is mediated by the endocytic receptors megalin and cubilin. *Am J Physiol Renal Physiol.* 2003; 285(3):F451-8.
- Gomez Lira M, Benetazzo MG, Marzari MG, Bombieri C, Belpinati F, Castellani C, Cavallini GC, Mastella G, Pignatti PF. High frequency of cystic fibrosis transmembrane regulator mutation L997F in patients with recurrent idiopathic pancreatitis and in newborns with hypertrypsinemia. *Am J Hum Genet.* 2000; 66(6):2013-4.
- Gordon M M, Brada N, Remacha A, Badell I, del Rio E, Baiget M, Santer R, Quadros E V, Rothenberg SP, Alpers DH. A genetic polymorphism in the coding region of the gastric intrinsic factor gene (GIF) is associated with congenital intrinsic factor deficiency. *Hum. Mutat.* 2004; 23(1): 85-91.
- Gräsbeck R, Gordon R, Kantero I, Kuhlback B. Selective vitamin B12 malabsorption and proteinuria in young people. *Acta Med. Scand.* 1960; 167: 289-296.
- Gravel RA, Mahoney MJ, Ruddle FH, Rosenberg LE. Genetic complementation in heterokaryons of human fibroblasts defective in cobalamin metabolism. *Proc. Nat. Acad. Sci.USA* 1975; 72(8): 3181-3185.

Gueant JL, Saunier M, Gastin I, Safi A, Lamireau T, Duclos B, Bigard MA, Gräsbeck R. Decreased activity of intestinal and urinary intrinsic factor receptor in Gräsbeck-Imerslund disease. *Gastroenterology*. 1995; 108(6):1622-8.

Gueant JL, Chery C, Namour F. Cubilin and the hydrophobic intrinsic factor receptor are distinct molecules. *Blood*. 2001; 97(10):3316-7.

Gulati S, Baker P, Li YN, Fowler B, Kruger W, Brody LC, Banerjee R. Defects in human methionine synthetase in cblG patients. *Hum Mol Genet*. 1996; 5(12):1859-65.

Gullberg R. Vitamin B 12 -binding proteins in normal human blood plasma and serum. *Scand J Haematol*. 1972; 9(6):639-47.

Guyon R, Lorentzen TD, Hitte C, Kim L, Cadieu E, Parker HG, Quignon P, Lowe JK, Renier C, Gelfenbeyn B, Vignaux F, DeFrance HB, Gloux S, Mahairas GG, Andre C, Galibert F, Ostrander EA. A 1-Mb resolution radiation hybrid map of the canine genome. *Proc Natl Acad Sci U S A*. 2003; 100(9):5296-301.

Hammad SM, Stefansson S, Twal WO, Drake CJ, Fleming P, Remaley A, Brewer HB Jr, Argraves WS. Cubilin, the endocytic receptor for intrinsic factor-vitamin B(12) complex, mediates high-density lipoprotein holoparticle endocytosis. *Proc Natl Acad Sci U S A*. 1999; 96(18):10158-63.

Hammad SM, Barth JL, Knaak C, Argraves WS. Megalin acts in concert with cubilin to mediate endocytosis of high density lipoproteins. *J Biol Chem*. 2000; 275(16):12003-8.

Hewitt JE, Gordon MM, Taggart RT, Mohandas TK, Alpers DH. Human gastric intrinsic factor: characterization of cDNA and genomic clones and localization to human chromosome 11. *Genomics*. 1991; 10(2):432-40.

Hippe E. Malabsorption of vitamin B12. Report of a case in a 1-year-old boy, including studies of the absorption of B12. *Acta Paediatr Scand*. 1966; 55(5):510-6.

Hooper DC, Alpers DH, Burger RL, Mehlman CS, Allen RH. Characterization of ileal vitamin B12 Binding using homogeneous human and hog intrinsic factors. *J Clin Invest*. 1973; 52(12):3074-83.

Idriss JM, Jonas AJ. Vitamin B12 transport by rat liver lysosomal membrane vesicles. *J Biol Chem*. 1991; 266(15):9438-41.

Imerslund O. Idiopathic chronic megaloblastic anemia in children. *Acta Paediatr. Scand*. 1960; 49: 1-115.

Imerslund O and Bjornstad P. Familial vitamin B12 malabsorption. *Acta Haemat*. 1963; 30:1-7.

Ismail EA, Al Saleh Q, Sabry MA, Al Ghanim M, Zaki M. Genotypic/phenotypic heterogeneity of selective vitamin B12 malabsorption (Gräsbeck-Imerslund syndrome) in two Bedouin families. *Acta Paediatr.* 1997; 86(4):424-5.

Israel DI. A PCR-based method for high stringency screening of DNA libraries. *Nucleic Acids Res.* 1993; 21(11):2627-31.

Janata J, Kogekar N, Fenton WA. Expression and kinetic characterization of methylmalonyl-CoA mutase from patients with the mut- phenotype: evidence for naturally occurring interallelic complementation. *Hum Mol Genet.* 1997; 6(9):1457-64.

Jensen HK, Jensen TG, Faergeman O, Jensen LG, Andresen BS, Corydon MJ, Andreasen PH, Hansen PS, Heath F, Bolund L, Gregersen N. Two mutations in the same low-density lipoprotein receptor allele act in synergy to reduce receptor function in heterozygous familial hypercholesterolemia. *Hum Mutat.* 1997; 9(5):437-44.

Kalantry S, Manning S, Haub O, Tomihara-Newberger C, Lee HG, Fangman J, Distèche CM, Manova K, Lacy E. The amnionless gene, essential for mouse gastrulation, encodes a visceral-endoderm-specific protein with an extracellular cysteine-rich domain. *Nat Genet.* 2001; 27(4):412-6.

Kapadia CR, Serfilippi D, Voloshin K, Donaldson RM Jr. Intrinsic factor-mediated absorption of cobalamin by guinea pig ileal cells. *J Clin Invest.* 1983; 71(3):440-8.

Katz M, Cooper BA. Solubilized receptor for intrinsic factor-Vitamin B12 complex from guinea pig intestinal mucosa. *J Clin Invest.* 1974a; 54(3):733-9.

Katz M, Mehlman CS, and Allen RH. Isolation and Characterization of an Abnormal Human Intrinsic Factor. *J Clin Invest.* 1974b; 53(5): 1274 -1283.

Kelley PM, Harris DJ, Comer BC, Askew JW, Fowler T, Smith SD, Kimberling WJ. Novel mutations in the connexin 26 gene (GJB2) that cause autosomal recessive (DFNB1) hearing loss. *Am J Hum Genet.* 1998; 62(4):792-9.

Kouvonen I. Solubilization of the pig ileal intrinsic factor receptor with papain treatment and studies on the solubilized receptor. *Biochim Biophys Acta.* 1980; 626(1):244-53.

Kozak M. Point mutations define a sequence flanking the AUG initiator codon that modulates translation by eukaryotic ribosomes. *Cell.* 1986; 44(2):283-92.

Kozak M. Recognition of AUG and alternative initiator codons is augmented by G in position +4 but is not generally affected by the nucleotides in positions +5 and +6. *EMBO J.* 1997; 16(9):2482-92.

Kozyraki R, Kristiansen M, Silahtaroglu A, Hansen C, Jacobsen C, Tommerup N, Verroust PJ, Moestrup SK. The human intrinsic factor-vitamin B12 receptor, cubilin:

molecular characterization and chromosomal mapping of the gene to 10p within the autosomal recessive megaloblastic anemia (MGA1) region. *Blood*. 1998; 91(10):3593-3600.

Kozyraki R, Fyfe J, Kristiansen M, Gerdes C, Jacobsen C, Cui S, Christensen EI, Aminoff M, de la Chapelle A, Krahe R, Verroust PJ, Moestrup SK. The intrinsic factor-vitamin B12 receptor, cubilin, is a high-affinity apolipoprotein A-I receptor facilitating endocytosis of high-density lipoprotein. *Nat Med*. 1999; 5(6):656-661.

Kozyraki R, Fyfe J, Verroust PJ, Jacobsen C, Dautry-Varsat A, Gburek J, Willnow TE, Christensen EI, Moestrup SK. Megalin-dependent cubilin-mediated endocytosis is a major pathway for the apical uptake of transferrin in polarized epithelia. *Proc Natl Acad Sci U S A*. 2001; 98(22):12491-12496.

Kristiansen M, Kozyraki R, Jacobsen C, Nexø E, Verroust PJ, Moestrup SK. Molecular dissection of the intrinsic factor-vitamin B12 receptor, cubilin, discloses regions important for membrane association and ligand binding. *J Biol Chem*. 1999; 274(29):20540-4.

Kristiansen M, Aminoff M, Jacobsen C, de La Chapelle A, Krahe R, Verroust PJ, Moestrup SK. Cubilin P1297L mutation associated with hereditary megaloblastic anemia 1 causes impaired recognition of intrinsic factor-vitamin B(12) by cubilin. *Blood*. 2000; 96(2):405-9.

Lander E, Kruglyak L. Genetic dissection of complex traits: guidelines for interpreting and reporting linkage results. *Nat Genet*. 1995; 11(3):241-7.

Lathrop GM, Lalouel JM, Julier C, Ott J. Strategies for multilocus linkage analysis in humans. *Proc Natl Acad Sci U S A*. 1984; 81(11):3443-6.

Le Panse S, Ayani E, Mulliez N, Chatelet F, Cywiner-Golenzer C, Galceran M, Citadelle D, Roux C, Ronco P, Verroust P. Antibodies to the 280-kDa coated pit protein, target of teratogenic antibodies, produce alterations in the traffic of internalized proteins. *Am J Pathol*. 1994; 145(6):1526-36.

Leclerc D, Campeau E, Goyette P, Adjalla CE, Christensen B, Ross M, Eydoux P, Rosenblatt DS, Rozen R, Gravel RA. Human methionine synthetase: cDNA cloning and identification of mutations in patients of the cblG complementation group of folate/cobalamin disorders. *Hum. Molec. Genet*. 1996; 5(12): 1867-1874.

Levine JS, Nakane PK, Allen RH. Immunocytochemical localization of human intrinsic factor: the nonstimulated stomach. *Gastroenterology*. 1980; 79(3):493-502.

Levine JS, Allen RH, Alpers DH, Seetharam B. Immunocytochemical localization of the intrinsic factor-cobalamin receptor in dog-ileum: distribution of intracellular receptor

during cell maturation. *J Cell Biol.* 1984; 98(3):1111-8.

Li N, Rosenblatt DS, Kamen BA, Seetharam S, Seetharam B. Identification of two mutant alleles of transcobalamin II in an affected family. *Hum Mol Genet.* 1994; 3(10):1835-40.

Lin SH, Sourial NA, Lu KC, Hsueh EJ. Imerslund-Gräsbeck syndrome in a Chinese family with distinct skin lesions refractory to vitamin B12. *J. Clin. Path.* 1994; 47(10): 956-958.

Lindblom A, Quadt N, Marsh T, Aeschlimann D, Morgelin M, Mann K, Maurer P, Paulsson M. The intrinsic factor-vitamin B12 receptor, cubilin, is assembled into trimers via a coiled-coil alpha-helix. *J Biol Chem.* 1999; 274(10):6374-80.

Ludvigsson P, Hassink SE, Bernstein M, Widzer S, Grover WD. Ataxia, cerebral atrophy, and abnormal somatosensory evoked potentials in a 9-year-old Boy with vitamin B12 deficiency. *Annals of Neurology.* 1980; 8: 234 only.

Mackenzie IL, Donaldson RM Jr, Trier JS, Mathan VI. Ileal mucosa in familial selective vitamin B 12 malabsorption. *N Engl J Med.* 1972; 286(19):1021-5.

Marcoullis G, Gräsbeck R, Salonen EM. Identification and characterization of intrinsic factor and cobalophilin from pig ileal and pyloric mucosa. *Biochim Biophys Acta.* 1977; 497(3):663-72.

Marcoullis G, Rothenberg SP, Labombardi VJ. Preparation and characterization of proteins in the alimentary tract of the dog which bind cobalamin and intrinsic factor. *J Biol Chem.* 1980; 255(5):1824-9.

Marcoullis G, Rothenberg SP. Intrinsic factor-mediated intestinal absorption of cobalamin in the dog. *Am J Physiol.* 1981; 241(4):G294-9.

Marsh EN. Coenzyme B12 (cobalamin)-dependent enzymes. *Essays Biochem.* 1999; 34:139-54. Review.

Martens JH, Barg H, Warren MJ, Jahn D. Microbial production of vitamin B12. *Appl Microbiol Biotechnol.* 2002; 58(3):275-85.

Martina JA, Bonangelino CJ, Aguilar RC, Bonifacino JS. Stonin 2: an adaptor-like protein that interacts with components of the endocytic machinery. *J Cell Biol.* 2001; 153(5):1111-20.

Mathan VI, Babior BM, Donaldson RM, Jr. Kinetics of the Attachment of Intrinsic Factor-Bound Cobamides to Ileal Receptors. *J Clin Invest.* 1974; 54(3): 598-608.

Mellersh CS, Hitte C, Richman M, Vignaux F, Priat C, Jouquand S, Werner P, Andre C, DeRose S, Patterson DF, Ostrander EA, Galibert F. An integrated linkage-radiation hybrid map of the canine genome. *Mamm Genome.* 2000; 11(2):120-30.

Metherell LA, Chapple JP, Cooray S, David A, Becker C, Ruschendorf F, Naville D, Begeot M, Khoo B, Nurnberg P, Huebner A, Cheetham ME, Clark AJ. Mutations in MRAP, encoding a new interacting partner of the ACTH receptor, cause familial glucocorticoid deficiency type 2. *Nat Genet.* 2005; 37(2):166-70.

Miller JW, Ramos MI, Garrod MG, Flynn MA, Green R. Transcobalamin II 775G-to-C polymorphism and indices of vitamin B12 status in healthy older adults. *Blood.* 2002; 100(2): 718-720.

Moestrup SK, Birn H, Fischer PB, Petersen CM, Verroust PJ, Sim RB, Christensen EI, Nexø E. Megalin-mediated endocytosis of transcobalamin-vitamin-B12 complexes suggests a role of the receptor in vitamin-B12 homeostasis. *Proc Natl Acad Sci U S A.* 1996; 93(16):8612-7.

Moestrup SK, Kozyraki R, Kristiansen M, Kaysen JH, Rasmussen HH, Brault D, Pontillon F, Goda FO, Christensen EI, Hammond TG, Verroust PJ. The intrinsic factor-vitamin B12 receptor and target of teratogenic antibodies is a megalin-binding peripheral membrane protein with homology to developmental proteins. *J Biol Chem.* 1998; 273(9):5235-42.

Moestrup SK, Verroust PJ. Megalin- and cubilin-mediated endocytosis of protein-bound vitamins, lipids, and hormones in polarized epithelia. *Annu Rev Nutr.* 2001; 21:407-28.

Mohamed SD, McKay E, Galloway WH. Juvenile familial megaloblastic anaemia due to selective malabsorption of vitamin B-12. A family study and a review of the literature. *Q J Med.* 1966; 35(139):433-53.

Mount SM. A catalogue of splice junction sequences. *Nucleic Acids Res.* 1982; 10(2): 459-472.

Nykjaer A, Fyfe JC, Kozyraki R, Leheste JR, Jacobsen C, Nielsen MS, Verroust PJ, Aminoff M, de la Chapelle A, Moestrup SK, Ray R, Gliemann J, Willnow TE, Christensen EI. Cubilin dysfunction causes abnormal metabolism of the steroid hormone 25(OH) vitamin D(3). *Proc Natl Acad Sci U S A.* 2001; 98(24):13895-900.

Okuda K. Mucosal adsorption and absorption of vitamin B12 in the intestine of the rat. *Proc. Soc. Exp. Biol. Med.* 1962; 111:3203.

Okuda K. Discovery of vitamin B12 in the liver and its absorption factor in the stomach: a historical review. *J Gastroenterol Hepatol.* 1999; 14(4):301-8.

Platica O, Janeczko R, Quadros EV, Regec A, Romain R, Rothenberg SP. The cDNA sequence and the deduced amino acid sequence of human transcobalamin II show homology with rat intrinsic factor and human transcobalamin I. *J Biol Chem.* 1991; 266(12):7860-3.

Prasad KV, Ao Z, Yoon Y, Wu MX, Rizk M, Jacquot S, Schlossman SF. CD27, a member of the tumor necrosis factor receptor family, induces apoptosis and binds to Siva, a proapoptotic protein. *Proc. Natl. Acad. Sci. U.S.A.* 1997; 94 (12): 6346-6351.

Quadros EV, Sai P, Rothenberg SP. Characterization of the human placental membrane receptor for transcobalamin II-cobalamin. *Arch Biochem Biophys.* 1994; 308(1):192-9.

Ramanujam KS, Seetharam S, Ramasamy M, Seetharam B. Expression of cobalamin transport proteins and cobalamin transcytosis by colon adenocarcinoma cells. *Am J Physiol.* 1991; 260(3):G416-22.

Ramanujam KS, Seetharam S, Seetharam B. Regulated expression of intrinsic factor-cobalamin receptor by rat visceral yolk sac and placental membranes. *Biochim Biophys Acta.* 1993; 1146(2):243-6.

Ramanujam KS, Seetharam S, Dahms NM, Seetharam B. Effect of processing inhibitors on cobalamin (vitamin B12) transcytosis in polarized opossum kidney cells. *Arch Biochem Biophys.* 1994; 315(1):8-15.

Ramasamy M, Alpers DH, Tiruppathi C, Seetharam B. Cobalamin release from intrinsic factor and transfer to transcobalamin II within the rat enterocyte. *Am J Physiol.* 1989; 257(5):G791-7.

Rappazzo ME, Hall CA. Cyanocobalamin transport proteins in canine plasma. *Am J Physiol.* 1972; 222(1):202-6.

Regec A, Quadros EV, Platica O, Rothenberg SP. The cloning and characterization of the human transcobalamin II gene. *Blood.* 1995; 85(10):2711-9.

Richman M, Mellersh CS, Andre C, Galibert F, Ostrander EA. Characterization of a minimal screening set of 172 microsatellite markers for genome-wide screens of the canine genome. *J Biochem Biophys Methods.* 2001; 47(1-2):137-49.

Rosenblatt DS and Fenton WA. Inborn errors of cobalamin metabolism. In: Banerjee, R., (ed.), *Chemistry and Biochemistry of Vitamin B12*. John Wiley and Sons, New York. 1999; pp. 367-384.

Rosenblatt DS and Fenton WA. In *The Metabolic and Molecular Bases of Inherited Disease* (Scriver, C. R., Beaudet, A. L., Sly, W. S., and Valle, D., eds) 8th Ed., 2001; pp. 3897-3933, McGraw-Hill, Inc., New York.

Roth JR, Lawrence JG, Rubenfield M, Kieffer-Higgins S, Church GM. Characterization of the cobalamin (vitamin B12) biosynthetic genes of *Salmonella typhimurium*. *J Bacteriol.* 1993; 175(11):3303-16.

Rubin HM, Giorgio AJ, Macdonald RR, Linarelli LG. Selective malabsorption of vitamin B 12: report of a case with metabolic studies. *Am J Dis Child.* 1974; 127(5):713-7.

Rumpelt HJ, Michl W. Selective vitamin B12 malabsorption with proteinuria (Imerslund-Najman-Gräsbeck-syndrome): ultrastructural examinations on renal glomeruli. *Clin Nephrol.* 1979; 11(4):213-7.

Sahali D, Mulliez N, Chatelet F, Dupuis R, Ronco P, Verroust P. Characterization of a 280-kDa protein restricted to the coated pits of the renal brush border and the epithelial cells of the yolk sac. Teratogenic effect of the specific monoclonal antibodies. *J Exp Med.* 1988; 167(1):213-8.

Saito A, Pietromonaco S, Loo AK, Farquhar MG. Complete cloning and sequencing of rat gp330/"megalin," a distinctive member of the low density lipoprotein receptor gene family. *Proc Natl Acad Sci U S A.* 1994; 91(21):9725-9.

Salameh MM, Banda RW, Mohdi AA. Reversal of severe neurological abnormalities after vitamin B12 replacement in the Imerslund-Gräsbeck syndrome. *J Neurol.* 1991; 238(6):349-50.

Sambrook J, Fritsch EF, Maniatis T. *Molecular Cloning: A Laboratory Manual*, 2nd ed. 1989 (Cold Spring Harbor, NY: Cold Spring Harbor Laboratory Press).

Sandoval C, Bolten P, Franco I, Freeman S, Jayabose S. Recurrent urinary tract infections and genitourinary tract abnormalities in the Imerslund-Gräsbeck syndrome. *Pediatr Hematol Oncol.* 2000; 17(4):331-4.

Sargan DR, Yang F, Squire M, Milne BS, O'Brien PC, Ferguson-Smith MA. Use of flow-sorted canine chromosomes in the assignment of canine linkage, radiation hybrid, and syntenic groups to chromosomes: refinement and verification of the comparative chromosome map for dog and human. *Genomics.* 2000; 69(2):182-95.

Schaffer AA, Gupta SK, Shriram K, Cottingham RW Jr. Avoiding recomputation in linkage analysis. *Hum Hered.* 1994; 44(4):225-37.

Schloesser LL, Deshpande P, Schilling RF. Biologic turnover rate of cyanocobalamin (Vitamin B12) in human liver. *Am J Med.* 1958; 101: 306-309.

Seetharam B, Alpers DH, Allen RH. Isolation and characterization of the ileal receptor for intrinsic factor-cobalamin. *J Biol Chem.* 1981; 256(8):3785-90.

Seetharam B, Alpers DH. Absorption and transport of cobalamin (vitamin B12). *Annu Rev Nutr.* 1982a; 2:343-69.

Seetharam B, Bagur SS, Alpers DH. Isolation and characterization of proteolytically derived ileal receptor for intrinsic factor-cobalamin. *J Biol Chem.* 1982b; 257(1):183-9.

Seetharam B, Levine JS, Ramasamy M, Alpers DH. Purification, properties, and immunochemical localization of a receptor for intrinsic factor-cobalamin complex in the

rat kidney. *J Biol Chem.* 1988; 263(9):4443-9.

Seetharam B, Christensen EI, Moestrup SK, Hammond TG, Verroust PJ. Identification of rat yolk sac target protein of teratogenic antibodies, gp280, as intrinsic factor-cobalamin receptor. *J Clin Invest.* 1997; 99(10):2317-22.

Seetharam B. Receptor-mediated endocytosis of cobalamin (vitamin B12). *Annu Rev Nutr.* 1999; 19:173-95. Review.

Sennett C, Rosenberg LE, Mellman IS. Transmembrane transport of cobalamin in prokaryotic and eukaryotic cells. *Annu Rev Biochem.* 1981; 50:1053-86. Review.

Si K, Das K, Maitra U. Characterization of multiple mRNAs that encode mammalian translation initiation factor 5 (eIF-5). *J Biol Chem.* 1996; 271(28): 16934-38.

Simpson KW, Alpers DH, De Wille J, Swanson P, Farmer S, Sherding RG. Cellular localization and hormonal regulation of pancreatic intrinsic factor secretion in dogs. *Am J Physiol.* 1993; 265(1):G178-88.

Stabler SP, Allen RH. Vitamin B12 deficiency as a worldwide problem. *Annu Rev Nutr.* 2004; 24:299-326. Review.

Strope S, Rivi R, Metzger T, Manova K, Lacy E. Mouse amnionless, which is required for primitive streak assembly, mediates cell-surface localization and endocytic function of cubilin on visceral endoderm and kidney proximal tubules. *Development.* 2004; 131(19):4787-95.

Tailor CS, Marin M, Nouri A, Kavanaugh MP, Kabat D. Truncated forms of the dual function human ASCT2 neutral amino acid transporter/retroviral receptor are translationally initiated at multiple alternative CUG and GUG codons. *J Biol Chem.* 2001; 276(29):27221-30.

Taira M, Iizasa T, Shimada H, Kudoh J, Shimizu N, Tatibana M. A human testis-specific mRNA for phosphoribosylpyrophosphate synthetase that initiates from a non-AUG codon. *J Biol Chem.* 1990; 265(27):16491-7.

Tang LH, Chokshi H, Hu CB, Gordon MM, Alpers DH. The intrinsic factor (IF)-cobalamin receptor binding site is located in the amino-terminal portion of IF. *J Biol Chem.* 1992; 267(32):22982-6.

Tanner SM, Aminoff M, Wright FA, Liyanarachchi S, Kuronen M, Saarinen A, Massika O, Mandel H, Broch H, de la Chapelle A. Amnionless, essential for mouse gastrulation, is mutated in recessive hereditary megaloblastic anemia. *Nat Genet.* 2003; 33(3):426-9.

Tanner SM, Li Z, Bisson R, Acar C, Oner C, Oner R, Cetin M, Abdelaal MA, Ismail EA, Lissens W, Krahe R, Broch H, Gräsbeck R, de la Chapelle A. Genetically heterogeneous

selective intestinal malabsorption of vitamin B12: founder effects, consanguinity, and high clinical awareness explain aggregations in Scandinavia and the Middle East. *Hum Mutat.* 2004; 23(4):327-33.

Tomihara-Newberger C, Haub O, Lee HG, Soares V, Manova K, Lacy E. The amn gene product is required in extraembryonic tissues for the generation of middle primitive streak derivatives. *Dev Biol.* 1998; 204(1):34-54.

Vaillant C, Horadagoda NU, Batt RM. Cellular localization of intrinsic factor in pancreas and stomach of the dog. *Cell Tissue Res.* 1990; 260(1):117-22.

Van Praet O, Argraves WS, Morales CR. Co-expression and interaction of cubilin and megalin in the adult male rat reproductive system. *Mol Reprod Dev.* 2003; 64(2):129-35.

Venter JC, Adams MD, Myers EW, Li PW, Mural RJ et al. The sequence of the human genome. *Science.* 2001; 291(5507):1304-51.

Vinogradov AE. Genome size and GC-percent in vertebrates as determined by flow cytometry: the triangular relationship. *Cytometry.* 1998; 31(2):100-9.

Wang X, Bornslaeger EA, Haub O, Tomihara-Newberger C, Lonberg N, Dinulos MB, Disteché CM, Copeland N, Gilbert DJ, Jenkins NA, Lacy E. A candidate gene for the amnionless gastrulation stage mouse mutation encodes a TRAF-related protein. *Dev Biol.* 1996; 177(1):274-90.

Watkins D, Ru M, Hwang HY, Kim CD, Murray A, Philip NS, Kim W, Legakis H, Wai T, Hilton JF, Ge B, Dore C, Hosack A, Wilson A, Gravel RA, Shane B, Hudson TJ, Rosenblatt DS. Hyperhomocysteinemia due to methionine synthetase deficiency, cblG: structure of the MTR gene, genotype diversity, and recognition of a common mutation, P1173L. *Am. J. Hum. Genet.* 2002; 71(1): 143-153.

Weng Z, Fluckiger AC, Nisitani S, Wahl MI, Le LQ, Hunter CA, Fernal AA, Le Beau MM, Witte ON. A DNA damage and stress inducible G protein-coupled receptor blocks cells in G2/M. *Proc Natl Acad Sci U S A.* 1998; 95(21):12334-9.

Werner P, Mellersh CS, Raducha MG, DeRose S, Acland GM, Prociuk U, Wiegand N, Aguirre GD, Henthorn PS, Patterson DF, Ostrander EA. Anchoring of canine linkage groups with chromosome-specific markers. *Mamm Genome.* 1999; 10(8):814-23.

Willigan DA, Cronkite EP, Meyer LM, Noto SL. Biliary excretion of Co60 labeled vitamin B12 in dogs. *Proc Soc Exp Biol Med.* 1958; 99(1):81-4.

Wilson A, Leclerc D, Rosenblatt DS, Gravel RA. Molecular basis for methionine synthetase reductase deficiency in patients belonging to the cblE complementation group of disorders in folate/cobalamin metabolism. *Hum Mol Genet.* 1999; 8(11):2009-16.

Xu D, Kozyraki R, Newman TC, Fyfe JC. Genetic evidence of an accessory activity required specifically for cubilin brush-border expression and intrinsic factor-cobalamin absorption. *Blood*. 1999; 94(10):3604-6.

Xu D, Fyfe JC. Cubilin expression and posttranslational modification in the canine gastrointestinal tract. *Am J Physiol Gastrointest Liver Physiol*. 2000; 279(4):G748-56

Yammani RR, Seetharam S, Seetharam B. Identification and characterization of two distinct ligand binding regions of cubilin. *J Biol Chem*. 2001; 276(48):44777-84.

Yang YM, Ducos R, Rosenberg AJ, Catrou PG, Levine JS, Podell ER, Allen RH. Cobalamin malabsorption in three siblings due to an abnormal intrinsic factor that is markedly susceptible to acid and proteolysis. *J Clin Invest*. 1985; 76(6):2057-65.

Yassin F, Rothenberg SP, Rao S, Gordon MM, Alpers DH, Quadros EV. Identification of a 4-base deletion in the gene in inherited intrinsic factor deficiency. *Blood*. 2004; 103(4):1515-1517.

Yetgin S, Altay C, Laleli Y. Familial selective vitamin B12 malabsorption in three families. *Turk J Pediatr*. 1978; 20(1-2):44-50.

Yki-Jarvinen H, Kouvonen I, Gräsbeck R. Solubilization and preliminary characterization of the human ileal vitamin B12-intrinsic factor receptor. *Scand J Clin Lab Invest*. 1979; 39(5):461-7.

Youngdahl-Turner P, Rosenberg LE, Allen RH. Binding and uptake of transcobalamin II by human fibroblasts. *J Clin Invest*. 1978; 61(1):133-41.

Zavadakova P, Fowler B, Zeman J, Suormala T, Pristoupilova K, Kozich V, Zavad'akova P. CblE type of homocystinuria due to methionine synthetase reductase deficiency: clinical and molecular studies and prenatal diagnosis in two families. *J Inherit Metab Dis*. 2002; 25(6):461-76.

Zhai XY, Nielsen R, Birn H, Drumm K, Mildenerberger S, Freudinger R, Moestrup SK, Verroust PJ, Christensen EI, Gekle M. Cubilin- and megalin-mediated uptake of albumin in cultured proximal tubule cells of opossum kidney. *Kidney Int*. 2000; 58(4):1523-33.

MICHIGAN STATE UNIVERSITY LIBRARIES



3 1293 02736 1231